APPLICATION OF *IN SITU* AU-AMALGAM MICROELECTRODES IN YELLOWSTONE NATIONAL PARK TO GUIDE MICROBIAL SAMPLING: AN INVESTIGATION INTO ARSENITE AND POLYSULFIDE DETECTION TO DEFINE MICROBIAL HABITATS

A Thesis Presented

by

Gregory Wade Lorenson

to

The Faculty of the Graduate College

of

The University of Vermont

In Partial Fulfillment of the Requirements
for the Degree of Master of Science
Specializing in Geology

October, 2006

Accepted by the Faculty of the Graduate College, The University of Vermont, in partial fulfillment of the requirements for the degree of Master of Science, specializing in Geology.

Thesis Examination Committee:

_____ Advisor
Gregory Druschel, Ph.D.

_____
Andrea Lini, Ph.D.

_____ Chairperson
Donna Rizzo, Ph.D.

_____ Vice President for
Frances E. Carr, Ph.D. Research and Dean
of the Graduate College

Date: May 11, 2006

Abstract

To better understand the links between microbial activity and geochemical cycling, geochemical parameters and microbial ecology must be defined together in both space and time. This can be accomplished with the help of gold-amalgam microelectrodes that provide real time *in situ* data of a number of redox species, including species of Fe, Mn, O, As, and S, to define the microbes' natural environment while those microbes are collected for characterization. Characterization of the microbes' natural environment provides insight into the location and sources of potential energy available to a microorganism.

The complete oxidation of sulfide is a complex pathway that provides a unique opportunity to study how subtle changes in the redox kinetics of a local environment can impact the environment's microbial ecology. The gold-amalgam microelectrode can detect subtle changes in sulfur substrates available to microbes, providing the opportunity to delineate different geochemical niches. As geochemical data are collected from the environment, microbial samples are also collected for culture-based studies, helping to address how much change in the local geochemical environment is required to invoke significant changes in the overall microbial population.

Yellowstone National Park is a unique place to study systems involving sulfur species because of its wide variety of springs, thermal and non-thermal, which contain elemental sulfur and products of sulfide oxidation. In 2004 electrochemical data and microbial samples were collected at Norris Geyser Basin and Gibbon Geyser Basin, in Yellowstone National Park, Wyoming, USA. Microbial samples were drawn through tubing attached to the working electrode, making sampling concurrent with electrochemical data collection.

Extensive laboratory work was conducted to determine the electrochemical signal for sulfide, polysulfide, elemental sulfur, and arsenite in natural waters. Arsenite, which has never before been quantified *in situ,* can now be determined and quantified with the Au-amalgam microelectrode for a wide range of pH values and temperatures down to nanomolar concentrations. Sulfide, polysulfide, and elemental sulfur can concurrently be determined in natural waters through the use of the Au-amalgam microelectrode in natural waters over a wide range of pH values and temperatures. Electrochemical signals collected from Yellowstone's hot springs were interpreted and concentrations of redox species that could not previously be defined were determined.

Microbial samples collected during electrochemical data collection were cultured using substrates designed to reflect the redox chemistry of the hot spring they were removed from. PCR and T-RFLP were run to classify microbial communities cultured on these substrates. Changes to microbial community fingerprints due to culturing with different substrates yielded inconclusive results. Energetic calculations were also conducted for reactions involving the intermediate sulfur species that can now be defined *in situ.* Polysulfide oxidation and reduction yield significant energy that could be used by microbial communities for metabolism in Yellowstone National Parks hot springs.

Table of Contents

Page

List of Tables

List of Figures

1.0 INTRODUCTION

Defining an environment in its undisturbed natural state is important to understanding the setting in which microbial communities thrive and may help to understand microbial response to geochemical change. The energy required for microbial life is harnessed through the use of reduced substrates coupled with oxidized electron acceptors (Amend et al., 2003). Geochemical energy potentially available to microbes in any environment is therefore dependent on the redox chemistry (involving all oxidized or reduced ions) of that environment. With minimal disruption to the environment, the real-time *in situ* redox chemistry important to microbial metabolism can be defined through the use of Au-amalgam microelectrodes. The Au-amalgam microelectrode can define many of the redox species (substrates and electron acceptors) involved in the half reactions that may be acted on by microbes (Amend and Shock, 2001; Luther et al., 2005). Many redox species within sampled water have a tendency to oxidize or precipitate before analysis is done in the lab, making microelectrode real-time *in situ* determinations of obvious value. The real-time redox data collected facilitates directed sampling of microbes from well-defined spatial intervals describing the geochemical niche they occupy. Redox chemistry data, collected through the use of microelectrodes, and microbial samples can be taken from the same location at the same time.

Microbiological research does not always include redox geochemical data (chemical speciation) from the exact location of microbial sampling (Spear et al., 2005), and may include little or no geochemical data gathered during microbial sampling (Tankere et al., 2002; Bernhard et al., 2003; Nunan et al., 2001, 2002). Data collection of

redox speciation using Au-amalgam microelectrodes provides information for Fe, Mn, As, S, and O species; helping to define redox species microorganisms may potentially use for chemolithothrophy. A better understanding of microbial metabolism will allow for more careful and site-tailored culturing of microorganisms, giving scientists and microbiologists the ability to cultivate novel organisms by inoculating environmental microbial samples with the proper substrates. Cultivating unknown microorganisms from natural environments, and understanding the chemical reactions they couple for survival, could lead to advances in the pharmaceutical industry, help to advance bioremediation technology, and impact science and microbiology significantly.

Many of the hot-spring pools in Yellowstone National Park (YNP) contain H_2S, many forms of S in various intermediate redox states [including polysulfides (S_5^{2-}, S_4^{2-}, S_2^{2-}), elemental sulfur (S_8), thiosulfate ($S_2O_3^{2-}$), and tetrathionate ($S_3O_4^{2-}$)], and chemical species of Fe, Mn, As, and O. These redox species act as substrates and electron acceptors, make the hot springs an ideal location to measure *in situ* redox chemistry while taking microbial samples of the hot spring microbial communities. The variety of thermal waters in YNP is reflected in differences in pH, temperature, and varying amounts of oxidized and reduced chemical species (Ball et al., 2001). Because a wide variety of redox species can exist, there are many possible combinations of substrates and electron acceptors available to microbes. Due to the variety of geochemical environments in YNP's hot springs there is a large diversity of microbial communities (Spear et al., 2005).

An environment's geochemistry can both affect the microbial community occupying the environment and be affected by the microbial community. Geochemical niches, the location in space where both a substrate and electron acceptor exist for microbial metabolism, can be extremely small (<0.2mm) (Tankere et al., 2002; Bernhard et al., 2003; Nunan et al., 2001, 2002). Redox transformations of chemical species within a geochemical niche can occur due to physiochemical changes in the environment or due to microbial metabolism, shifting the location of the geochemical niche or affecting the microbial community occupying that space. Understanding the physical/geochemical processes that select for specific microbes requires that we gather highly correlated geochemical and microbial data that is well defined in space and time.

This thesis will show the importance of collecting detailed redox chemical data to calculate potential energy available from thermodynamic modeling, so that energy yielding reactions in natural environments can be better defined. In order to understand and interpret data collected in the field by *in situ* voltammetric electrodes, the chemical species that can be detected with the electrode must be defined. Au-amalgam microelectrodes have been used for the *in situ* detection of redox species in environments where the environmental conditions (pH and temperature) fluctuate; however, changes in the electrochemical signal due to changing environmental conditions is not well quantified. In order to use Au-amalgam electrodes in Yellowstone's hot springs, changes in electrochemical signals due to varying conditions must be understood.

1.1 Thesis Statement and Objectives

This thesis will examine the use of voltammetric microelectrodes for *in situ* determination of redox chemistry important to microbial metabolism. Work contained in this thesis will identify the electroactive redox species of arsenic and sulfur, in both laboratory and natural solutions, at Au-amalgam microelectrodes. Electrochemical signals for the chemical redox species of arsenic and sulfur were examined in great detail at selected Yellowstone National Park environments to determine what redox species Au-amalgam microelectrodes were useful in detecting. The careful evaluation of certain chemical species was carried out to determine how environmental changes, mainly pH and temperature, affect electrochemical data interpretation. By better defining the *in situ* redox chemistry of an environment, it is possible to describe geochemical reactions that have previously been overlooked to determine if they yield energy to microbial metabolism. Defining the *in situ* redox chemistry and the energy yielding geochemical reactions of an environment can allow for improvement in culturing techniques. It is important to determine if culturing techniques effectively represent the real *in situ* environment of microbial communities and if the substrate supplied to microbial cultures has a significant impact on community selection.

The thesis objectives are to:

1. Better characterize the *in situ* water chemistry of several of Yellowstone National Parks hot springs by evaluating the reactions occurring at the Au-amalgam microelectrode surface involving arsenic and sulfur species;

2. Determine the potential energy available for microbial metabolism; and,

3. Understand how changes to an environment's geochemistry affect changes in microbiology.

1.2 Yellowstone Geology and Geochemistry

Yellowstone National Park (YNP) is located in the northwest corner of the state of Wyoming and incorporates over 2,000,000 acres (Figure 1.2.1); including four major types of hydrothermal features associated with volcanic activity. Since 1888 geochemical data from many of Yellowstone's thermal features have been collected.

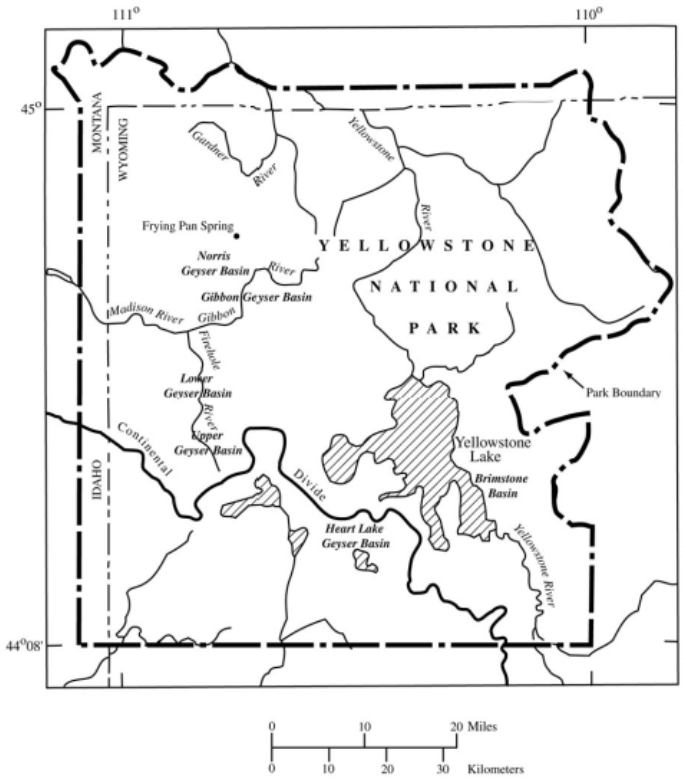

Figure 1.2.1. Map of Yellowstone National Park, WY. (From Ball et al., 2001).

Yellowstone National Park is of much interest to scientists because of its volcanic activity and history; it is home to a large percentage of the worlds geysers, and has a remarkable diversity of thermal waters and microbial habitats. Geochemical and geological data collected by many different scientific groups over the past century

provides background information about YNP's present hydrothermal systems and geologic past (Gooch and Whitfield, 1888; Hague, 1911; Allen and Day, 1935; Craig et al., 1956; Mazor and Wasserburg, 1965; Gunter and Musgrave, 1966; White et al., 1971; Mazor and Fournier, 1973; Thompson and Hutchinson, 1981; Welhan, 1981; Truesdell and Thompson, 1982; Fournier, 1989; Xu et al., 1998; Christiansen, 2001). Yellowstone has also been of great interest to microbiologists, and the study of microorganisms in YNP hot springs has led to significant advances in microbiology (Setchell, 1903; Barns et al., 1994; Reysenbach and Shock, 2002; Brock, 1978; Huganholtz et al., 1998; Graber et al., 2001; Fishbain et al., 2003; Meyer-Dombard et al., 2004; Spear et al., 2005).

1.2.1 Geologic History

YNP and its surrounding area make up a rhyolite plateau of late Pliocene and Quaternary age covering 17,000 km^2 (Christiansen, 2001). The Yellowstone Plateau Volcanic Field (YPVF) is made up of three major rhyolitic welded ash-flow tuff sheets. Unconformities separate the three sheets that make up the Yellowstone Group, and are, from oldest to youngest, Huckleberry Ridge, Mesa Falls, and Lava Creek Tuffs, respectively (Figure 1.2.2). The three major sheets of welded ash-flow tuff represent the climax of three cycles in the volcanic history of YNP. All three cycles had a similar sequence of volcanic events; all climaxed with large volume rhyolitic ash-flows and tuffs; all had eruptive events both before and after the major eruption of rhyolitic lavas and tuffs from the source area; and all had eruptions of basalts around the margins of the major rhyolitic volcanism. More than half of the erupted material from the YPVF during

its last three cycles is from the sheet flows making up the Yellowstone Group. The overall volume of these magmas is approximately 3700 km^3 (Christiansen, 2001).

Age	Volcanic cycle	Precaldera rhyolite	Caldera-forming ash-flow tuff (Yellowstone Group)	Postcaldera rhyolite	Contemporaneous plateau-marginal basalts
Pleistocene	Third			Plateau Rhyolite	Basalts of Snake River Group Osprey Basalt Madison River Basalt Basalt of Geode Creek Swan Lake Flat Basalt Gerrit Basalt Falls River Basalt Basalt of Mariposa Lake
			Lava Creek Tuff		
		Mount Jackson Rhyolite Lewis Canyon Rhyolite			Undine Falls Basalt Basalt of Warm River Basalt of Shotgun Valley
	Second			Island Park Rhyolite	Basalt of the Narrows
		Big Bend Ridge Rhyolite[1]	Mesa Falls Tuff		
Pliocene	First			Big Bend Ridge Rhyolite[1]	
		Rhyolite of Snake River Butte	Huckleberry Ridge Tuff		
					Junction Butte Basalt

Figure 1.2.2. YPVF's three volcanic cycles and their associated rocks. (From Christiansen, 2001.)

Each of the cycles in the Yellowstone group lasted one half to one million years (Christiansen, 2001). Active extensional tectonics started in the late Miocene, creating north to northwest trending fault blocks via normal faulting. Continued uplift and tilting of these fault blocks has accompanied volcanism, and controlled the volcanic structure of the YPVF (Christiansen, 2001).

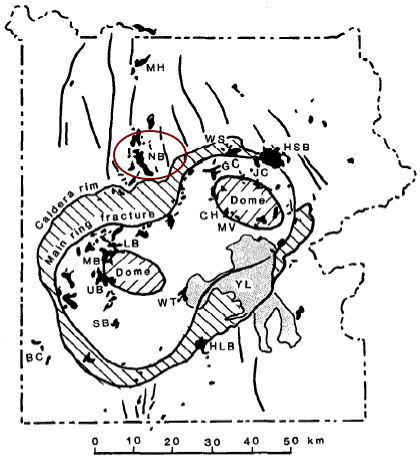

Figure 1.2.3. Current Yellowstone caldera showing major NW trending faults and the location (circled) of Norris Geyser Basin (NB) (From Fournier, 1989).

Most of the seismic and tectonic activity in YNP is currently located along the eastern edge of the YPVF, while most of the present day hydrothermal activity in YNP lies within the most recent 0.6 Ma caldera (Figure 1.2.3). The majority of these hydrothermal features are located along the main ring fracture zone or along the edges of the two resurgent domes. However, features such as Norris Geyser Basin (NGB) lie outside the caldera following fault trends (Figure 1.2.3). These faults trend northwest from the northern edge of the caldera rim and link NGB and Mammoth Hot Springs (MH, Figure 1.2.3).

Permeable rhyolite flows are sandwiched between impermeable ash-flow tuffs and have created very large fluid reservoirs (Truesdell et al., 1977). These reservoirs are recharged by runoff from the mountains to the north and west of the Yellowstone caldera, and provide water to Yellowstone's geothermal system (Fournier, 1989). Meteoric waters within rhyolite reservoirs are conductively heated; cold when entering the reservoir, the water is dense and will sink or move downward through faults and fractures. Fluid pressures steadily increase downward through the crust influencing the maximum temperature obtainable by infiltrating waters at a given depth. This temperature maximum is determined by a boiling-point curve at specific hydrostatic conditions (Fournier, 1989); therefore the infiltrating water can become superheated, not boiling until the pressure decreases. The water convects at this hydrostatic pressure to a depth of about 4-5 km within the caldera, and deeper outside the caldera, reaching a maximum temperature of 350-430 °C, and obtaining up to 300-500 mg/kg of Cl^- from the rock it passes through and possibly from mixing with deep brine of magmatic origin

(Fournier, 1989). In addition to chlorine, geothermal water also picks up gaseous components, dissolved minerals, and leached elements from the magma and crystalline magmatic rocks through which it flows (Fournier, 1989).

1.2.2 Hydrothermal System

Geothermal systems can be found on the earth's surface where there are large thermal gradients associated with one of three tectonic settings; tectonic plate boundaries, "hot spots", or rift zones (Webster and Nordstrom, 2003). Yellowstone National Pak (YNP) is a high temperature geothermal system, associated with a shallow depth magma chamber within the earths crust; a "hot spot". Extensive isotopic studies have shown that geothermal fluids commonly originate from meteoric waters (Craig et al., 1956; Fournier, 1989; Giggenbach, 1971; Webster and Nordstrom, 2003) and are not significantly of magmatic origin. The thin crust under YNP easily transports the heat from the "hot spot" magma chamber to meteoric water filling the fractures in the overlying rock. Gooch and Whitfield (1888) were the first scientists to study many of the YNP hot springs and geysers. A thorough study by Allen and Day (1935), in which the chemistry of most of YNP thermal features were characterized was conducted between 1925-1930. This study was incredibly detailed for its time and even included thiosulfate ($S_2O_3^{2-}$) titrations. Since this study, many other groups have collected and analyzed thermal waters and gases from Yellowstone's hot springs and geysers (Ball et al., 1998; Ball et al., 2001; Ball et al., 2002; Fournier, 1989; Fournier and Thompson, 1992; Mazor and Wasserburg, 1965; Truesdell and Fournier, 1976; Sheppard et al., 1992; Welhan, 1981; White et al., 1971; Xu et al., 2000). These studies have shown that there have been significant

changes in some individual features over time, while others have remained essentially the same since Allen and Day (1935) first studied them; but the range of hydrothermal water compositions in YNP has remained the same (Fournier, 1989). This wide range of geothermal waters within YNP have pH values ranging from 1 to 10, temperatures ranging from ambient to boiling, and relative to most natural waters the waters in YNP have high concentrations of H_2S, SO_4^{2-}, As, and HCO_3 (Ball et al., 2001). The diversity of geothermal fluids that can be found in YNP is due to equilibrium processes, physical processes, redox reactions, and mineral-precipitation reactions occurring both at depth and at the surface of the Yellowstone hydrothermal system.

Fluid temperature and host rock composition are the factors controlling the chemical composition of geothermal fluids making up the geothermal reservoir (Weres, 1988; Webster and Nordstrom, 2003). Hot water is a solvent that has a high dielectric constant, giving it the ability to dissolve ionic crystalline minerals in the host rock (Webster and Nordstrom, 2003). Minerals dissolved or leached from the host rock form new hydrated minerals that are easily transported with the bulk geothermal fluid. High temperature water-rock interactions have been studied over a wide range of temperatures using many different host rock types (Ellis and Mahon, 1964; 1977). Convection drives these heated waters upward and the decrease in pressure allows some geothermal fluids to boil changing them from a superheated single-phase liquid into steam and water. As these geothermal fluids rise towards the surface of the crust they are able to mix with shallow groundwaters and feed the geyser basins (Truesdell et al., 1977). Variations in dissolved gases and chloride concentrations present in individual pools or springs can

provide an idea as to whether boiling or mixing occurred at depth or in a shallow reservoir (Fournier, 1989).

The geothermal features present at the surface are a result of the direct discharge of the hot water phase, the hot water phase mixing with warm shallow groundwaters, or the interaction of the steam phase with shallow aquifer waters (Webster and Nordstrom, 2003). Four distinct types of mixed hot water systems exist within the park and create geyser basins where faults cut across topographically low basins in places such as Norris and Gibbon Geyser Basins (Fournier, 1989).

- Chloride rich waters that have low sulfate concentrations and reservoir temperatures greater than 260 °C, usually include large amounts of siliceous material that deposits to form terraces and mounds around the hot springs.
- Low pH-sulfate rich waters typically have low chloride concentrations with reservoir temperatures less than 200 °C.
- High pH-carbonate rich waters typically have low chloride concentrations with reservoir temperatures less than 200 °C.
- Low temperature pools are relatively low in both sulfate and chloride and exhibit little or no discharge from the source.

Neutral pH hot springs that are rich in chloride and silica are a result of direct discharge of the hot water phase (Webster and Nordstrom, 2003; See Figure 1.2.4). Mixing of the hot water phase with warmer aquifer waters results in low temperature waters that are relatively dilute with respect to dissolved chemical species and exhibit little to no discharge at the surface. When the steam phase is able to mix with shallow meteoric waters, (Figure 1.2.4) acidic, sulfate-rich waters or high pH HCO_3-rich waters are created, leading to the precipitation of elemental sulfur or carbonate (Webster and Nordstrom, 2003).

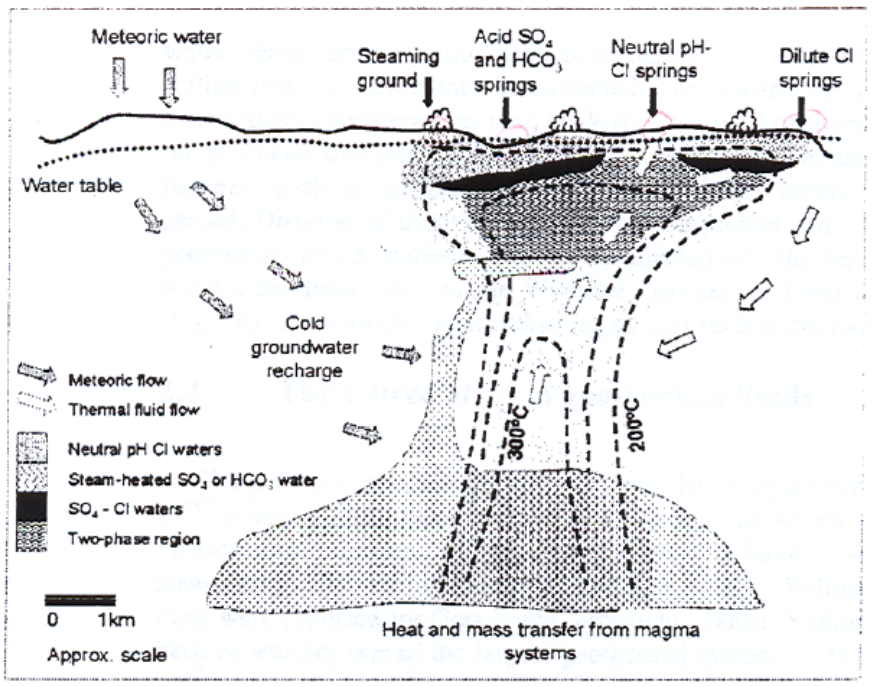

Figure 1.2.4. Structure of the geothermal system at Yellowstone National Park. (From Webster and Nordstrom, 2003).

Mixing of two or more of the three distinct types of mixed hot water systems can occur at or near the surface, creating surface waters that have a unique chemistry representative of the waters that mixed.

The sulfate/chloride ratios of the three hydrothermal feature types vary annually due to episodes of boiling brought on by changes in pressure within the hydrothermal system. Some hot springs will alternate seasonally between vapor-dominated and liquid-dominated; becoming low pH sulfate rich springs when sulfide gas released directly into surface waters dissociates or oxidizes (Webster and Nordstrom, 2003). Pressure changes can be due to seasonal changes in the water table, geyser eruptions, or the clogging of channels in which meteoric water flows due to earthquakes (Fournier, 1989). Large annual changes in the water table are due to rapid snowmelt events in spring. Runoff

from the mountains during spring recharges rhyolite aquifers exposed at the surface and increases the overall potentiometric surface of the water table in the valleys.

Since the end of the last glaciation, hydrothermal activity in YNP has been continuous at its present level; and it is not known whether the thermal energy that drives the system is increasing or decreasing (Fournier, 1989). Christiansen (2001) has proposed that continuing injection of basaltic magma (1200-1300 °C) from the mantle into the crust over a long period of time supplies the thermal energy to melt the crustal material, forming large volumes of silicic magmas at 800-900 °C. This crystallization of basalt is thought to provide enough heat for Yellowstone's present day hydrothermal system (Fournier, 1989).

1.2.3 Arsenic Sources

Arsenic has been known to exist in hydrothermal waters of YNP since they were first studied in the late 19th century (Gooch and Whitfield, 1888). Arsenic exists in most of Yellowstone's geothermal waters, prior to mixing, and ranges from less than 0.1 mg/kg to 10.0 mg/kg (Stauffer and Thompson, 1984). This range is common for As concentrations in most of the world's geothermal systems, and is three orders of magnitude greater than As found in most uncontaminated ground and surface waters (Webster and Nordstrom, 2003); and much higher than the USEPA drinking water standard of 0.01 mg/L total As (Federal Register, 2001).

Magmatic fluids containing arsenic, arsenic mineralization at depth, and arsenic leached from host rocks in the geothermal reservoir are the three potential As sources in geothermal waters (Webster and Nordstrom, 2003). Arsenic has been found to leach out

of host rocks such as greywacke and andesite at temperatures lower than most geothermal waters (Ellis and Mahon, 1964; Ellis and Mahon, 1967; Ewers and Keays, 1977). Leaching experiments have shown that As concentrations can reach 1.3 mg/kg in the leachate, making high As concentrations possible in hydrothermal waters without the input of magmatic fluids or As mineralization at depth (Webster and Nordstrom, 2003). Geothermal reservoir fluids, derived from meteoric waters, are typically undersaturated with respect to arsenic minerals, arsenopyrite and other arsenic minerals, and will more easily leach these minerals from host rocks into solution (Ballantyne and Moore, 1988).

Arsenic exists in reduced hydrothermal fluids, and its speciation is dependent on the sulfide concentration in the water (Webster and Nordstrom, 2003). In hydrothermal environments with low sulfide concentrations, arsenic exists primarily as arsenious acid [$H_3As^{III}O_3^o$] (Ballantyne and Moore, 1988; Heinrich and Eadington, 1986). Sulfide can react with arsenic to form thioarsenite complexes in environments with high sulfide concentrations because the solubility of arsenious acid is inhibited and the solubility of thioarsenite complexes increases (Helz et al., 1995; Webster and Nordstrom, 2003). Laboratory experiments have found that the reduction of arsenate (133 μM) by sulfide (266 μM) at pH 4 forms thioarsenite complexes, up to 100 μM, that decrease in concentration over time as they are further reduced to arsenite (Rochette et al., 2000).

The redox state of arsenic changes as hydrothermal fluids are transported through the geothermal system. Hot springs and geysers in YNP, supplied by geothermal fluids discharged directly from the reservoir, are dominated by arsenite [As(III)] (Ball et al., 1998; Webster and Nordstrom, 2003). As geothermal waters rise and are exposed to

oxygen, either from mixing with shallow groundwater or from exposure to the atmosphere, As(III) will oxidize to arsenate [As(V)] (Webster and Nordstrom, 2003).

1.2.4 Sulfur Sources

Chemical sulfur species are present in geothermal fluids due to two major sources: leaching from host rocks in the geothermal reservoir (Ellis and Mahon, 1964) and hydrogen sulfide gases formed at depth and brought to the surface (Fournier, 1989). As reduced hydrothermal fluids convect upwards into shallow reservoirs, reduced sulfur species will be oxidized when mixing occurs with shallow groundwaters containing oxygen.

Sulfur species can be formed by oxidation, reduction, and disproportionation reactions, taking on many intermediate forms (Figure 1.2.5). As sulfur is oxidized or reduced it goes through many redox states because an oxidation or reduction step can only transfer one or two electrons at a time and the complete oxidation of sulfide to sulfate involves the transfer of eight electrons.

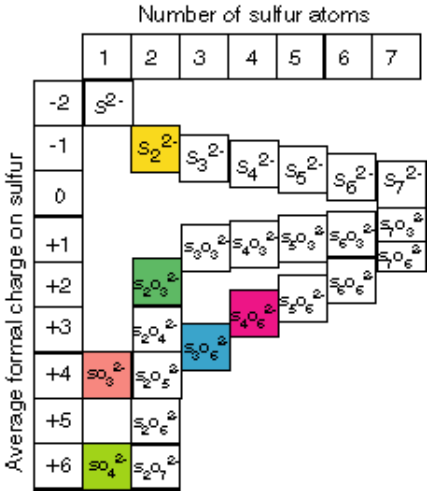

Figure 1.2.5 Sulfur speciation chart showing number of sulfur atoms and average formal charge. Adapted from Williamson and Rimstidt, 1992.

Sulfide is the most reduced redox form of sulfur and can exist as HS^- or H_2S (pK_1 =7) in lower pH environments (Webster and Nordstrom, 2003). Hydrogen sulfide gases that are discharged directly into surface waters will create low pH hot springs due to H_2S oxidation by atmospheric oxygen (1.1) (Webster and Nordstrom, 2003), or by H_2S dissociation in water (1.2).

$$H_2S + 2O_2 \rightarrow 2H^+ + SO_4^{2-}. \quad (1.1)$$
$$H_2S + H_2O \rightarrow HS^- + H^+ + H_2O. \quad (1.2)$$

Reduced sulfur species are oxidized due to both abiotic and biotic processes (Amend et al., 2003) and the rate of the oxidation process is dependent on pH, temperature, the presence of other chemical redox species, and the presence of microbial communities. The abiotic oxidation of sulfide leads to the formation of sulfur, thiosulfate, sulfite, and sulfate through the following reactions:

$$HS^- + ½\ O_2 \rightarrow S^0 + OH^-, \quad (1.3)$$
$$HS^- + O_2 \rightarrow ½\ S_2O_3^{2-} + ½\ H_2O, \quad (1.4)$$
$$HS^- + 3/2\ O_2 \rightarrow SO_3^{2-} + H^+, \quad (1.5)$$
$$HS^- + 2\ O_2 \rightarrow SO_4^{2-} + H^+, \quad (1.6)$$

where the product of the reaction is dependent on the pH and the sulfide/oxygen ratio (Kleinjan et al., 2005a) and the reactions are generally catalyzed by metal ions (Steudel, 2003).

Inorganic polysulfide ions, S_x^{2-}, are important intermediates in the inorganic sulfur system, and are important to the redox reactions involving sulfide, pyritization reactions, metal complexation, and elemental sulfur, playing a vital role in the geochemical and microbial sulfur cycle. Polysulfide ions can form due to the oxidation of monosulfide ions (1.7), due to the reaction involving monosulfide and elemental sulfur

(Wackenroeder solution) (1.8), or due to the reduction of elemental sulfur (1.9) (Steudel, 2003):

$$2HS^- - 2e^- \rightarrow S_2^{2-} + 2H^+, \quad (1.7)$$
$$2HS^- + S_8 \rightarrow 2S_5^{2-} + 5H^+, \quad (1.8)$$
$$\tfrac{1}{2}\, S_8 + 2e^- \leftrightarrow S_4^{2-}. \quad (1.9)$$

The only sulfur redox species that are thermodynamically stable in natural solutions are sulfide, elemental sulfur, and sulfate in the presence of water (Figure 1.2.6); however, it is possible to prepare metastable redox sulfur species, such as polysulfides, in aqueous solutions under conditions where they will not rapidly degrade.

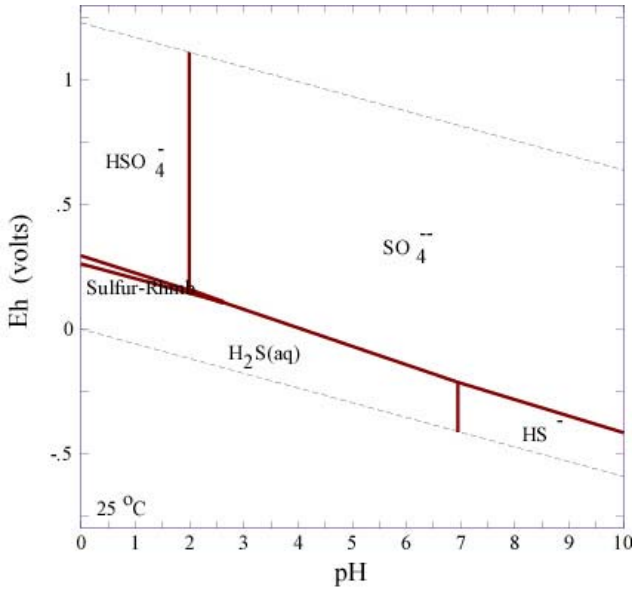

Figure 1.2.6. Eh-pH diagram of aqueous sulfur species in natural solutions at 1 bar pressure and 25°C.

Polysulfide ions, S_x^{2-}, can be formed due to the reaction of dissolved hydrogen sulfide with either elemental sulfur in its most common form (1.10) or biologically produced sulfur (1.11) (Steudel, 1996; Kleinjan, 2005b):

$$HS^- + (x\text{-}1)\ 1/8S_8 \leftrightarrow S_x^{2-}, \quad (1.10)$$
$$HS^- + (x\text{-}1)\ 1/8S_8 \leftrightarrow S_x^{2-} + H^+. \quad (1.11)$$

Aqueous solutions containing sulfide can dissolve elemental sulfur through the following pathway:

$$S_8 + HS^- + OH^- \leftrightarrow S_9^{2-} + H_2O, \quad (1.12)$$
$$S_9^{2-} + HS^- + OH^- \leftrightarrow 2S_5^{2-} + H_2O, \quad (1.13)$$

where the direction of this pathway is dependent on the pH of the solution. If the pH of a solution containing pentasulfide is lowered below 6, the precipitation of elemental sulfur is expected (Steudel, 2003). Polysulfide ions can be oxidized via chemical and biological processes. The chemical oxidation of polysulfide ions (1.14), leads to the formation of thiosulfate and elemental sulfur (Steudel et al., 1986; Steudel, 1996).

$$S_x^{2-} + 3/2\ O_2 \rightarrow S_2O_3^{2-} + (x-2)S^0. \quad (1.14)$$

Thiosulfate can also be formed due to sulfur hydrolysis in both alkaline and acidic solutions (1.15) where molten sulfur exists (Giggenbach, 1974; Xu et al., 2000):

$$4S_{(l)} + 3H_2O_{(l)} = S_2O_3^{2-}{}_{(aq)} + 2H_2S_{(aq)} + 2H^+_{(aq)}. \quad (1.15)$$

Thiosulfate is stable above pH 4.0 and up to 120 ºC and decomposes below this pH and above this temperature according to the following reactions (Xu, 1997):

$$S_2O_3^{2-} + H^+ = HSO_3^- + 1/8\ S_8, \quad (1.16)$$
$$3SO_3^{2-} + 2H^+ = 2SO_4^{2-} + 1/8\ S_8 + H_2O. \quad (1.17)$$

Tetrathionate can be formed due to the oxidation of thiosulfate in the presence of a pyrite catalyst (Xu and Schoonen, 1995):

$$2S_2O_3^{2-} + 0.5O_2 + 2H^+ = S_4O_6^{2-} + H_2O. \quad (1.18)$$

Sulfur cycling in natural environments is a very complex process due to the transfer of eight electrons between H_2S and SO_4^{2-} producing many intermediate redox species and numerous mineral forms. The ability to analyze multiple sulfur intermediates

in situ will yield information that could help better understand the biotic and abiotic sulfur transformations in natural environments.

1.2.5 Microbial Studies in Yellowstone's Hot Springs

Yellowstone's microbial ecology has been studied for over a century; with many scientists being interested in the thermophilic organisms living at such high temperatures (Setchell, 1903; Barns et al., 1994; Reysenbach and Shock, 2002; Brock, 1978; Huganholtz et al., 1998; Graber et al., 2001; Fishbain et al., 2003; Meyer-Dombard, 2004; Spear et al., 2005). Microorganisms living in Yellowstone's hot springs can undergo chemosynthesis or photosynthesis at lower temperatures; however, at higher temperatures (> 75C°) photosynthesis does not occur and microorganisms can only use chemical sources of energy (chemosynthesis) (Brock, 1978). Chemosynthesis involves microbial utilization of the energy yielded from coupling half reactions involving substrates (electron donors) and electron acceptors. Microbes commonly use oxidized and reduced forms of hydrogen, nitrogen, carbon, sulfur, iron, manganese, and oxygen as substrates and electron acceptors (Amend and Shock, 2001). Substrates are reduced redox species that once oxidized, give up an electron. The redox species that accepts this electron and become reduced are called the electron acceptors. Microbial communities will occupy space where both oxidized and reduced chemical species exist out of equilibrium; gaining valuable energy by coupling thermodynamically favorable reactions. Changes in an environment's geochemistry can both affect the microbial community occupying the environment and be affected by the microbial community. Microbial communities therefore play an important role in the redox chemistry of Yellowstone's hot

springs; of particular interest are microorganisms of the Aquificales spp. bacterial phylogenetic division, which have been found in abundance in hot spring environments (Reysenbach et al., 1994; Huber et al., 1998; Hugenholtz et al., 1998; Skirisdottir et al., 2000; Blank et al., 2002) and mainly use H_2 as an energy source (Spear et al., 2005). The abundance of Aquificales in Yellowstone's hot springs suggests that H_2 may be the main energy source for chemolithotrophy in select areas (Spear et al., 2005). It is possible that microorganisms in Yellowstone's hot springs could link H_2 oxidation with the reduction of sulfur species to gain energy; and this metabolic pathway needs to be explored further.

1.3 Metabolic Energy

For life to exist in natural environments, the environment's redox geochemistry cannot be in equilibrium. When a geochemical system is out of equilibrium there is a potential for chemical reactions to occur (Shock et al., 2005). Calculating the Gibbs energy of the system, at constant temperature and pressure, can determine the potential for chemical reactions to occur, and finding the difference between the real system from its equilibrium state yields quantifiable geochemical energy in the system (Amend et al., 2003; Spear et al., 2004; Shock et al., 2005). It is this energy that chemoautotrophic microorganisms utilize, gaining metabolic energy by catalyzing electron transfer reactions (oxidation-reduction reactions) that are thermodynamically favored but kinetically inhibited (Shock et al., 2005). Microorganisms are able to overcome kinetic barriers by providing an alternative pathway for the reaction, through the catalytic action of enzymes (Shock et al., 2005). The elements hydrogen, oxygen, nitrogen, carbon,

sulfur, iron, and manganese are essential to life and most of the electron transfer reactions that support life involve these elements (Amend and Shock, 2001). Microorganisms are able to harness energy by taking advantage of the potential energy available in natural geochemical gradients.

1.3.1 Calculating Microbial Energetics

The amount of chemical energy potentially available to microbial communities from a particular redox reaction can be quantified by calculating the Gibbs free energy:

$$\Delta G_r = \Delta G_r^o + RT\ln Q, \tag{1.19}$$

where, ΔG_r is the free energy change for a particular reaction, ΔG_r^o is the standard Gibbs free energy, R is the gas constant (8.3141 kJ/mol*K), T is the *in situ* temperature in degrees Kelvin, and Q is the activity product of compounds involved in the reaction.

The activity product, Q, is solved for all reactions of interest by:

$$Q = \Pi\, a_i{}^{r}{}_{(products)} / \Pi\, a_i{}^{r}{}_{(reactants)}, \tag{1.20}$$

where, $a_{i\ (products/reactants)}$ is the activity of the *i*th (product/reactant) chemical species involved in the reaction and r is the stoichiometric reaction coefficient for the *i*th chemical species. The activity (a_i) of a particular chemical species was calculated by

$$a_i = \gamma_i \bullet m_i; \tag{1.21}$$

where, m_i is the molar concentration of the particular chemical species and Debye-Hückel theory is used to solve the activity coefficient (γ) from the molar concentration and the charge of the ion. The activities of all the potential chemical species in solution are solved using the USGS computer-modeling program PHREEQC Interactive 2.10 for the

in situ conditions of the environment. The standard Gibbs free energy, ΔG_r^o, is calculated at *in situ* temperature and 1 bar pressure for reaction of interest through:

$$\Delta G_r^o = \Sigma\ r \bullet \Delta G_i^o, \qquad (1.22)$$

where, ΔG_i^o is the Gibbs free energy of formation for the *i*th chemical species and r is the stoichiometric reaction coefficient for the *i*th chemical species and is negative for reactants and positive for products. The values of ΔG_r^o are calculated using SUPCRT92 and a thermodynamic database including all chemical species of interest. If the overall Gibbs free energy for a particular reaction is negative (exergonic), the reaction will yield potential energy that could be used for microbial metabolism. Knowing the Gibbs free energy of potential half-reactions occurring at *in situ* conditions can help to define the microbial energetics of a particular environment; leading to proper selection of substrates for microbial culturing.

1.3.2 Geochemical Gradients

Geochemical gradients exist in all types of natural environments including lakes, soils, hydrothermal systems, and microbial mats (Thamdrup et al., 1994; Tankere et al., 2002; Bernhard et al., 2003; Nunan et al., 2001, 2002; Sundby et al., 2005). Chemical gradients are essential to life, maintaining disequilibrium and the possibility for microorganisms to harvest energy from coupled oxidation/reduction reactions. An electron tower can help to determine the potential energy available from redox reactions (Figure 1.3.1, Left). Electron towers can be created for any natural environment where the chemical speciation is well defined. The energy potential of chemical species on an

electron tower is equal to the Eh of that chemical species at a particular pH (Figure 1.3.1, Right), based on an Eh-pH diagram for the environments conditions.

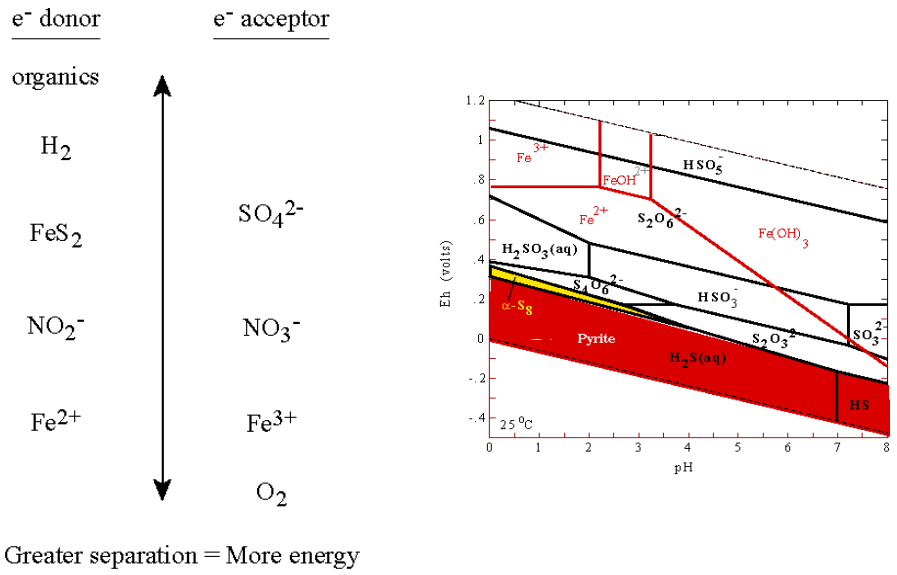

Figure 1.3.1. Left) Electron tower of common substrates and electron acceptors. Right) Construction of S intermediates by suppressing SO_4^{2-} species T=25 ºC, $\sum$ S = $1x10^{-4}$ M, $\sum$ Fe = $1x10^{-5}$ M.

Greater separation of the electron donor and the electron acceptor on the electron tower yields greater amounts of energy potentially available to microorganisms. Microorganisms have the ability to couple chemical redox reactions to gain metabolic energy. In order to gain energy from coupled half-reactions, microorganisms must situate themselves at a point in space where two chemical species out of equilibrium coincide.

Defining where geochemical gradients exist can be important to locating microbial communities important to redox cycling. A location in space that has oxidized and reduced chemical species used by microorganisms for metabolism or catabolism can support microbial communities. Once established, these microbial communities can

maintain, influence, or enhance sharp geochemical gradients between the oxidized and reduced chemical species.

1.4 Applied Electrochemistry

Electrodes and microelectrodes can be applied for geochemical analysis of natural environments, yielding valuable information about the environments' chemical speciation. Microelectrodes can define the spatial distribution of chemical species on a sub-millimeter scale, with only minor disruption to the environment's natural state (Taillefert et al., 2000). Electrodes and electrochemical techniques have been used since the 1970's for analysis of natural waters (Batley and Gardner, 1978; Piotrowicz et al., 1982; van den Berg, 1984; Florence, 1986; Capodaglio et al., 1990; Henneke et al., 1991), and recently have been used to make *in situ* measurements of chemical species (Taillefert et al., 2000; Luther et al., 1996; Luther et al., 1999; Nolan and Gaillard, 2002; Luther et al., 2005; Sundby et al., 2005).

Electroanalytical chemistry is a group of quantitative analytical methods that are based on the electrical properties of a solution containing an analyte (an electroactive chemical species) when it is made part of an electrochemical cell (Skoog and Leary, 1998). Electroanalytical methods can have low detection limits and have several advantages over other analytical techniques: they are specific for particular oxidation states of an element; the equipment needed is relatively inexpensive; and they can provide activities rather than concentrations of chemical species (Skoog and Leary, 1998). Several electrochemical methods including conductimetric, potentiometric, and amperometric/voltammetric types are used to quantify dissolved chemical species,

providing information about geochemical and microbial processes occurring in a natural environment (Taillefert et al., 2000; Luther et al., 2005).

Conductimetric methods can be useful in determining how well certain solutions conduct electrical current. Conductimetry uses two platinum electrodes of opposite polarities that are rapidly switched between positive and negative (up to 1000 times per second) to measure the resistance of the solution (Rubinson and Rubinson, 2000). Commercially available examples of conductimetric type electrodes provide the resistance measurement to a hand held computer unit that calculates the conductance or specific conductance and are used widely in monitoring environmental contamination for a general estimate of the number of ions in a solution.

Potentiometric type electrodes measure the potential through an electrochemical cell consisting of a working and reference electrode (Luther et al., 2005). The potential measured when passing a near zero current through the electrochemical cell is proportional, through the use of the Nernst equation, to the concentration of the analyte in solution (Luther et al., 2005; Rubinson and Rubinson, 2000; Skoog and Leary, 1998). Potentiometric type electrodes include the carbon dioxide electrode (Cai and Reimers, 1993; 1995), the Ag/Ag_2S electrode for determining S^{2-} (Visscher et al., 1991;Gundersen et al., 1992; Eckert and Truper, 1993), and the commonly used pH electrode (Archer et al., 1989; Cai and Reimers, 1993; 1995; deBeer et al., 1997). Potentiometric microelectrodes have also been designed to measure nitrate, nitrite, and ammonium, with detection limits of 10 μM in freshwater environments (deBeer and Vandenheuvel, 1988; Sweerts and deBeer, 1989; Jensen et al., 1993; deBeer et al., 1997). Trace copper (Cu^{2+})

concentrations can also be determined by potentiometric stripping through the use of a three-electrode system with a gold working electrode (Wang et al., 1995). Potentiometric electrodes are ideal when measuring one analyte in a solution and are highly specialized for that particular analyte (Rubinson and Rubinson, 2000).

Amperometry measures the current that passes through a solution to cause oxidation or reduction of an analyte (Rubinson and Rubinson, 2000). The current measured, the limiting current (i_L), is linearly proportional to the concentration of the chemical species being oxidized or reduced at the working electrode (Rubinson and Rubinson, 2000). The concentration of an electroactive chemical species is related to the limiting current through a constant:

i_L = constant * concentration of analyte;

where the constant can be determined through the use of standards, and the constant may change over large concentration ranges. The current measured in amperometric techniques can either be measured at a fixed potential or as a function of a changing potential (Rubinson and Rubinson, 2000). Amperometric *in situ* sensors include the oxygen electrode, or Clark electrode (Hitchman, 1978; Gnaiger and Forstner, 1983), and have been used to measure oxygen in the water column, in sediment porewaters, and in microbial mats (Kester, 1975; Gnaiger and Forstner, 1983; Reimers et al., 1986; Reimers, 1987; Archer et al., 1989; Gundersen and Jorgensen, 1990; Gundersen and Jorgensen, 1992; Glud et al., 1994; Millero and Sohn, 1992; Cai and Reimers, 1993; Cai and Reimers, 1995; Tengberg et al., 1995). Amperometric type electrodes also have been designed to measure nitrous oxide (Revsbech et al., 1988) and hydrogen sulfide

(Jeroschewski et al., 1988; Jeroschewski and Braun, 1996; Stuben et al., 1998; Kuhl et al., 1998). Electrodes built to detect nitrous oxide have been used rarely for *in situ* work, can degrade in the presence of excess sulfides, and have interference problems in the presence of elevated CO_2 (Revsbech et al., 1988). However, these electrodes have been adapted recently for the detection of nitrate in marine environments (Larsen et al., 1997) because they don't suffer from the chloride inferences of potentiometric type electrodes (Taillefert et al., 2000). Because oxygen doesn't interfere with the detection of H_2S on hydrogen sulfide amperometric electrodes, they are more useful than Ag/Ag_2S potentiometric electrodes for *in situ* work; however, H_2S amperometric electrodes are sensitive to pH, temperature, and salinity changes, effecting the detection limits for H_2S.

1.4.1 Voltammetric Methods

Voltammetry is comprised of a group of electrochemical methods that provide information about an analyte by measuring the current as a function of applied potential and is obtained under conditions that promote polarization of the working electrode (Skoog and Leary, 1998). Polarization is defined as the change of potential of an electrode from its equilibrium potential upon the application of a current (Electrochemistry Dictonary, 2006). Techniques that vary the potential being applied yield several voltammetric methods including: differential pulse polarography, cyclic voltammetry, square wave voltammetry, and anodic stripping voltammetry. These techniques are used to measure the concentration of electroactive species in solution; where one technique may be more effective than another at detecting a certain chemical

species because of the method differences in sensitivity and signal to noise ratios (Rubinson and Rubinson, 2000).

Voltammetric methods use a three-electrode system consisting of a working electrode, reference electrode, and a counter electrode. The current is measured at the working electrode while the potential is changed over the voltage range of the electrode or microelectrode being used (Luther et al., 2005; Rubinson and Rubinson, 2000). The dimensions of the working electrode are kept small to promote polarization during use (Skoog and Leary, 1998). Reference electrodes are electrodes whose potential remains constant throughout the experiment. To protect the reference electrode from changes in potential, a counter electrode is used to conduct electricity through the solution to the microelectrode and a resistor is used to ensure current leakage does not occur (Skoog and Leary, 1998). The counter electrode measures the background current of a solution so that no current passes through the reference electrode as it is applying a voltage against the working electrode (Luther et al., 2005).

Voltammetric type electrodes are extremely useful because of their ability to scan an entire voltage range and their ability to detect more than one analyte in a solution (Brendel and Luther, 1995). The voltage range that can be applied depends on the overpotential of the electrode or microelectrode being used, and is dependent on both the material the electrode is made of and the electrolyte in the solution being analyzed. The overpotential, or overvoltage, is a measure of the degree of polarization of an electrode, and is equivalent to the difference between the actual electrode potential and the thermodynamic or equilibrium potential (Skoog and Leary, 1998). Metals such as

mercury have a high overpotential for water, allowing electrode potentials to become more negative than the thermodynamic or equilibrium potential for the reduction of water to hydrogen gas (Skoog and Leary, 1998). This allows for the detection of chemical species with more negative electrode potentials than hydrogen to be deposited on the mercury surface without the interference of hydrogen gas production during electrodeposition.

Data obtained through the use of voltammetric methods result in potential vs. current curves, voltammograms, which are analogous to the absorbance vs. wavelength curves obtained in spectroscopy. Specific oxidation or reduction of a chemical species at the working electrode results in a current signal at a specific potential, where the measured current(s) is proportional to the analyte(s) concentration in the solution. Voltammetry is a non-selective method because it provides a better background or zero current than amperometry, and can therefore measure more than one chemical species at a given time in the same location (Luther et al., 2005).

1.4.2 Signals in Voltammetry

Voltammetry uses four major types of excitation signals in order to vary the potential: linear scan, differential pulse, square wave, and triangular (Figure 1.4.1). Each variable potential excitation signal is applied to the electrochemical cell containing a microelectrode over time and induces a characteristic current response (Skoog and Leary, 1998). Linear and triangular excitation signals vary the potential applied to the working electrode linearly over time (Figure 1.4.1; (a) and (d)).

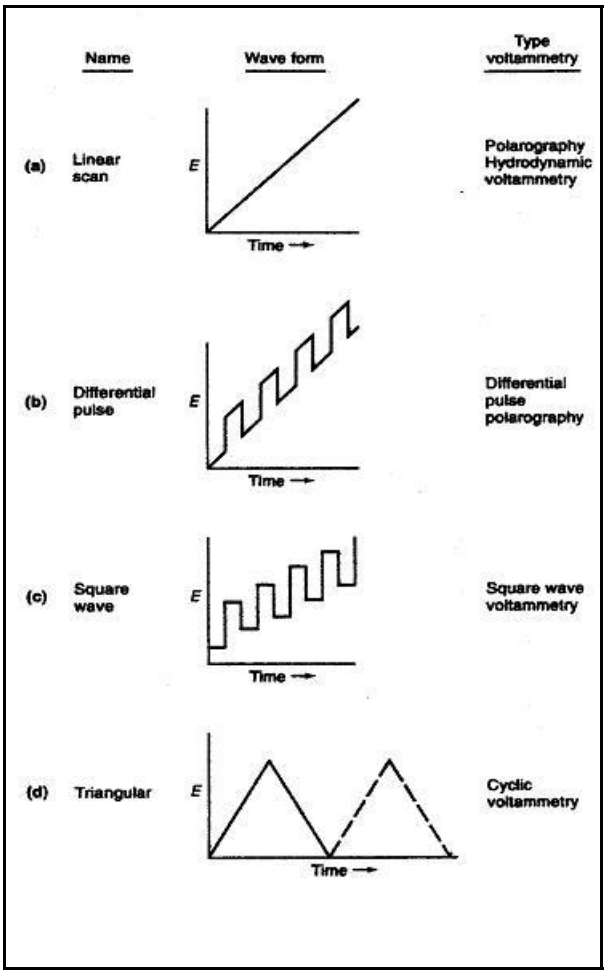

Figure 1.4.1. Four Types of Voltammetric Signals. (From Skoog and Leary., 1998).

When triangular excitation signals are used, we call the voltammetric method cyclic voltammetry. Pulsed voltammetric methods include differential pulse and square wave excitation signals, which vary the potential differently over time (Figure 1.4.1; (b) and (c)) and are of great analytical use because they minimize the interference of capacitive or nonfaradaic currents. A current that is due to electrolysis is a faradaic current and is the useful current in pulsed voltammetric methods. Changing the potential applied to an electrode contributes a second current, called a nonfaradaic current, to the overall observed current, where the total current measured is the sum of the faradaic and

nonfaradaic currents (Rubinson and Rubinson, 2000). As the potential is changed, the electrode must be charged resulting in a nonfaradaic current. Advances in voltammetry have led to improvements in the sensitivity of pulsed voltammetric methods, allowing interfering nonfaradaic currents to be separated from analytically useful faradaic currents (Rubinson and Rubinson, 2000). The manipulation of the voltage applied to the working electrode provides three useful types of voltammetry; cyclic voltammetry, square wave voltammetry, and differential pulse voltammetry.

1.4.3 Cyclic Voltammetry

In cyclic voltammetry (CV), a triangular wave form (Figure 1.4.1; (d)) is used to vary the potential applied to the working electrode linearly in both the forward and reverse direction. Because of the large overpotential of mercury electrodes, CV scans in natural waters are typically run from –0.1V to –1.8V and back to –0.1V (I-F-I scans) so that reversible electrochemical reactions can be detected. The rate at which the potential is changed (voltage/time) is called the scan rate. The potential range used when running a CV scan depends on the type of working electrode and the electrolyte it is in. As the varying potential is applied to the working electrode, the current is recorded. An advantage of CV over linear sweep voltammetry is the ability to determine if an electrochemical reaction is reversible by comparing the forward (cathodic) and reverse (anodic) peak currents and peak potentials. If a reaction is truly reversible the peak separation between the cathodic peak potential and the anodic peak potential will be 0.0592 V/ electron (Kounaves, 1997).

1.4.4 Square Wave Voltammetry

In square wave voltammetry (SWV), the square wave form (Figure 1.4.1; (c)) consists of a symmetrical square wave pulse of the potential applied to the working electrode, where the amplitude and step height can be defined by the user. The result of the staircase waveform is a forward pulse that produces a cathodic current and a reverse pulse that produces an anodic current (Skoog and Leary, 1998). The net current, or resultant current, is the difference between the forward and reverse currents and is centered on the base potential of the wave pulse. Current peak heights, from the resultant current, are directly proportional to the concentration of the electroactive species reduced at the working electrode. Advantages to SWV include its excellent sensitivity, rejection of background currents, and the fast speeds at which scans can be run (Kounaves, 1997; Skoog and Leary, 1998).

1.4.5 Differential Pulse Voltammetry

Differential pulse polarography (DPP) uses the differential pulse excitation signal (Figure 1.4.1; (b)) where a series of small pulses are made to the potential applied to the working electrode. Each potential pulse is fixed, has a small amplitude, and is superimposed on a slowly changing base potential (Kounaves, 1997). In order to separate the faradaic and nonfaradaic currents, the total current is measured twice; once just prior to the voltage pulse providing a baseline current, and once close to the end of the pulse when the nonfaradaic currents have decreased significantly (Rubinson and Rubinson, 2000). The difference between the two currents at each pulse, the resultant current, is determined and centered on the base potential of the pulse. DPP has two major advantages, the ability to separate peaks at similar potentials and excellent sensitivity.

With DPP, individual peaks of chemical species with very similar electropotentials (e.g. differing by as little as 0.04 V to 0.05 V) can be separated and defined (Skoog and Leary, 1998). DPP techniques are also very sensitive because they enhance the faradaic current while decreasing the nonfaradaic charging current (Skoog and Leary, 1998).

1.4.6 Stripping Voltammetry

Stripping voltammetry involves the pre-concentration of an analyte on the surface of the working electrode before running a voltammetric scan. Pre-concentrating an analyte on the surface of the working electrode can be accomplished by applying a potential to the working electrode for a certain amount of time. Certain analytes in solution are able to react with the surface of the electrode forming an amalgam that can then be measured or stripped from the electrode by running a potential scan (CV, SWV, DPP). The amount of time the potential is held during the pre-concentration step, while consistently stirring the solution, directly affects the sensitivity of the electrochemical method, lowering the detection limits of certain analytes.

1.4.7 In Situ Voltammetry

Voltammetric techniques can be applied to environments where redox chemistry needs to be defined *in situ*. The ability to detect and measure multiple chemical species in the same potential scan makes voltammetric techniques useful for investigating redox chemistry. Several electrode systems, based on voltammetric methods, have been designed for *in situ* detection of chemical species of oxygen, sulfur, iron, manganese, iodide, and many trace metals (Tercier-Waeber et al., 1998; Tercier et al., 1998; Herdan et al., 1998; Luther et al., 1998; Luther et al., 1999; Taillefert et al., 2000). Working

electrodes designed for these systems make it possible to detect particular chemical species; however, they are not able to detect metals and redox species important to anaerobic oxidation processes simultaneously (Luther et al., 2005). Development of the solid-state Au-Hg (Au-amalgam) microelectrode (Brendel and Luther, 1995) made it possible to determine both metals (Fe and Mn) and other chemical species (S and O) in the same location at the same time. This electrode system allows for a better understanding of natural redox cycling, yielding real-time *in situ* measurements of the redox chemistry in environments where redox species important to microbial metabolism and geochemical cycling need to be defined.

2.0 GOLD-MERCURY AMALGAM MICROELECTRODE SYSTEM

The need for solid-state microelectrodes arose from a need to define chemical redox species of O_2, H_2S, Fe, and Mn simultaneously; in order to better define microbial oxidation and reduction (Luther et al., 2005). Brendel and Luther (1995) designed a single Au-Hg voltammetric microelectrode that is capable of measuring many of the important redox species simultaneously. The Au-amalgam electrodes that are used to collect redox chemistry information are based on voltammetric methods and generate output scans called voltammograms that show distinct peaks for certain redox species. Based on voltammetric scans, the peak size is proportional to the concentration of a certain analyte (redox species), while the peak location (the voltage at which the peak appears) is based on the overall electropotential of the reaction.

2.1 Voltammetric System

The overall voltammetric system is comprised of a signal source, a potentiostat control circuit, three electrodes, and a recorder and integrator.

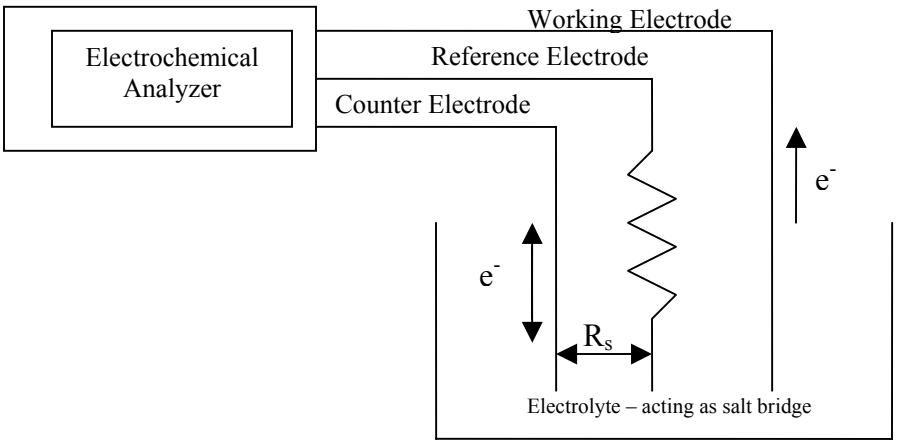

Figure 2.1.1. Schematic of voltammetric type electrode system showing electron flow direction.

The signal source, potentiostat, and control circuit are all part of an electrochemical analyzer that is connected directly to the three electrodes (Figure 2.1.1).

Two electrochemical analyzers are used for laboratory and field data collection; the DLK-60 and the DLK-100, both made by Analytical Instrument Systems, Inc. The electrochemical analyzers are controlled by a computer using Analytical Instrument Systems, Inc. software, that records the output data from voltammetric scans. The three electrodes used for voltammetric analysis are a working electrode, reference electrode, and a counter electrode. The working electrode can be a hanging drop electrode or a solid-state electrode that can be made from several different materials. Voltammograms represent the current response (I) of the working electrode when the potential (E) between the working electrode and the reference electrode is changed over time by one of the voltammetric methods previously discussed.

2.1.1 Signal Source

A linear-scan voltage generator is used for the signal source. The voltage generator is similar to an integration circuit and outputs a potential. The type of voltammetric scan and the selected parameters for the scan (scan rate, amplitude, step size) are input into the computer software. The computer relays this information to the signal source inside the electrochemical analyzer, so that the output potential can be applied accordingly. This output potential is sent to the potentiostat circuit to be used by the microelectrodes.

2.1.2 Potentiostat

The potentiostat is an electronic device that maintains the potential of the working electrode at a constant level relative to the reference electrode. The resistance between the counter electrode and the tip of the reference electrode is known as R_s (Figure 2.1.1). R_u represents the resistance that is not compensated for, which is the resistance between the working electrode and R_s. The background potential of the entire system is maintained at a constant reference potential, such as the potential of the saturated calomel electrode (E_{SCE}). The operational amplifier, inside the potentiostat, works to keep the potential of the reference electrode (E_1) at the constant potential (E_{SCE}) by supplying a current I_c to maintain this condition. If we consider the path between the input and the output, we see that:

$$E_1 = E_{SCE} + I_c R_u. \tag{2.1}$$

In order for E_1 to remain constant, R_u must also remain constant. A change in R_u or R_s would change the operational output voltage. If R_u were to increase, due to an increase in resistance or polarization due to concentration, the operational amplifier would decrease the output voltage, by decreasing I_c. Because the potentiostat is able to maintain a constant background potential, it can then vary the potential applied to the working electrode according to the excitation signal chosen.

2.1.3 Three Electrode System

An amperometric type microelectrode system, based on voltammetric methods, includes a working, a reference, and a counter electrode. At a fixed potential, the current is measured between the working and the reference electrodes. For this thesis work, the working electrode is a small Hg surface that applies a varying potential over time. The

working electrode can either be a hanging mercury drop electrode (HMDE) or a gold-mercury amalgam microelectrode (Au-amalgam). The reference electrode, a Ag/AgCl electrode, acts as an anchor for the system keeping the background potential equal to 0.197 V vs. the standard hydrogen electrode. The counter electrode, a Pt electrode, is used as a shuttle for electrons between it and the working electrode, and the current between the two is measured by the potentiostat. The current measured over time is proportional to the concentration of an analyte in solution. The working potential range for mercury electrodes is 0 to -1.8 V and can be so negative due to the overpotential of water on the Hg surface. For most scans the potential is varied from -0.1 V (or holding potential chosen) to -1.8 V, conditioning the working electrode at -0.1 V for two seconds before running a scan.

2.2 Basic Electrode Reactions

2.2.1 Voltammograms

Voltammograms represent the redox chemistry of a system at the point in time when they were run. They represent the current response (I) of the working electrode when the potential (E) between the working and reference electrodes is changed over time. Figure 2.2.1 summarizes most of the reactions that can occur at the electrode surface, showing the potential (E_p) where a peak will occur on the voltammogram. S-shaped peaks with a maxima that is hard to determine can be reported by their half-wave potential ($E_{1/2}$).

		E_p ($E_{1/2}$) (V)	MDL (μM)
1a)	$O_2 + 2H^+ + 2e^- \rightarrow H_2O_2$	-0.30	5
1b)	$H_2O_2 + 2H^+ + 2e^- \rightarrow H_2O$	-1.2	5
2a)	$HS^- + Hg \rightarrow HgS + H^+ + 2e^-$	adsorption onto Hg	<-0.60
2b)	$HgS + H^+ + 2e^- \leftrightarrow HS^- + Hg$	~ -0.60	<0.1
3a)	$S(0) + Hg \rightarrow HgS$	adsorption onto Hg	<-0.60
3b)	$HgS + H^+ + 2e^- \leftrightarrow HS^- + Hg$	~ -0.60	<0.1
4a)	$Hg + S_x^{2-} \rightarrow HgS_x + 2e^-$	adsorption onto Hg	<-0.60
4b)	$HgS_x + 2e^- \leftrightarrow Hg + S_x^{2-}$	~ -0.60	<0.1
4c)	$S_x^{2-} + x H^+ + (2x-2)e^- \rightarrow x HS^-$	~ -0.60	<0.1
5)	$2 RSH \leftrightarrow Hg(SR)_2 + 2H^+ + 2e^-$	typically more positive than H_2S/HS^-	
6)	$2 S_2O_3^{2-} + Hg \leftrightarrow Hg(S_2O_3)_2^{2-} + 2e^-$	-0.15	10
7)	$2 I^- + Hg \leftrightarrow HgI_2 + 2e^-$	-0.30	<0.1
8)	$FeS + 2e^- + H^+ \rightarrow Fe(Hg) + HS^-$	-1.1	molecular species
9)	$Fe^{2+} + Hg + 2e^- \leftrightarrow Fe(Hg)$	-1.43	10
10)	$Fe^{3+} + e^- \leftrightarrow Fe^{2+}$	-0.2 to -0.9 V	molecular species
11)	$Mn^{2+} + Hg + 2e^- \leftrightarrow Mn(Hg)$	-1.55	5
12)	$Cu^{2+} + Hg + 2e^- \leftrightarrow Cu(Hg)$	-0.18	<0.1
13)	$Pb^{2+} + Hg + 2e^- \leftrightarrow Pb(Hg)$	-0.41	<0.1
14)	$Cd^{2+} + Hg + 2e^- \leftrightarrow Cd(Hg)$	-0.58	<0.1
15)	$Zn^{2+} + Hg + 2e^- \leftrightarrow Zn(Hg)$	-1.02	<0.1
16)	$S_4O_6^{2-} + 2e^- \rightarrow 2 S_2O_3^{2-}$	-0.45	50
17)	$2 HSO_3^- + Hg \leftrightarrow Hg(SO_3)_2^{2-} + 2H^+ + 2e^-$ requires low pH as sulfite (SO_3^{2-}) is not electroactive	-0.50	20

Figure 2.2.1. Electrode reactions at the Au/Hg electrode surface, showing each reactions potential, (E_p), and the minimum detection limit (MDL) for that redox species. (From Luther et al., 2005).

Electrolysis involving the reduction of any analyte species (A) at the mercury surface of the microelectrode gives you a product (B). A solution with an electrolyte, acting as a salt bridge, a known concentration of an analyte, A, and no B gives the half-reaction at the microelectrode:

$$A + ne^- \leftrightarrow B, \tag{2.2}$$

which is a reversible reaction with a standard potential (E^0). The standard potential of a reaction is related to ΔG^0_R (the free energy of reaction) by:

$$E^0 = \Delta G^0_R / -nF, \tag{2.3}$$

where F is Faraday's constant. From equation (2.2), a reaction occurs with an initial concentration (C_A). It is assumed the reaction is completely reversible and rapid enough so that the concentration of A and B in the solution adjacent to the Hg electrode surface are given at any point in time by the Nernst Equation:

$$E_p = E^0_A - (0.0592/n) \log (C_B{}^0/C_A{}^0) - E_{ref}, \quad (2.4)$$

where E_p is the potential between the working and counter electrodes. The concentration does not change over time due to the small size of the electrode surface and the small time interval. Typical E_p values for the Au/Hg electrode are given in Figure 2.2.1.

2.2.2 Example Voltammogram: Oxygen waves on Hg surface

Dissolved oxygen is readily available in any solution exposed to the atmosphere and is readily reduced at the mercury surface. The reduction of dissolved oxygen to peroxide is shown in the half-reaction (2.5) (Figure 2.2.2):

$$O_{2\,(g)} + 2H^+ + 2e^- \leftrightarrow H_2O_2. \quad (2.5)$$

Further reduction of hydrogen peroxide to water occurs, (2.6), as the potential becomes more negative (Figure 2.3.1):

$$H_2O_2 + 2H^+ + 2e^- \leftrightarrow 2\ H_2O. \quad (2.6)$$

The current response from this set of reactions is measured, and through a two-point calibration, the dissolved oxygen in solution can be determined. The presence of oxygen often interferes with the accurate determination of other species, and O_2 is therefore removed from a solution by purging that solution with an inert gas. Lab solutions are purged with argon or nitrogen for four minutes and continually passed over the surface during analysis to prevent the reabsorption of oxygen.

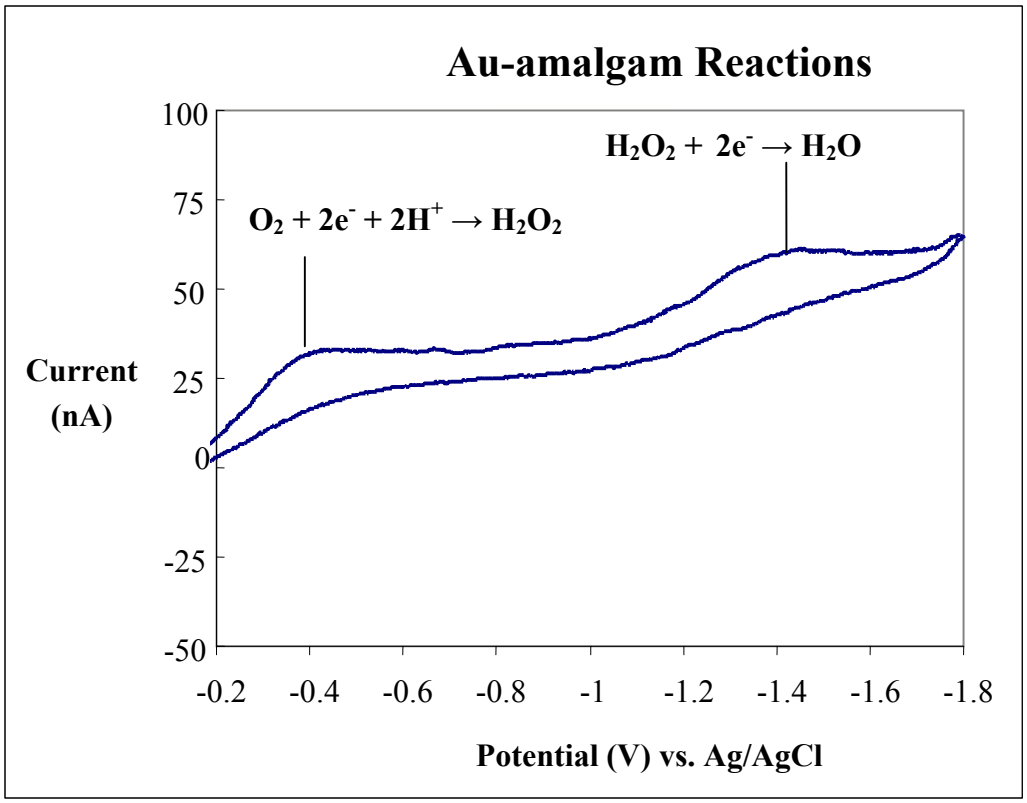

Figure 2.2.2. Oxygen Signal on Au-amalgam microelectrode.

2.3 Microelectrodes

2.3.1 Working Electrode

Two types of solid state working microelectrodes are currently made in our lab; a glass Au-amalgam microelectrode, and a polyethyletherketone (PEEK) Au-amalgam microelectrode. The glass electrode is made to be pushed through biomats and sediments, but is easily broken when rocks or shells are encountered in the sediment. The PEEK electrode is used for surface water work and can be used for hydrothermal work, even at high temperatures (up to 150 °C) (Luther et al., 2005). The dimensions of the working electrode are kept small, enhancing the tendency for the electrode become

polarized. The gold amalgam solid-state electrodes are built as Brendel and Luther (1995) described with some modifications. One advantage of the mercury-gold amalgam microelectrode is its large negative potential range. The Hg electrode has this large range due to the high overvoltage of hydrogen on the Hg. Also, the chemistry at the electrode surface is simplified due to the fact that many metal ions are reversibly reduced to amalgams.

To construct the electrodes, prepare a 3 to 6 foot long copper coaxial cable (Belden RG-174/U Type 50 OHM) by stripping both ends down to the copper wire. To one end connect a BNC or underwater connector, in order to attach the electrode to the electrochemical analyzer. To the other end of the coaxial cable, solder a gold wire (100 μm in diameter) to the copper wire with Ag solder. The gold wire is pushed through either a 4 inch long section of PEEK tubing or the small end of a 6 mm piece of glass tubing that has been pulled on one end to a tip about 0.3 mm in diameter. The inside of the glass/PEEK tubing is filled slowly with epoxy resin (West System brand 105 epoxy resin mixed with 205 hardener) that has been centrifuged at 2000 rev/min for 45 seconds to remove air bubbles after mixing. For the glass electrode, epoxy will slowly fill the tip of the pulled glass; and the Au/Cu soldered junction can be pulled down to the neck of the glass tube. A screw is attached to the gold wire hanging from the bottom of the glass/PEEK tubing to keep the Au wire completely straight and left to set up over night. After the epoxy has dried, the top end of the electrode is coated with Scotchkote, wrapped with Scotchfil electrical putty, and sealed with another coat of Scotchkote to seal the gap between the coaxial cable and glass/PEEK tubing. The bottom end on the

electrode has a protruding gold wire that can be trimmed off. The thin end of the glass electrode can be trimmed to size by scoring the glass with a diamond file and quickly snapping the scored location.

The small electrode surface is polished using sandpaper and diamond polishes. The glass electrode is held by a micromanipulator during the polishing process so that the tip does not break. When the PEEK electrode is polished, it is held by hand. First a 100 grit sandpaper is used to make epoxy and glass or PEEK surfaces even. The electrode is then sanded with 400 grit sandpaper to remove all the major scratches on the electrode surface. Then a series of four diamond polishes (Buehler Metadi Diamond polishing compound) 15, 6, 1, and 0.25 μm are used to give the electrode a perfectly flat, smooth surface.

After the gold wire electrode surface is polished, it is ready to be plated with Hg. The polished electrode is placed in 0.1 M $HgCl_2$ solution with 0.05 N HNO_3 that has been purged with argon for 4 minutes. The gold wire is plated with Hg by reducing Hg^{2+} from solution for four minutes at a potential of -0.1 V. The Au-Hg amalgam is then polarized by attaching the working electrode to the negative terminal and a Pt wire to the positive terminal of a 9 V battery, and placing them both in 1 N NaOH solution for 90 seconds.

2.3.2 Reference Electrode

The reference electrode is also made in the lab with materials similar to the working electrode. A 500 μm diameter silver wire is soldered to a copper coaxial cable with Ag solder. The soldered junction of the Ag/Cu connection is epoxyed inside PEEK tubing so that about 2 inches of Ag is coming out of the PEEK tubing. The extruding Ag

wire is coated with AgCl by placing it in 0.1 M KCl solution and polarizing it for 90 seconds. A 9 V battery is used to polarize the Ag in the chloride solution by attaching a Pt wire in the solution to the negative terminal and the Ag is attached to the positive terminal. A glass frit is placed in shrink tubing and heated to seal around the frit. The shrink tubing is trimmed so that the bottom of the frit is completely exposed. The shrink tubing is then filled with saturated KCl and the Ag wire coated with AgCl is placed in the KCL. The shrink tubing is then heated and wrapped around the PEEK tubing. Scotchkote and Scotchfil need to be applied to the other end of the PEEK tubing in the same fashion as the working electrode to make a water tight seal between the coaxial cable and the PEEK tubing.

2.3.3 Counter Electrode

A solid state Pt counter electrode is made in a similar fashion to the reference electrode. A Pt wire is soldered to a copper wire in a coaxial cable and epoxyed inside a piece of PEEK tubing so that about 2 inches of Pt wire are sticking out at the end. Once epoxy sets, more will need to be added to the end so that the soldered connection is sealed inside the PEEK tubing. Scotchkote and Scotchfil need to be applied to the other end of the PEEK tubing in the same fashion as the working and reference electrodes to make a water tight seal between the coaxial cable and the PEEK tubing.

3.0 *IN SITU* DETECTION OF ARSENITE USING AU-AMALGAM MICROELECTRODES

3.1 Introduction

Arsenic (As) is known to be toxic to humans and is a widespread environmental problem. The World Health Organization (WHO) declared As a carcinogen in 1993, finding cancer widespread among populations exposed to high levels of As (WHO, 1993). The WHO drinking water guideline for As is 0.1 mg/L total As, while the USEPA has set a much lower drinking water standard of 0.01 mg/L total As (WHO, 1993; Federal Register, 2001). Dissolved arsenic in natural waters primarily exists as the oxyanions arsenite [AsO_3^{3-}] and arsenate [AsO_4^{3-}] (McCleskey et al., 2004; Smedley and Kinniburgh, 2002); however, numerous other organic and inorganic dissolved As species do exist (Kumaresan and Riyazuddin, 2001). The redox state of As is of particular interest because arsenite is known to be 10 times more toxic to humans than arsenate (Kumaresan and Riyazuddin, 2001; National Research Council, 1999; Squibb and Fowler, 1983). Arsenic speciation will also affect mobility (Amirbahman et al., 2006) in natural waters; affecting how As will be absorbed to mineral oxides (Arai et al., 2001; Dixit and Hering, 2003; Raven et al., 1998). Arsenic speciation can change due to the presence of other chemical species in solution (McCleskey et al., 2004). It is easily reduced in the presence of hydrogen sulfide and oxidized in the presence of iron and manganese (Cherry et al., 1979). For these reasons there has been much interest in the development of methods for determining As speciation in natural waters.

Mineral oxides, particularly Fe, Mn, and Al oxides, in natural water systems play a pivotal role in the behavior of As (Amirbahman et al., 2006; Inskeep et al., 2004;

McCleskey et al., 2004). Arsenic, both arsenite and arsenate forms, develop strong complexes with mineral oxides, where sorption is dependent on pH (Chui and Hering, 2000; Manning et al., 1997; Raven et al., 1998; Sun and Doner, 1998). In general, As(III) sorption onto mineral oxides occurs at circumneutral pH, while As(V) sorption onto mineral oxides occurs at low pH (Arai et al., 2001; Dixit and Hering, 2003; Raven et al., 1998). Under reducing conditions, sorbed As will be released into solution due to the reductive dissolution of mineral oxides (Cummings et al., 1999; Zorbrist et al., 2000). The photochemical reduction of Fe(III) causes As(III) oxidation (McCleskey et al., 2004). Minerals containing Mn(III) and Mn(IV) will oxidize As(III) (Oscarson et al., 1981; Brannon and Patrick, 1987); however, the absorption of As onto manganese oxides consisting predominantly of Mn(IV) has only been shown to occur for As(V) (Amirbahman et al., 2006; Tani et al., 2004). Changes in environmental conditions and the presence of other redox species can lead to the sorption, release, or oxidation of As in natural environments, effecting the overall As(III)/As(V) ratio.

Microbial activity can influence the As(III)/As(V) ratios in natural waters by significantly influencing redox transformations (Newman et al., 1998; Gihring et al., 2001; Mukhopadhyay et al., 2002; Oremland and Stolz, 2005). As(V) is used as the electron acceptor by prokaryotes for respiration or detoxification, causing As(V) reduction (Donahoe-Christiansen et al., 2004; Gihring et al., 2001; Ji et al., 1983; Oremland and Stolz, 2005). Likewise, organisms can oxidize As(III) to provide a source of energy for growth (Anderson et al., 1992; Donahoe-Christiansen et al., 2004; Gihring et al., 2001; Santini et al., 2000). Microorganisms' ability to oxidize As(III) has been

shown to be slowed down by the presence of sulfide (Donahoe-Christiansen, 2004) and the redox speciation of Fe has been shown to be critical to the oxidation or reduction of As by microorganisms (Inskeep et al., 2004). The ability to detect the redox state of important redox species such as As, Fe, and S in an environment is therefore useful to investigating microbial activity in an environment.

Many analytical techniques for the determination of As have been developed; however, none are able to detect arsenite directly *in situ*. For an excellent critical review of the methods and procedures used for the laboratory detection of As species from many different environmental settings, refer to Francesconi and Kuehnelt (2004). The method by which environmental samples are collected and preserved for analysis of As(III) and As(V) is important; for a comprehensive review of proper methods for sampling and preserving As species, refer to McCleskey et al. (2004). As with all redox-active samples, once the sample is removed from its natural environment, the As(III)/As(V) ratio can change due to oxidation or precipitation (McCleskey et al., 2004). Proper sampling techniques can preserve the As ratio for up to a month; but if these procedures are not followed correctly, the As ratio (easily effected by light, pH, and other chemical species in solution), could change (McCleskey et al., 2004). *In situ* determination of arsenic species allows direct measurement of speciation without the concern for sampling bias.

Voltammetric techniques are a useful tool for making rapid and accurate measurements of redox species at low concentrations *in situ* (Brendel and Luther, 1995; Luther et al., 2001; Taillefert et al., 2000). Voltammetric techniques are based on electrochemical methods in which a potential is applied to an electrode while the current

flowing through the electrochemical cell is monitored. The potential applied is varied over time. Varying the potential can drive redox reactions to occur at the surface of the electrode. Specific redox reactions occur at certain potentials, resulting in increased current flowing through the electrochemical cell. By measuring current amplitude at specific potentials, redox species present can be quantified.

Voltammetric procedures for the direct determination of As(III) using differential pulse polarography (DPP) at a hanging mercury drop electrode (HMDE) have been attempted with some success (Forsburg et al.,1975; Holak, 1980; Myers and Osteryoung, 1973; Sharma, 1995). As(III) has been determined on a HMDE for waste water samples using DPP (Sharma, 1995) and the arsenite peak was found to be linear from 0.01 to 14.00 ppm. Sharma (1995) was the first to determine arsenite in neutral pH solutions and found the reduction of As(III) to occur at –1.1 V.

Arsenite has been determined on a HMDE down to 2 ng/mL and yields a sharp peak using DPP at a potential of –0.72 V in the presence of copper or selenium (Holak, 1980; Sadana, 1983); however, these early experiments were conducted in acid solutions at low pH. In the presence of copper(II) or selenium(IV) the mercury at the surface of the HMDE forms a Cu-Hg or Se-Hg amalgam when held at a negative potential (3.1). The As in solution reacts with the amalgam surface (3.2) creating a [Cu/Se]-As complex at a potential between –0.25 and –0.5 V (Holak, 1980). The metal-As complex is reduced at a more negative potential (3.3), affecting the measured current and allowing for the quantification of As(III).

$$Hg(0) + M^{x+} + (x)e^- \rightarrow HgM. \quad (3.1)$$

$$2As^{3+} + 3MHg + 6e^- \rightarrow M_3As_2 + 3Hg. \quad (3.2)$$

$$M_3As_2 + 3Hg + 12H^+ + 12e^- \rightarrow AsH_3 + H_2 + 3MHg. \quad (3.3)$$

As(III) has been detected in natural water samples, using a HMDE, at low-ppb levels by making an addition of Cu(II) or Se(IV) to the sample (Ferreira and Barros, 2002; Holak, 1980; Hung et al., 2004; Kotoucek et al., 1993; Li and Smart, 1996; Sandana, 1983; Zima and Vandenberg, 1994). The amount of copper or selenium added to the solution affects the size of the arsenite peak, so adding more of the metal will increase the size of the peak and lower the detection limit for As(III). No previous information exists to our knowledge on the effect metals have on arsenite detection at a pH range more likely to be found in natural environments.

Gold-Mercury amalgam (Au-amalgam) voltammetric microelectrodes (Brendel and Luther, 1995) are used as an *in situ* tool for determining S, Mn, Fe, and O redox species in natural solutions, and have the ability to determine more than one of these species at a time (Luther et al., 2001; Taillefert et al., 2000). The application of these electrodes can help determine the redox state of these species directly (*in situ*), providing detailed geochemical speciation of the redox environment in both space and time. The Au-amalgam microelectrode can be an excellent tool for characterizing the redox species in environments where microorganisms live, providing more information on possible oxidation/reduction reactions occurring because of microbial activity, and other geochemical transformations.

In order to interpret data collected by Au-amalgam microelectrodes from the natural environment, we must understand the way As(III) reacts with the Hg surface of the electrode. To do this, we have completed a large set of As addition experiments in

the laboratory. Published experiments on As(III) detection using a HMDE have been redone using the microelectrode system and the results have been compared. We have looked at the effect environmental conditions have on the As(III) voltammetric signal and have optimized the procedure of cyclic voltammatry (CV) for As(III) determination. Laboratory experiments were used to interpret data collected from an As-rich hot spring, Realgar Spring, in Yellowstone National Park, WY.

3.2 Experimental

3.2.1 Instrumentation

A solid-state three electrode voltammetric system consisting of a Au-amalgam solid state working electrode, a platinum wire counter electrode, and a Ag/AgCl reference electrode, was used in tandem with a DLK60 electrochemical analyzer by Analytical Instrument Systems, Inc. The electrochemical analyzer is controlled by a laptop computer that uses Analytical Instrument Systems, Inc. software. This system is extremely portable, running off batteries, and can be used in the field and in the lab.

A hanging mercury drop electrode (HMDE) from Princeton Applied Research attached to a DLK 100 electrochemical analyzer by Analytical Instrument Systems, Inc was used in the lab for comparison studies between the solid-state electrode experiments with published experiments previously done on the HMDE. Reactions occurring at the HMDE are the same as those occurring at the surface of the Au-amalgam electrode; however, the surface area of the HMDE is much larger making it a more sensitive instrument.

3.2.2 Reagents

All chemicals were reagent grade and dissolved in 18.2 MΩ water. As(III) standard: A standard stock solution of arsenite, containing 1000 mg/L As(III), was prepared by dissolving As_2O_3 in a minimum amount of 20% (w/v) NaOH, then quickly acidified to pH 2 with 20% (v/v) sulfuric acid and diluted to 1 L with purged water (after Holak, 1980). As(V) standard: A standard stock solution of arsenate, containing 1000 mg/L As(V), was prepared by dissolving $Na_2HAsO_4 \bullet 7H_2O$ in 1 L of water. Cu(II) standard: A standard stock solution of copper(II), containing 1000 mg/L Cu(II) was prepared by dissolving $CuCl_2 \bullet 2H_2O$ in 1 L of 0.5% HCl. Se(IV) standard: A standard stock solution of selenium(IV), containing 1000 mg/L Se(IV), was prepared by dissolving selenium powder in a minimum volume of nitric acid, evaporating to dryness, adding 3 mL of 18.2 MΩ water, and evaporating to dryness. The addition and evaporation was repeated twice. The residue was dissolved in 10% (v/v) HCl and diluted to 1 L with 10% HCl (after Holak, 1980). Sulfide standard: Stock solution of sulfide was made by rinsing a solid chunk of Sigma sodium sulfide, nonahydrate ($Na_2S \bullet 9H_2O$), with N_2 purged water to remove the oxidized outer layer. The sulfide chunk was then dried and weighed, before being dissolved in N_2 purged water. Thiosulfate Standard: Thiosulfate stock solution was made by adding anhydrous Fisher Brand $Na_2S_2O_3$ to N_2 purged water.

3.2.3 Experiments

All experiments (unless otherwise noted) were run using the solid-state three electrode system described. The experimental conditions presented in this paper are described in Table 3.2.1.

Table 3.2.1. The experimental conditions used for all experiments explained above and the figures presented in this paper.

Experiment Set #	pH	Temperature (C°)	Scan Rate (mV/s)	Media	Arsenite concentration (μM)	Figure #	Notes
1	6.2-6.5	20	1000	0.1M KCl	5-25	Figure 3.3.1	
2	5.5	20	Several	0.1M KCl	10	Figure 3.3.2	Conditioning changed
3	2.2-6.64	20	1000	0.1M KCl	60	Figure 3.3.3	
3	5	20-80	1000	0.1M KCl	30	Figure 3.3.4	
3	2.2-5.7	20	1000	0.1M KCl	60	Figure 3.3.6	
4	2.5	20	1000	0.1M KCl	25	Figure 3.3.7	Cu(II) added
4	6	20	1000	St. Albans Bay Water	10	Figure 3.3.8	10μM Se(IV) added
4	6.6	20	1000	0.1M KCl	4	Figure 3.3.9 (Top)	40μM Sulfide
4	6.7	20	1000	0.1M KCl	1	Figure 3.3.9 (Bottom)	50μM Thiosulfate
5	6.7	20	1000	0.1M KCl	25-100	Figure 3.3.10	
5	6	20	1000	0.1M KCl	0.005-0.075	Figure 3.3.11	
6	3.37	87.1	1000	Realgar Water	?	Figure 3.3.12	
6	Varies	60	1000	Realgar Water	25	Figure 3.3.13 (Bottom)	
6	2.89	Varies	1000	Realgar Water	25	Figure 3.3.13 (Top)	
6	3.37	87.1	1000	Realgar Water	0.125-0.375	Figure 3.3.14	

Initial experiments were performed to define the experimental conditions that optimized the reproducibility of the As(III) peak, shown in Table 3.3.1. Once these optimal conditions were defined, they were used for most of the experiments conducted.

Experiment Set 1: Arsenic Species Detection

As(III) Signal Identification

To determine whether arsenite could be detected by the Au-amalgam microelectrode, 5 μM As(III) additions were made to 0.1 M KCl buffered with PIPES (Piperazine Diethane Sulfonic Acid, $C_8H_{16.5}N_2O_6S_2 \cdot 1.5Na$). First the KCl was purged with nitrogen to remove any oxygen from the solution and to remove the electrochemical oxygen and peroxide signals detected by the Au-amalgam microelectrode. Sequential As(III) additions in 5 μM increments were made to the KCl solution, stirring after each addition. The pH was carefully monitored and adjusted with NaOH to maintain a range between 6.2 and 6.5.

As(V) Signal Detection

Arsenate [As(V)] has been reported as not being electroactive (Sharma, 1995). To test this theory, As(V) additions were made to 0.1 M KCl to determine if a current peak was created. The KCl was purged with nitrogen to remove any oxygen from solution. Sequential 5 μM additions of As(V) were made to the purged solution, stirring after each addition.

Experiment Set 2: Conditioning Steps and Scan Rate

To determine if the conditioning step, scan type, or scan rate has any effect on the As(III) peak, a large matrix of experiments was performed for CV, DPP, and SW scan types at several combinations of conditioning times and scan rates. A solution of 0.1 M KCl at near neutral pH was used for all experiments and was purged with nitrogen to remove any oxygen from solution. Multiple concentrations ranging from 5 nM to 100 μM As(III) were added to the KCl and the pH was adjusted so that it was close to 6. The conditioning steps were changed from no conditioning to conditioning at –0.05, -0.1, -0.2, -0.3, -0.4, and –0.5 V for 2, 10 , and 20 seconds each. Each was done for CV, DPP, and SW signals at scan rates of 100, 500, 1000, and 2000 mV/sec.

Experiment Set 3: pH and Temperature

A matrix of experiments was run to determine how pH and temperature affect the arsenite peak. Temperature was controlled by adding 0.1 M KCl to an insulated vessel attached to a water bath circulating water at a constant temperature. At temperatures of 20 °C, 40 °C, 60 °C, and 80 °C, the KCl was purged with nitrogen; and As(III) was sequentially added to yield a concentration of 0-60 μM. After a concentration of 60 μM As(III) was reached, the pH of the solution was decreased slowly from 7 to 1, by the addition of 0.05 M HCl. A set of 1000 mV/sec CV scans were run and recorded for each of the seven pH values.

Experiment Set 4: As(III) Detection Limitations

As(III) and Cu(II)

A set of experiments was run to determine how Cu(II) can effect the detection of As(III) with the Au-amalgam microelectrode. A solution containing 25 μM As(III) was made by adding As(III) to purged 0.1 M KCl. Sequential additions of Cu(II) where made from a concentration of 1 ppb to 20 ppm Cu(II). Published experiments from: Ferreira and Barros (2002); Hung et al. (2004); Kotoucek et al. (1993); Li and Smart (1996); Sandana (1983); and Zima and Vandenberg (1994) were reproduced so that results would be comparable.

As(III) and Se(IV)

A solution containing 10 μM As(III) was prepared by adding As(III) to a purged water sample collected from the surface of St. Albans Bay in Lake Champlain, VT. Sequential additions of Se(IV) where made from a concentration of 1 ppb to 20 ppm. Experiments following the experimental conditions of Holak (1980) were done for comparison.

$FeS_{(aq)}$ clusters and As(III)

Because aqueous iron-sulfur clusters have a peak potential similar to As(III), a set of experiments was preformed to determine if the peaks interfered with one another. A 0.1 M KCl solution buffered with PIPES to pH 6.8, was purged with nitrogen. 15 μM sulfide and 20 μM Fe^{2+} were added to the solution to create $FeS_{(aq)}$ clusters (after Theberg

and Luther, 1997). To this solution, As(III) was added to determine the voltammetric signal for both species in solution.

Interference of Sulfur Species

The experimental procedure of Rochette et al. (2000) was followed to determine how well the reduction of As(V) by dissolved sulfide could be monitored using the Au-amalgam microelectrodes and to determine if As-S complexes were electroactive (Helz et al., 1995). In addition, a set of experiments were conducted making additions of various sulfur species (sulfide, polysulfide, and thiosulfate) to purged 0.1 M KCl containing As(III). The concentrations of the sulfur species and the arsenite were varied from nM to μM.

Experiment Set 5: Concentration Curves

Additions of As(III) were made to a nitrogen purged 0.1 M KCl pH 6.7 solution at 20 °C to determine if increases in concentration affect the As(III) peak and if the As(III) peak increases linearly with concentration. Both low concentration (1-15 nM) and high concentration (25-100 μM) additions were made and the peak height was determined using CV scans at 1000 mV/sec.

Experiment Set 6: Field Results from Yellowstone National Park

Voltammetric scans were collected from Realgar Spring in Yellowstone National Park in August, 2004. Laboratory experiments controlling the addition of As(III) were preformed on water collected from the spring to determine the effect of pH and temperature on the As(III) electrochemical signal. At the *in situ* pH and temperature of the hot spring, additions of As(III) were made to determine a true matrix-match

calibration curve to define As(III) concentration in the spring. The collected water used for these addition experiments no longer had any As(III) present because it had all oxidized to As(V).

3.3 Results & Discussion

3.3.1 Arsenic Species Detection

As(III) Signal Identification

Arsenic(III) shows a forward cyclic voltammatry (CV) peak in 0.1 M KCl solution at standard lab conditions (25 °C, pH 6, 1000 mV/sec) at a potential E_p of –1.18 V and a $E_{1/2}$ of –0.98 V (Figure 3.3.1).

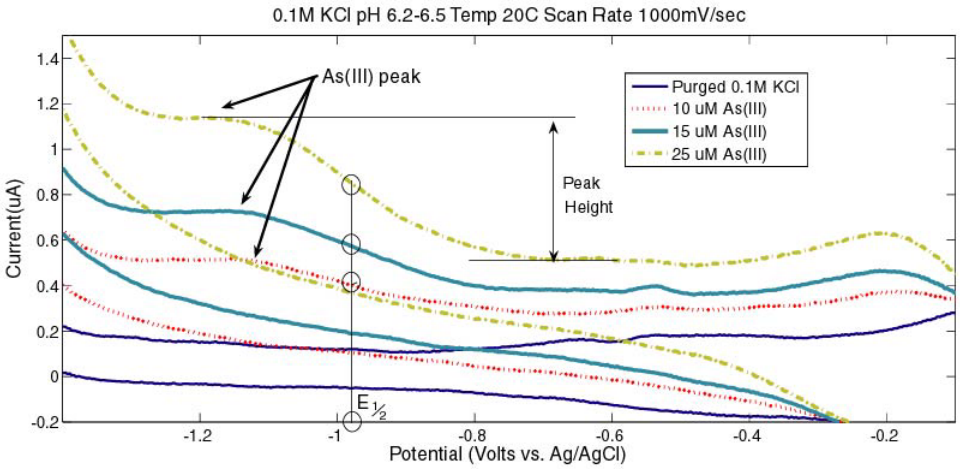

Figure 3.3.1. Peak for As(III) over a range of concentrations in 0.1 M KCl and pH 6 at 20 °C. Scan rate is 1000 mV/sec.

The As(III) peak potential is dependent on the As(III) concentration, scan rate, pH, temperature, and presence of certain chemical species (Cu, Se) in the environment. The Au-amalgam voltammetric signal for arsenite, Figure 3.3.1, has a peak height that is dependent on the concentration of As(III) in the solution being tested. The peak height is

measured as the difference in current from the bottom of the peak to the top of the peak (Figure 3.3.1). $E_{1/2}$ is equal to the inflection points circled in Figure 3.3.1, and the exact potential of each point can be precisely determined using the peak of the first derivative.

As(V) Signal Identification

Arsenate [As(V)], even up to molar concentrations, is not electroactive and therefore cannot be determined using a Au-amalgam microelectrode system. As(V) added to 0.1 M KCl yields a scan that looks identical to purged KCl scans (see the purged signal in Figure 3.3.1).

3.3.2 Voltammetric Conditions and Scan Rate

Voltammetric conditions (conditioning step, scan type, and scan rate) are important in identifying redox species with a microelectrode because they affect the observed peak potential and peak current height for a particular species by affecting the rate of the reaction occurring at the electrode surface. To properly identify the As(III) peak in any natural environment, the voltammetric conditions where the As(III) peak can be identified under changing natural conditions must be determined. This includes optimizing the conditioning step, scan type, and scan rate in laboratory solutions so that the As(III) peak potential and peak height can be reproduced.

A conditioning step is where a potential is applied to the working electrode for a set amount of time before a electrochemical scan is run, at which time plating reactions can concentrate certain species on the surface of the electrode. Changes to the potential and length of the conditioning step do not effect the size of the As(III) peak; proving that the electrochemical reaction occurring at the surface of the electrode is not a plating or

stripping reaction. As(III) is irreversibly reduced at the surface of the electrode, as there is no return signal for arsenite. Changing the starting or ending potential does not effect the As(III) peak; however, limiting the potential range could eliminate the possibility of detecting certain redox species. Cyclic voltammetry, differential pulse polarography, and square wave voltammetry have all been used to determine As(III) with microelectrodes in this study. Cyclic voltammetry is most widely applicable in natural systems for As(III) analysis because the reduction of water to H^+ forms a large peak that will interfere with the As(III) peak at pH less than 5 when SW or DPP scans are run; however, the H^+ peak does not effect the detection of As(III) by CV until the pH becomes less than 2.

Background noise from hydrodynamic turbulence makes slow scan rates less useful for detecting chemical species *in situ* because of a lower signal to noise ratio. To increase the signal to noise ratio, electrodes with a small surface area are used for *in situ* work; however, small electrodes are less sensitive. Faster scan rates increase sensitivity (Rozan et al., 2000); and when combined with small electrodes, As(III) can be determined at low concentrations in turbulent environments. The scan rate affects the As(III) peak potential and the peak size (Figure 3.2.2). Faster scan rates shift the As(III) peak to more negative potentials (500 mV/sec $E_{½}$ = -0.95 V, 1000 mV/sec $E_{½}$ = -0.98 V, 2000 mV/sec $E_{½}$ = -1.01 V) and increase the As(III) peak size (Figure 3.3.2). We have found a scan rate of 1000 mV/sec to be a useful scan rate in many types of environments and in the lab because redox species can still be detected when there is significant turbulence.

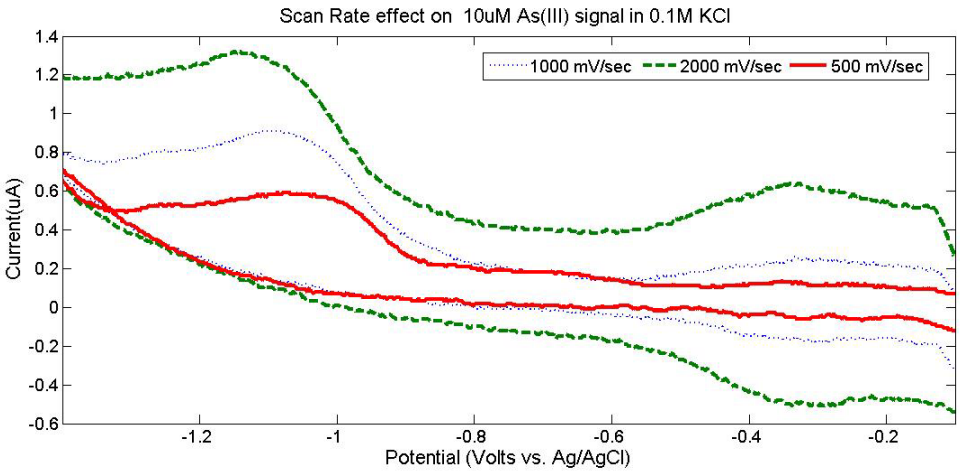

Figure 3.3.2. Voltammogram showing how scan rate (500-2000 mV/sec) changes the peak potential and peak current for As(III). 10 µM As(III) in 0.1 M KCl at pH 5.5 and 20 ºC.

The optimal conditions determined in this study for As(III) analysis are shown in Table 3.3.2. It is important to use the same conditioning step, scan type, scan rate, and potential scan range in the lab as used in the field when calibrating the electrode for data interpretation.

Table 3.3.2. Optimum conditions for As(III) determination using a 100µM Au-amalgam voltammetric microelectrode.

Conditioning Step	-0.05 V for 2 seconds
Scan Potential Range	-0.05 V to –1.80 V
Scan Type	Cyclic Voltammetry
Scan Rate	1000 mV/sec

3.3.3 pH and Temperature

The peak potential and peak current for As(III) are affected by changes in both pH and temperature. As pH increases, the peak potential of As(III) becomes more negative and the peak current decreases (Figure 3.3.3).

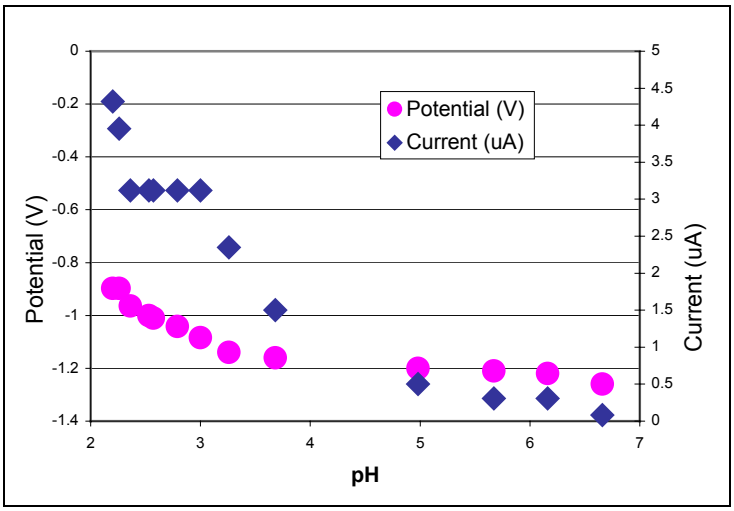

Figure 3.3.3. Changes in the peak current (uA) and peak potential (V) over a range of pH for 60 µM As(III) in 0.1 M KCl at 1000 mV/sec and 20 °C.

As temperature increases, the As(III) peak potential will become more positive and the peak size will become slightly larger (Figure 3.3.4); however, the pH of a solution has a much larger effect on the arsenite peak then does temperature.

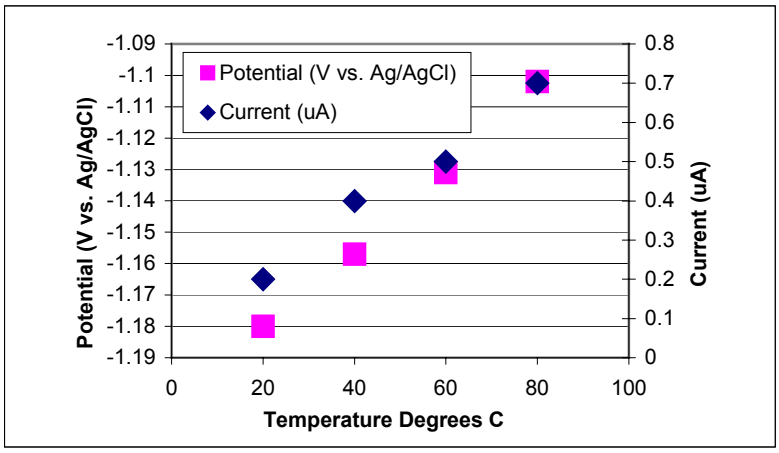

Figure 3.3.4. Temperature (20-80 °C) Affect on As(III) (30 µM) signal in 0.1 M KCl at pH 5, CV 1000 mV/Sec.

The changes in the As(III) peak potential could be a function of some effect at the electrode surface, or due to changes in chemical speciation. Changes in temperature affect the arsenite signal due to the diffusion characteristics around the surface of the

electrode and the temperature dependence of the equilibrium reaction, having a smaller effect then pH on the potential at which a chemical species reacts.

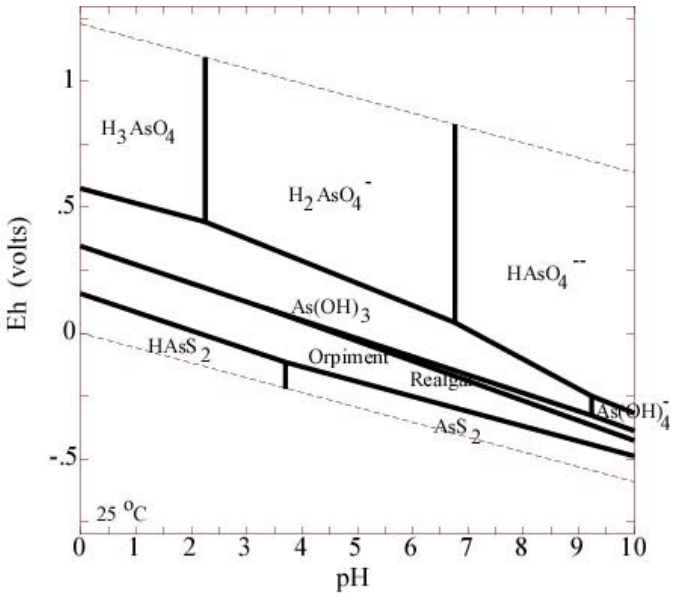

Figure 3.3.5. Eh-pH diagram for As(III) speciation in natural waters at 25 °C.

More significant changes in pH could affect the arsenite signal due to both diffusional changes at the electrode surface and possible chemical speciation changes. A Eh-pH diagram for As at standard state conditions (Figure 3.3.5**)** shows that $As(OH)_3$ is the arsenite species present from pH 0 to 9; however, little is known or published about arsenic speciation at low pH. A Previous study conducted at high pH has suggested that changes in the peak shape and peak position are due As(III)-CO_3^- speciation changes (Kim et al., 2006). At pH 4 there is a major increase in the size of the As(III) signal **(**Figure 3.3.6**)**, suggesting a change in the As(III) speciation. Another change occurs below pH 2.5, where the shape of the arsenite peak changes from an 'S'-shape to a peak shape (Figure 3.3.6).

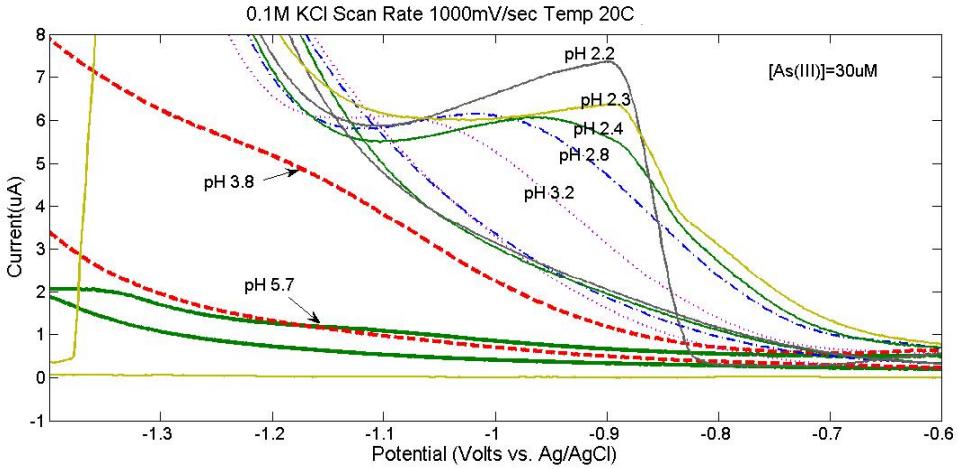

Figure 3.3.6. Changes in the 60 µM As(III) voltammetric signal due to changes in pH. Done in 0.1 M KCl at 20 °C, CV 1000 mV/sec.

These changes in the size and shape of the arsenite peak suggest a speciation change for As chemistry in 0.1 M KCl solution at both pH 4 and 2.5; however, more work needs to be done to show exactly what this speciation change is related to. Neither the changes in the arsenite voltammetric signal due to pH or temperature compromise the use of Au-amalgam microelectrodes as a detection tool. Since the peak current response is much larger and the peak potential becomes more positive at low pH, lower concentrations of As(III) can be detected at lower pH; however, below pH 2, it may not be possible to detect As(III) because the H^+ reduction wave will interfere with the As(III) peak.

3.3.4 As(III) Detection Limitations

Effect of Copper and Selenium on Arsenite Detection

The detection of arsenite by the Au-amalgam microelectrode can be affected by other chemical species in solution. Chemical species of copper and selenium common in natural waters containing reduced arsenic will affect the arsenite peak as well as the chemistry occurring at the surface of the electrode. The As(III) peak potential changes in

the presence of Cu(II) and Se(IV) because the electrochemical reaction occurring at the mercury surface changes (Holak, 1980; Sadana, 1983). Instead of the simple reduction of As(III) at the electrode surface, the Cu(II) or Se(IV) cause a stripping reaction to take place (reactions 3.1-3.3). The metal will form an amalgam with the mercury surface of the electrode, changing the interaction of As(III) with the electrode surface.

Small amounts (1 ppb to 1 ppm) of Cu(II) in solution will change the electrochemical reaction occurring at the electrode surface, changing the electrochemical signal and the peak potential of the As(III) peak, from Ep= -0.94 to –0.89 V (Figure 3.3.7). The resulting positive potential shift with the addition of Cu(II) (Figure 3.3.7) is due to As(III) reacting with the Cu-Hg amalgam instead of the direct reduction of As(III) at the Au-amalgam electrode surface.

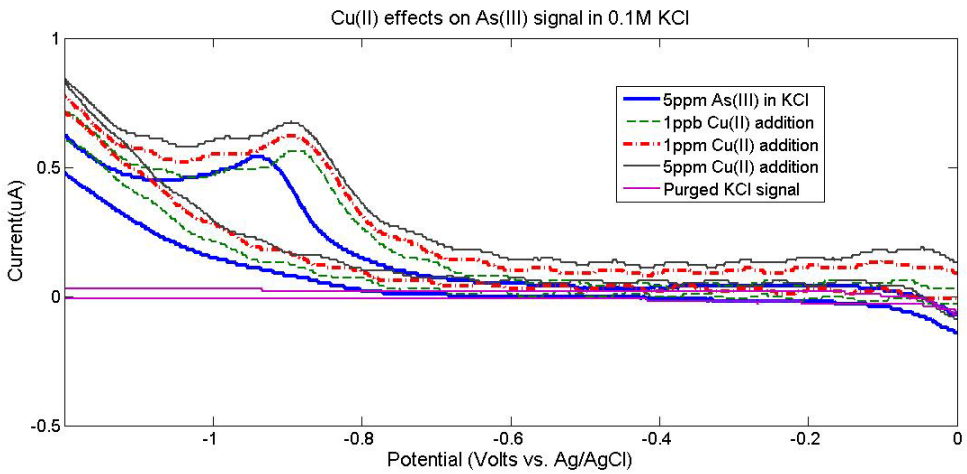

Figure 3.3.7. Effect of Cu(II) on the As(III) electrochemical signal. Done in 0.1 M KCl, 1000 mV/sec, pH 2.5, 20 °C.

Cu(II) in solution at high concentrations, greater than 1ppm, has the same affect as small Cu(II) concentrations except it increases the baseline of the electrochemical scan slightly (Figure 3.3.7). The As(III) peak in the presence of Cu(II) will also shift to more positive peak potentials as the pH decreases (Forsburg, 1975; Sadana, 1983).

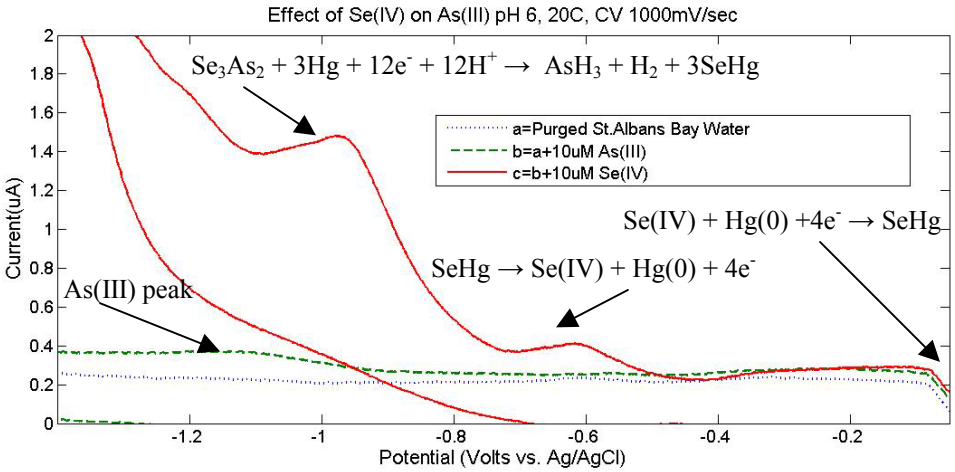

Figure 3.3.8. Effect of Se(IV) on the As(III) electrochemical signal. Done in SAB surface water at pH 6, CV 1000 mV/sec, 20 °C.

Selenium and arsenic in the same solution (Figure 3.3.8) create two peaks when an electrochemical scan is run. The more positive peak represents the reduction of the Se-Hg amalgam formed during the conditioning step. This peak is present when Se(IV) standards are added to the same solution matrix without any arsenic present. The more negative of the two peaks represents the reduction of the As-Se complex (reactions 3.1-3.3). Selenium(IV), just like Cu(II), shifts the As(III) peak to more positive potentials; however, unlike Cu(II), Se(IV) increases the sensitivity significantly, making As(III) quantifiable at even lower concentrations in the presence of Se(IV). Experiments conducted (Ferreira and Barros, 2002; Holak, 1980; Hung et al, 2004; Kotoucek et al, 1993; Li and Smart, 1996; Sandana, 1983; Zima et al., 1994) are consistent with what we have found, but the peak potentials are shifted to more positive potentials due to the lower pH of their experiments. Very acidic solutions (pH <2) that contain selenium or copper will create a quantifiable As(III) peak at a more positive potential and are described by methods already published (Holak, 1980; Li, 1996). Experiments

containing less than 1 ppb Cu(II) or Se(IV) were not conducted; therefore, it is unknown at what concentration these metals change the As(III) peak potential when the electrode is conditioned. The amount of Cu-Hg or Se-Hg that is formed on the electrode surface is dependent on the conditioning time, and if the Cu or Se concentrations are low, a longer conditioning step would be needed.

Interference of Sulfur Species

The Au-Hg amalgam microelectrode is a useful tool because of its ability to determine multiple redox species simultaneously (Druschel et al, 2003; Luther et al., 2005). The sulfur species sulfide and thiosulfate do not interfere with the arsenite voltammetric signal (Figure 3.3.9), making it possible to determine the presence of arsenite and these sulfur species simultaneously. The presence of arsenate (133 μM) and sulfide (266 μM) in solution is known to form thioarsenate complexes up to 100 μM concentrations (Rochette et al., 2000). Addition experiments of sulfide to solutions containing As(V) that produce As-S complexes (after Rochette et al., 2000) didn't form an peak on collected electrochemical signals. Reason may be that thioarsenates are not electrochemically active on the Au-amalgam microelectrode, or because the concentration was below the detection limit for these complexes on the Au-amalgam microelectrode.

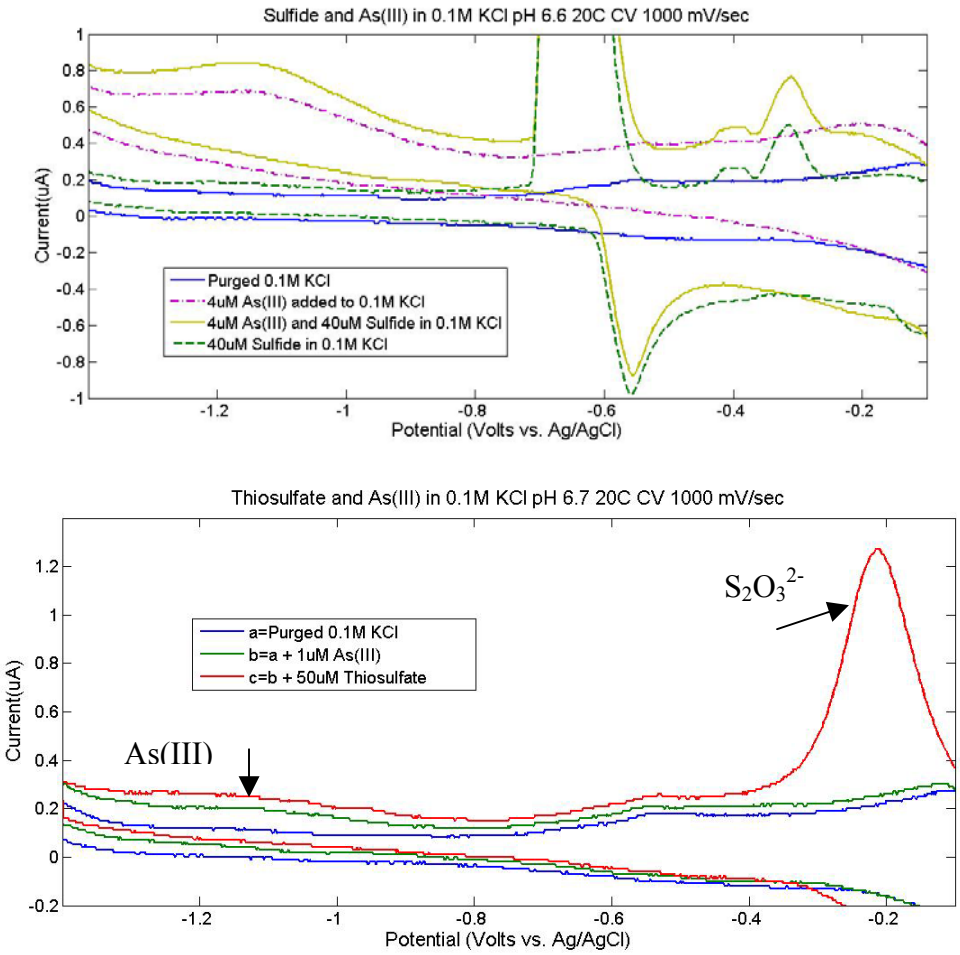

Figure 3.3.9. Top) Sulfide and As(III) may be determined simultaneously on the Au-amalgam microelectrode. Bottom) Thiosulfate and As(III) may be determined simultaneously on the Au-amalgam microelectrode.

Certain sulfur species present at similar peak potentials as As(III) in an environment containing arsenite may interfere with the detection of arsenite by the Au-amalgam microelectrode. Aqueous iron-sulfur clusters are electrochemically active at potentials similar to As(III). The electrochemical signal for $FeS_{(aq)}$ clusters is much larger than the As(III) signal, dwarfing the arsenite signal; however it is possible to differentiate the two signals because the $FeS_{(aq)}$ signal has a return peak that can be used to identify it. Elemental Sulfur dissolved in solution has also been found to have an

electropotential that is very similar to the As(III) electropotential; and its presence may make the quantification of As(III) with Au-amalgam microelectrodes difficult. However, the peak shapes and reactions of S_8 and As(III) are very different and therefore, can be distinguished from one another. Addition experiments of sulfide to solutions containing As(V) (following Rochette et al., 2005), reduced the As(V) to As(III) but did not produce any As-S complexes that are electroactive on the Au-amalgam microelectrode.

3.3.5 Concentration Curves

Concentration curves can be determined in the laboratory to calibrate the electrode to a particular chemical species. The addition of As(III) to 0.1 M KCl at a particular pH and temperature will result in a concentration curve for that particular electrode (Figure 3.3.10).

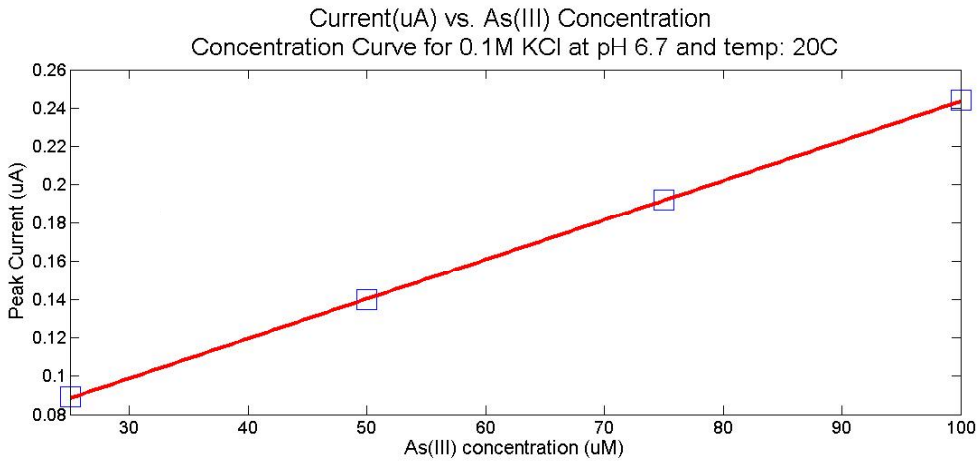

Figure 3.3.10. Concentration curve for As(III) in 0.1 M KCl at pH 6.7 and 20 °C.

The difference in current, the peak current, can then be plotted against the arsenite concentration data (Figure 3.3.10) and a best fit line may be used for this electrode in determining future concentrations of As(III). The concentration curve in Figure 3.3.10 is

valid for determining the concentration of arsenite in 0.1 M KCl at scan rates of 1000 mV/sec, pH 6.7, and 20 °C.

As(III) can be determined at concentrations as low as 5 nM (1 ppb) using the solid-state Au-amalgam microelectrode under standard lab conditions, 20 °C, pH 6, CV 1000 mV/sec (Figure 3.3.11). At low concentrations (5-75 nM) the As(III) peak current increases linearly with increasing arsenite concentration.

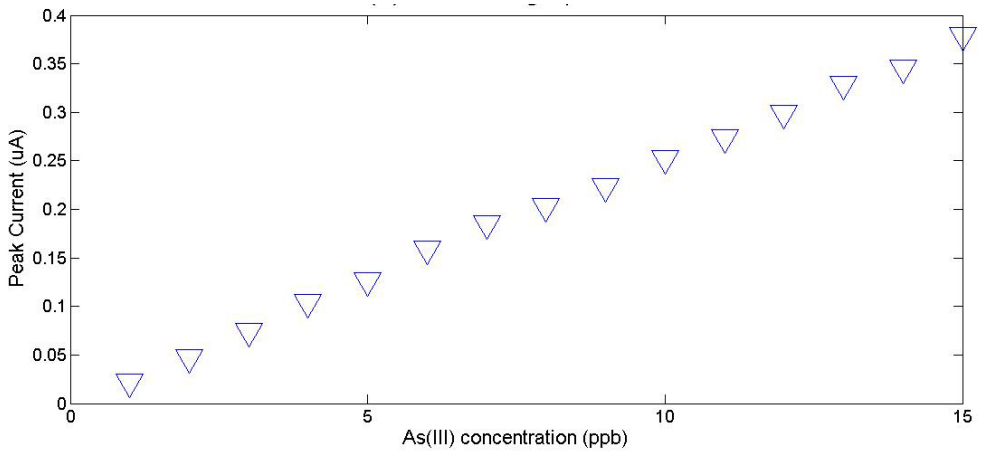

Figure 3.3.11. Low ppb concentrations of As(III) at pH 6, 20 °C, CV 1000 mV/sec in 0.1 M KCl.

At higher As(III) concentrations (> 0.01 μM) the peak current increases linearly and the peak potential will change, moving to more negative potentials with increasing concentration; however, the $E_{½}$ potential stays constant.

3.3.6 Field Results from Yellowstone National Park

Realgar spring (Latitude: 44º44'05.7" Longitude: 110º42'24.3") is an acid sulfate arsenic rich hot spring within Norris Geyser Basin in Yellowstone National Park, Wyoming. In August of 2004, Au-amalgam microelectrodes were placed in the hot spring and its outlet stream, which varied in temperature (61.7-87.1 ºC) and pH (2.87-3.37) with location in the outflow channel.

Table 3.3.2. ICP-OES water analysis of Realgar Spring for selected chemical species

	mg/L		mg/L
Al	0.07	Ni	0.00
As	0.05	Pt	0.00
Ba	0.00	Se	0.00
Co	0.00	Si	1.11
Cr	0.00	Sr	0.00
Cu	0.00	V	0.00
Mn	0.00	Zn	0.00

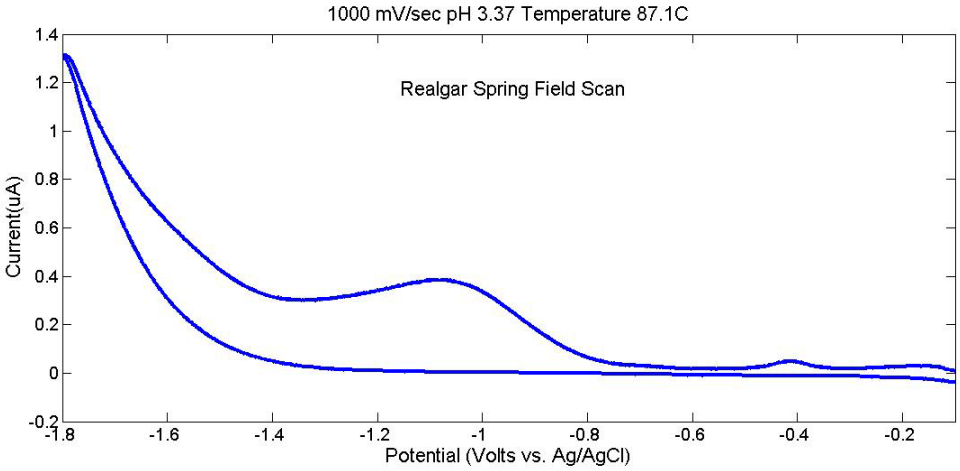

Figure 3.3.12. Field Scan Collected from the outlet of Realgar Spring, YNP, WY.

Voltammetric and environmental conditions were recorded as the electrochemical data were collected (Figure 3.3.12), so that identical conditions might be reproduced in the lab to identify the chemical species and determine its concentration. Since other chemical species can affect the detection of As(III), a sample of the water was collected from the environment where the scans were run and analyzed by ICP-OES to determine selected total element concentrations present in the sample (Table 3.3.2). Cu and Se have been found to exist in Realgar springs in very low quantities (Cu <0.0006 mg/L, Se<0.05 mg/L) from previous studies (Ball et al., 2002) and were not in high enough concentrations to be detected in this study by ICP-OES. The water sample was used to matrix match calibrations in the lab was a filtered, unacidified sample that once used for

calibrations, had no As(III) due to oxidation of As(III) to As(V). Fresh As(III) standards were added to this water sample to determine the As(III) concentration in the hot spring.

The effects of pH and temperature on the As(III) peak in a natural solution collected from Realgar Spring in Yellowstone National Park, WY are shown in Figure 3.3.13. The peak potential and peak current of Realgar Spring water at a constant temperature of 60 °C decrease with increasing pH (Figure 3.3.13, Top). As the temperature increases, the peak potential of As(III) becomes more positive and the peak current increases (Figure 3.3.13, Bottom).

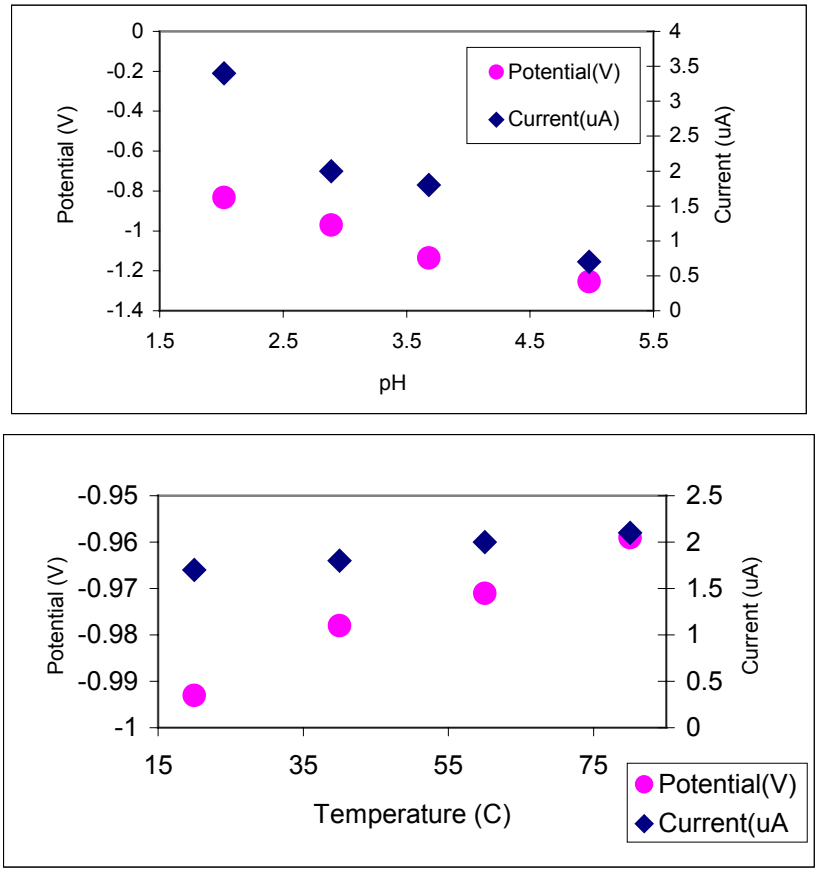

Figure 3.3.13. Changes in the As(III) peak due to pH (Top, temp constant 60 ºC) and temperature (Bottom, pH constant 2.89) in realgar spring water sample with 25 µM As(III).

A similar change is observed in the As(III) peak current in 0.1 M KCl (Figure 3.3.3) as in water collected from Realgar Spring; where in both solutions there is a change in the peak height at pH 4 and pH 2.5. It is interesting that we see evidence suggesting a chemical speciation change of arsenic in both solutions at a very similar pH.

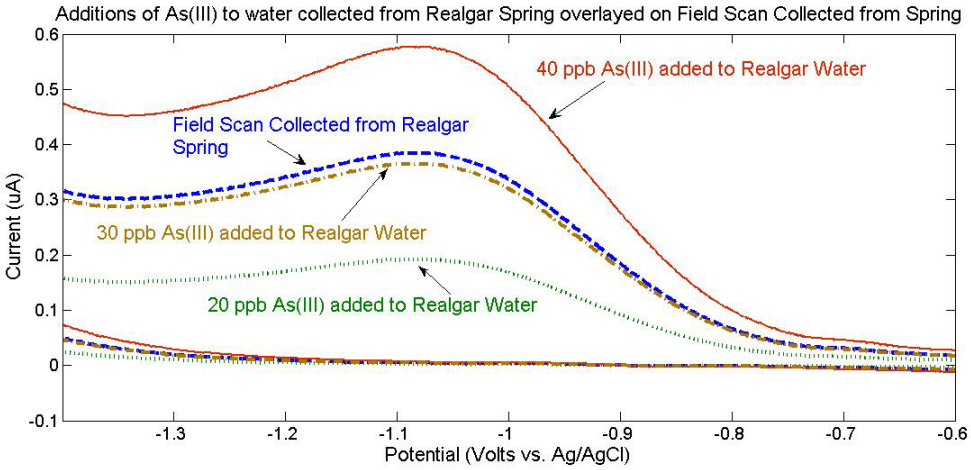

Figure 3.3.14. Overlay of As(III) additions made to Realgar water with a field scan collected from the spring. CV 1000 mV/sec. The additions were made at in situ conditions, 87.1 °C, pH 3.37.

In the lab, using the same electrode that was used in the field, additions of As(III) to purged water collected from Realgar Spring at the field pH and temperature conditions (Figure 3.3.14) yield the concentration of As(III) in the hot spring at the time it was sampled. Lab experiments show that Realgar spring had arsenite concentrations of 0.031 mg/L and a small amount of sulfide present. The addition of the correct amount of As(III) to the water at the *in situ* conditions yields a scan that is almost identical to the field scans collected at Realgar Spring (Figure 3.3.14). Previous results from Realgar Spring (Ball et al., 2002) have reported 0.060 mg/L As(III) and 0.090 mg/L As(total) present in the spring. Our ICP result gave us an As(total) value of 0.05 mg/L. The

difference between As(total) and As(III) equals the concentration of As(V) present in the spring, which was 0.019 mg/L on August 20, 2004.

3.4 Conclusion

Au-amalgam microelectrodes with cyclic voltammetry are a useful tool for determining and quantifying As(III) *in situ*. The ability to determine the redox state of arsenic and other important redox species simultaneously and *in situ*, through the use of a Au-amalgam microelectrode, provides detailed geochemical speciation of the redox environment in both space and time. The Au-amalgam microelectrode proved to be an excellent tool for characterizing the redox species in environments where microorganisms live, providing more information on the possible oxidation/reduction reactions occurring because of microbial activity.

As(III) is the only arsenic species known that can be determined and quantified with the Au-amalgam microelectrode. Arsenite concentrations can be determined by the microelectrode, arsenic total can be determined by an ICP, and arsenate concentrations can be determined by the difference between arsenic total and arsenite. The Au-amalgam microelectrode is the first real-time tool for collecting activities of arsenite *in situ*.

CV scans collected from Realgar Spring in Norris Geyser Basin, Yellowstone National Park, WY provides insight into the arsenite distribution throughout the outlet stream of the spring. The use of the Au-amalgam microelectrodes is helpful in determining how fast As(III) oxidizes in the outlet stream and where arsenite was available to microorganisms for energy. Using microelectrodes as geochemical tools for *in situ* determination of arsenite will prove useful in defining geochemical niches and

microbial environments and may lead to the cultivation of novel microorganisms and a better understanding of microbial physiology.

4.0 *IN SITU* DETECTION OF POLYSULFIDE, ELEMENTAL SULFUR, SULFIDE, AND THIOSULFATE IN YELLOWSTONE NATIONAL PARK'S HOT SPRINGS TO GUIDE MICROBIAL SAMPLING.

4.1 Introduction

Defining an environment in its undisturbed natural state is important to understanding the setting in which microbial communities thrive and may help to understand microbial response to geochemical change. The energy required for microbial life is harnessed through the use of reduced substrates and oxidized electron acceptors, creating coupled half reactions (Amend et al., 2003). Geochemical energy potentially available to microbes in any environment is therefore dependent on these coupled half reactions, where many combinations are possible involving all oxidized or reduced ions in that environment. The oxidation and reduction of sulfur bearing compounds is a widely present energy-yielding process to microorganisms, especially chemolithoautotrophic thermophiles (Amend et al., 2003).

With minimal disruption to the environment, the real-time *in situ* redox chemistry important to microbial metabolism can be defined through the use of Au-amalgam microelectrodes. The Au-amalgam microelectrode can identify many of the redox species (substrates and electron acceptors) involved in the half reactions that provide energy to microbes (Amend and Shock, 2001; Luther et al., 2005). Some redox species within sampled water have a tendency to oxidize or precipitate before analysis is done in the lab, and can be better defined through *in situ* analysis. Redox chemistry data, collected through the use of microelectrodes, and microbial samples can be taken from the same location at the same time. The real-time redox data collected facilitates directed

sampling of microbes from well-defined spatial intervals, describing the geochemical niche they occupy and defining possible metabolic reactions.

Sulfur cycling in natural environments is a complex process due to the transfer of eight electrons between the most reduced and most oxidized forms stable in water, producing many intermediate redox sulfur species (Figure 4.1.1) and sulfur minerals. Sulfur species can be formed by oxidation, reduction, and disproportionation reactions, taking on many intermediate forms (Figure 4.1.1). The ability to analyze multiple sulfur intermediates *in situ* will yield information that could help our understanding of the biotic and abiotic sulfur transformations in natural environments.

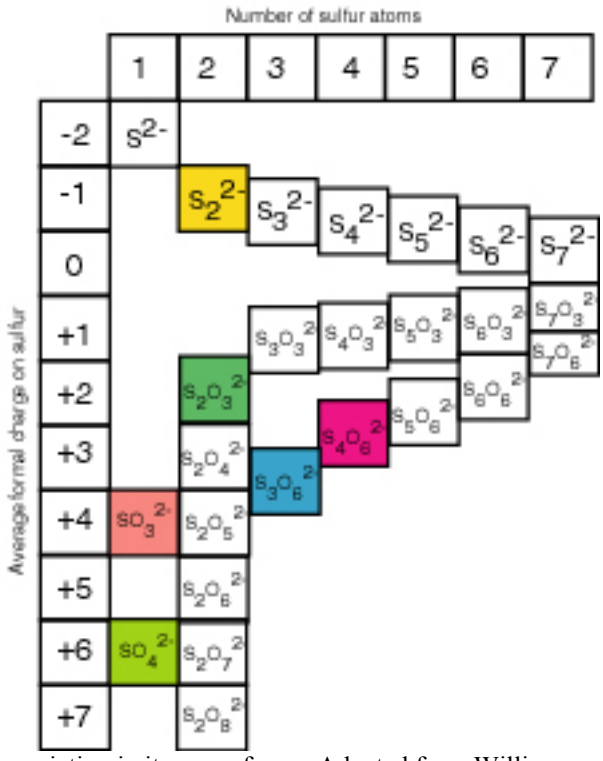

Figure 4.1.1. Sulfur speciation in its many forms. Adapted from Williamson and Rimstidt, 1992.

Reduced chemical sulfur species are often found in marine sediment porewaters (Luther et al., 1985), fresh water lakes (Ginzburg et al., 1999), anoxic groundwaters

containing sulfur bearing hydrocarbons (Sonne and Dasgupta, 1991), and reduced geothermal fluids making up hydrothermal systems (Rozan et al., 2000). Reduced sulfur species are oxidized due to both abiotic and biotic processes (Amend et al., 2003). The rate of the oxidation process is dependent on pH, temperature, the presence of other chemical redox species, and the presence of microbial communities. The abiotic oxidation of sulfide leads to the formation of sulfur, thiosulfate, sulfite, and sulfate through the following reactions:

$$HS^- + \tfrac{1}{2}\, O_2 \rightarrow S^0 + OH^-, \quad (4.1)$$
$$HS^- + O_2 \rightarrow \tfrac{1}{2}\, S_2O_3^{2-} + \tfrac{1}{2}\, H_2O, \quad (4.2)$$
$$HS^- + 3/2\, O_2 \rightarrow SO_3^{2-} + H^+, \quad (4.3)$$
$$HS^- + 2\, O_2 \rightarrow SO_4^{2-} + H^+, \quad (4.4)$$

where the product of the reaction is dependent on the pH and the sulfide/oxygen ratio (Kleinjan et al, 2005a); and the reactions are generally catalyzed by metal ions (Steudel, 2003).

Several microorganisms, including chemoautotrophic bacteria (Burgess et al., 2001; Buisman, 1990), oxidize sulfide to elemental sulfur through aerobic oxidation (4.1) (Kleinjan et al., 2005a,b). Biologically produced sulfur, often referred to as S^0, is different from the mineral of ring molecular form of sulfur and the two should not be confused. S^0 is a widely misused term and generally implies 1/8 S_8, or one sulfur atom at a zero-valence state. If biologically produced sulfur, S^0, is truly one sulfur atom, it will quickly form S_8 rings, which will in turn form sulfur colloids (4.5) (Kleinjan et al., 2005a,b).

$$S_{8(s)} \Leftrightarrow S_{8(dissolved)} \quad (4.5)$$

Sulfur colloids produced from biological activity have been determined to be two size ranges centered at 0.3μm and 1.0 μm (Kleinjan et al., 2005a/b) and are able to remain dissolved in solution because organics dissolve the elemental sulfur in a micellar structure (Janssen et al., 1999; Kleinjan et al., 2003). Inorganic elemental sulfur is extremely hydrophobic and will form from dissolved elemental sulfur joining together if the micellar structure around the colloids is lost (5).

Inorganic polysulfide ions, S_x^{2-}, are important intermediates in the inorganic sulfur system, and are important to the redox reactions involving sulfide, pyritization reactions, metal complexation, and elemental sulfur, playing a vital role in the geochemical and microbial sulfur cycle (Steudel, 2003; Williamson and Rimstidt, 1992). Polysulfide ions can form due to the oxidation of monosulfide ions (4.6), due to the reaction involving monosulfide and elemental sulfur (Wackenroeder solution) (4.7), or due to the reduction of elemental sulfur (4.8) (Steudel, 2003):

$$2HS^- - 2e^- \rightarrow S_2^{2-} + 2H^+, \quad (4.6)$$
$$2HS^- + S_8 \rightarrow 2S_5^{2-} + 5H^+, \quad (4.7)$$
$$\tfrac{1}{2}\, S_8 + 2e^- \leftrightarrow S_4^{2-}. \quad (4.8)$$

The only sulfur redox species that are thermodynamically stable in natural solutions are sulfide, elemental sulfur, and sulfate in the presence of water (Figure 4.1.2); however, it is possible to prepare metastable redox sulfur species, such as polysulfides, in aqueous solutions under conditions where they will not rapidly degrade.

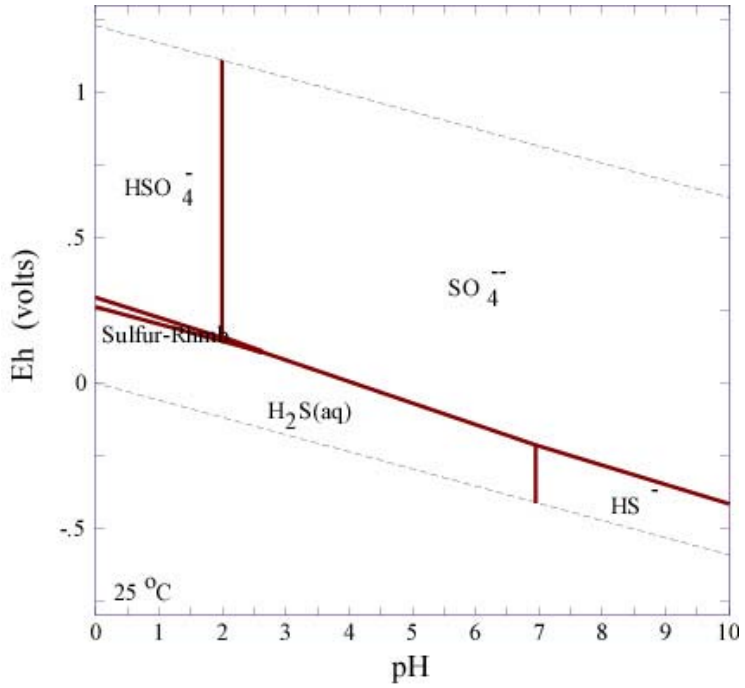

Figure 4.1.2. Eh-pH diagram of aqueous sulfur species in natural solutions at 1 bar pressure and 25 °C.

Polysulfide ions S_x^{2-} can be formed due the reaction of dissolved hydrogen sulfide with either elemental sulfur in its most common form (4.9) or biologically produced sulfur (4.10) (Steudel, 1996; Kleinjan, 2005).

$$HS^- + (x\text{-}1)1/8\ S_8 \leftrightarrow S_x^{2-}, \quad (4.9)$$
$$HS^- + (x\text{-}1)\ S^0 \leftrightarrow S_x^{2-} + H^+. \quad (4.10)$$

Aqueous solutions containing sulfide can dissolve elemental sulfur through the following pathway:

$$S_8 + HS^- + OH^- \leftrightarrow S_9^{2-} + H_2O, \quad (4.11)$$
$$S_9^{2-} + HS^- + OH^- \leftrightarrow 2S_5^{2-} + H_2O, \quad (4.12)$$

where the direction of the pathway is dependent on the pH of the solution. If the pH of a solution containing pentasulfide is lowered below 6, the precipitation of elemental sulfur is expected (Steudel, 2003). The presence of elemental sulfur and polysulfides in a

solution can change the rate of polysulfide formation because polysulfide is present as an auto-catalyst (4.13 and 4.14) (Kleinjan et al., 2005b):

$$S_2^{2-} + S_8 \leftrightarrow S_{10}^{2-}, \quad (4.13)$$
$$S_{10}^{2-} + S_2^{2-} \leftrightarrow 2S_6^{2-} \leftrightarrow S_5^{2-} + S_7^{2-}. \quad (4.14)$$

Kinetic experiments have shown that the presence of polysulfide ions accelerates the dissolution of elemental sulfur (Gerischer, 1949) and that the reaction takes place at the surface of sulfur granules (Hartler et al, 1967). Reactions as stated by equations (4.11) and (4.12) will proceed slower than reactions stated by equations (4.13) and (4.14), if elemental sulfur is dissolved in a solution containing polysulfide (Steudel, 2003). Dissolved elemental sulfur, biologically produced sulfur, would consist of smaller sized particles with a smaller surface area than inorganic sulfur (Janssen et al, 1996; Janssen et al, 1999), speeding up the formation of polysulfide ions (Kleinjan et al., 2005b).

The most thermodynamically stable polysulfide ions, dominant under most environmental conditions, are tetrasulfide (S_4^{2-}) and pentasulfide (S_5^{2-}), and S_n^{2-} ions with n >7 should be neglected (Giggenbach, 1971; Steudel, 2003). Polysulfide ions present in aqueous solutions are of different chain lengths due to their complex equilibrium:

$$2S_4^{2-} \leftrightarrow S_3^{2-} + S_5^{2-}, \quad (4.15)$$
$$2S_5^{2-} \leftrightarrow S_4^{2-} + S_6^{2-}, \quad (4.16)$$

and can be affected by the pH and the presence of elemental sulfur (Steudel, 2003). At neutral and more alkaline pH, S_4^{2-}, S_5^{2-}, and S_6^{2-} ions dominate (Kleinjan, 2005b); while S_2^{2-}, S_3^{2-} have only been found to exist at pH >14 (Gigganbach, 1974). At acidic pH, polysulfide ions are not stable (Kleinjan, 2005b) disproportionating into elemental sulfur

and sulfide. It has also been found that the average chain length of polysulfide ions increases with increasing temperature (Teder, 1971).

Polysulfide ions can be oxidized via chemical and biological processes. The chemical oxidation of polysulfide ions (4.17), leads to the formation of thiosulfate and elemental sulfur (Steudel, 1986; Steudel, 1996):

$$S_x^{2-} + 3/2\ O_2 \rightarrow S_2O_3^{2-} + (x\text{-}2)S^0. \quad (4.17)$$

Although Steudel (1986) reports that no sulfate, sulfite, or polythionate ($S_xO_6^{2-}$) are produced from polysulfide oxidation, other studies have found sulfite and thiosulfate to be the resulting products of polysulfide oxidation (Chen and Morris, 1972; Pasiuk-Bronikowska et al., 1992). The biological oxidation of polysulfide ions has been shown to produce sulfate as the oxidation product of haloalkaliphilic sulfur-oxidizing bacterium (Banciu et al., 2004). Thiosulfate present in environments incurring biotic and abiotic hydrogen sulfide removal processes has been suggested to be produced via chemical oxidation of polysulfide ions (Kleinjan et al., 2005b). It is possible that environments undergoing biological oxidation of polysulfide ions in the absence of chemical polysulfide oxidation would not have any thiosulfate; however, to our knowledge no known microbial metabolic pathway taking polysulfide to other intermediate sulfur species have been documented.

For life to exist in natural environments, the environment's redox geochemistry cannot be in equilibrium. When a geochemical system is out of equilibrium there is a potential for chemical reactions to occur (Shock et al., 2005). Calculating the Gibbs energy of the system, at constant temperature and pressure, can help determine the

potential for chemical reactions to occur. Finding the difference between the real system from its equilibrium state yields quantifiable geochemical energy in the system (Amend et al., 2003; Spear et al. 2004; Shock et al., 2005). Chemoautotrophic microorganisms utilizethis energy, gaining metabolic energy by catalyzing electron transfer reactions (oxidation-reduction reactions) that are thermodynamically favored but kinetically inhibited (Shock et al., 2005). Microorganisms are able to avoid kinetic barriers by providing an alternative pathway for the reaction, through the catalytic action of enzymes (Shock et al, 2005). The elements hydrogen, oxygen, nitrogen, carbon, sulfur, iron, and manganese are essential to life and most of the electron transfer reactions the support life involve these elements (Amend and Shock, 2001).

In order to properly describe the geochemical speciation of any important redox species involved in providing metabolic energy, a complete geochemical data set needs to be obtained. Defining an environment's *in situ* redox chemistry will better describe the environment's geochemistry and can allow for the calculation of geochemical energy available from chemical reactions that have previously been overlooked. The geochemical energy in hot spring environments has been determined for many chemical reactions including reactions involving hydrogen, sulfide, sulfate, thiosulfate, and elemental sulfur (Amend et al., 2003; Spear et al., 2005; Shock et al., 2005); however, reactions involving other intermediate sulfur species, particularly polysulfides, have not been determined.

Voltammetric Au-amalgam microelectrodes can be used to determine chemical redox species of sulfur, oxygen, manganese, iron, and arsenic, and have been used in the

past to distinguish sulfide, polysulfide, thiosulfate, and tetrathionate (Wang and Ariel, 1978; Wang and Greene, 1983; Herdan et al, 1998; Rozan et al., 2000; Taillefert et al., 2000; Druschel et al., 2003, 2004; Luther et al., 2005). Real-time *in situ* data collection of redox chemistry can help in determining potential redox reactions taking place, which will provide data necessary for defining sources of energy for microbial metabolism, and help to define small-scale redox gradients important for describing geochemical niches where specific microbial communities inhabit common space and compete or synergistally utilize resources. The ability to define the *in situ* geochemical redox speciation allows for culturing of microorganisms removed from a particular environment with substrates and electron donors known to exist in that environment. Inoculating cultures with the redox species known to exist in a microorganisms' natural environment, could lead to culturing of novel organisms from these environments.

Previous studies to define electrochemical signals for intermediate sulfur species have been conducted in both saline and freshwater environments where pH and temperature are constant (Rozan et al., 2000; Kariuki et al., 2001; Druschel et al., 2003; Luther et al., 2005). However, the effects of changes in pH and temperature on these electrochemical signals have not previously been defined. Polysulfides (S_4^{2-},S_5^{2-}) have been determined using voltammetric electrodes and these studies have shown that the scan rate used impacts the size and peak potential of the polysulfide peak, becoming more negative and larger as the scan rate increases (Rozan et al., 2000; Kariuki et al, 2001).

In August, 2004 three acid sulfate hot springs; Cinder Pool, Evening Primrose Spring, and a small hot spring in Gibbon geyser basin that we will call "Mini-Primrose", were visited in Yellowstone National Park (YNP). At each location the *in situ* redox speciation was determined while simultaneously collecting microbial and water samples. The hot springs offer sulfide rich environments that include ample amounts of elemental sulfur, making them an ideal environment to study the formation of polysulfides. To determine the activity of intermediate sulfur species found in YNP's hot springs, detailed lab experiments have been carried out to confirm and quantify these signals, associated with these intermediates. This study documents the effect that pH and temperature have on the electrochemical signal for intermediate sulfur species over the range of pH and temperature observed in YNP's hydrothermal waters. This information can be used to define the potential energy available to microorganisms in their natural environment and help in determining new culturing techniques to select for different microbial communities and eventually guide culturing practices to isolate previously uncultured organisms.

4.2 Experimental

4.2.1 Instrumentation

A solid-state three electrode voltammetric system consisting of a Au-amalgam solid state working electrode, a platinum wire counter electrode, and a Ag/AgCl reference electrode, was used in tandem with a DLK60 electrochemical analyzer by Analytical Instrument Systems, Inc. The electrochemical analyzer is controlled by a laptop computer

that uses Analytical Instrument Systems, Inc. software. This system is extremely portable, running off batteries, and is used in the field and in the lab.

After prolonged exposure to high temperatures in Yellowstone's hot springs, the epoxy used to build the working electrode irreversibly expanded, rendering the electrode useless after it was removed from the hot spring. Recent advances in the construction of the working electrode have lead to an electrode made of PEEK completely surrounding a gold wire. Because the coefficient of thermal expansion is very similar for PEEK material and gold, these working electrodes should be good after being placed in high temperature environments.

4.2.2 Sampling

The simultaneous collection of electrochemical data, water samples, and microbial samples was accomplished through the use of a sampling tube attached to the working electrode. A peristaltic pump was connected to the sample tubing to draw the water and microbial samples from the environment. The working electrode and sampling tube were zip tied to a rope and run through rigging on a pole so that they could be suspended in the hot springs away from the side of the pool (Figure 4.2.1).

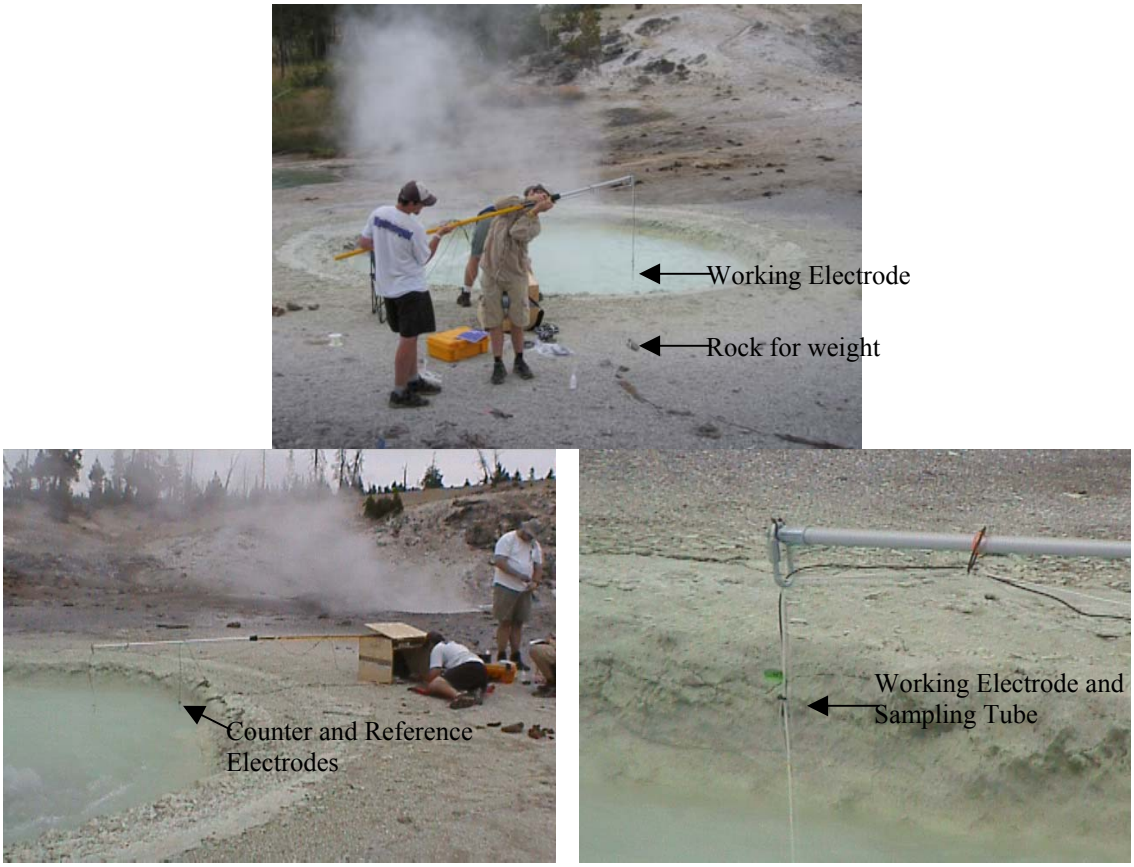

Figure 4.2.1. Top) Pole rig with weight (rock) before being placed in hot spring. Bottom Left) Sampling setup at Yellowstone National Park. Bottom Right) Working Electrode, sampling tube, and rope holding weight through end of pole rig before being dropped into hot spring.

A rock, found close to the hot springs, was tied to the end of the rope for weight and was suspended one foot below the working electrode (Figure 4.2.1). The distance between the working electrode surface and the sampling tube was minimized so that the geochemical redox chemistry defined by the electrode was representative of the water and microbial sample environment. The counter and reference electrodes were suspended from the side of the hot springs. The pole rig was attached to a large wooden box, that also acted as shade and protection for the computer, electrochemical analyzer, and batteries.

Parameters collected at the time of geochemical data collection and microbial sampling include pH, temperature, and conductivity. Field parameters are important to the proper calibration of microelectrodes and were thus recorded in the field. The pH, temperature, and conductivity of the *in situ* environment were measured using a Fisher Scientific Accumet AP85 pH/Conductivity/TDS/ºC/ºF meter. The conductivity of an aqueous solution is measured by the Accumet electrode, and the measurement is based of conductimetric methods. The conductivity and pH electrodes must be calibrated often to retrieve accurate measurements, and were thus calibrated before every use.

An Induced Coupled Plasma Optical Emission Spectrometer (ICP-OES) was used to define basic cations and selected ions in the water collected from the studied hot springs. Water samples collected from Yellowstone's hot springs were filtered in the field and acidified in the lab with nitric acid before being run on the ICP-OES.

4.2.3 Reagents

All chemicals were reagent grade and made using 18.2 MΩ water. The potassium chloride (KCl) used was made by Fluka.

Sulfide and Thiosulfate

Stock solution of sulfide was made by rinsing a solid chunk of Sigma sodium sulfide, nonahydrate ($Na_2S \bullet 9H_2O$), with N_2 purged water to remove the oxidized outer layer. The sulfide chunk was then dried and weighed, before being dissolved in N_2 purged water. Thiosulfate stock solution was made by adding anhydrous Fisher Brand $Na_2S_2O_3$ to N_2 purged water.

Elemental Sulfur

Elemental Sulfur standards were made by dissolving Fisher Brand precipitated sulfur in solutions containing Alfa Aesca soduim n-dodecyl sulfate (SDS) and Alfa Aesca n-hexadecyltrimethylammonium bromide (CTAB) as surfactants to drive micellar S_8 to form, making the elemental sulfur soluble. The procedure for dissolving the elemental sulfur was taken from Steudel and Holdt, 1988.

Polysulfide

To prepare polycrystalline pure polysulfide salts $Na_2S_2^{2-}$, $Na_2S_4^{2-}$, and $Na_2S_5^{2-}$, the procedure published by Rosen and Tegman (1971) was followed, where the polysulfide salts were prepared by the reaction between Na_2S (anhydrous) and elemental sulfur:

$$Na_2S_{(s)} + nS_{(l)} \rightarrow Na_2S_{n+1(s,l)}. \quad (4.18)$$

Elemental sulfur (Fisher Scientific Precipitated Sulfur) and anhydrous sodium sulfide (Alfa Aesar) were used for these preparations. The elemental sulfur was dried in an oven at 80˚C and placed in a desiccator to remove any water. All preparation and handling of the polysulfide salts were done in a dry glove box because anhydrous sodium sulfide and sodium polysulfides are extremely hydroscopic and very sensitive to oxidation in humid air (Rosen and Tegman, 1971). In order to keep the glove box anoxic and the humidity low, it was filled with oxygen stripped dried N_2 by passing N_2 gas through a Restak catalytic indicatory O_2-stripper and a column filled with dryrite. Oxygen stripping Campy Paks (BD BBL) and humidity sponges (Control Company) were also used inside the glove box to remove any remaining oxygen and humidity. Stoichiometric amounts of

sodium sulfide and elemental sulfur (Table 4.2.1) were weighed and mixed together by grinding, then placed in quartz tubes and sealed.

Table 4.2.1. Stoichometric amounts of Na-sulfide and sulfur needed to make 2.5 g. of polysulfide salts.

Salt	Na_2S	1/8 S_8	Na_2S (g/mol)	S_8 (g/mol)	Amount Na_2S (g)	Amount S_8 (g)
Na_2S_2	1	1	78.04	32.07	1.77	0.73
Na_2S_4	1	3	78.04	96.21	1.12	1.38
Na_2S_5	1	4	78.04	128.28	0.95	1.55

The quartz tubes were evacuated on a vacuum line for 48 hours and sealed for heat treatment. The heat treatment procedure given by Rosen and Tegman (1971) was followed using the following temperatures (Table 4.2.2):

Table 4.2.2. Reaction steps involved in polysulfide synthesis.

Step #	**Reaction Temp (˚C)**	**Reaction Time (hrs)**
1	210	12
2	350	1/2
3	200	10

The first step is a solid-state reaction with 80%-90% conversion, followed by raising the temperature for a short period of time (Step 2) to obtain a homogeneous melt and ensure a complete reaction. Once cool, the polysulfide forms a glass that needs to be removed from the glass tube and crushed at room temperature. It is important that this removal and crushing of the polysulfide be done in a glove box under anoxic and low humidity conditions. The crushed polysulfide is then placed in another glass tube, evacuated, sealed, and tempered at 200˚C (Step 3) to obtain a well-crystallized polysulfide salt.

Polysulfide Standards

Once polysulfide salts $Na_2S_2^{2-}$, $Na_2S_4^{2-}$, and $Na_2S_5^{2-}$ are synthesized, laboratory standards can be made for electrochemical analysis. The polysulfide salts should be kept

in the sealed quartz tubes until standards are ready to be made. All polysulfide standards were made in the oxygen free, low humidity environment of a glove box. This is critical because polysulfide will oxidize in humid air and is subject to oxidation in the presence of molecular oxygen (Steudel, 2003):

$$S_{(4,5)}^{2-} + 3/2O_2 \rightarrow S_2O_3^{2-} + 1/4S_8. \quad (4.19)$$

Inside the glove box, the polysulfide salt is removed from the glass tube, weighed, and added to N_2 purged 18.2 MΩ water. All laboratory polysulfide standards were made fresh daily.

4.2.4 Experiments

Thiosulfate in Natural Solutions

A solution of 0.1 M KCl was purged to remove all oxygen from the solution. To the purged solution, 10 μM additions of thiosulfate stock solution were made. Cyclic voltammetric scans were run at 1000 mV/sec for each addition of thiosulfate.

Sulfide Electrochemical Signal Dependence on pH and Temperature

A solution of 0.1 M KCl was purged with N_2 to remove all oxygen from the solution. 28 μM additions of sulfide stock solution were made to the purged 0.1 M KCl at pH 6 and at 20 °C and 80 °C. Cyclic voltammetric scans were run at 1000 mV/sec.

Water collected from Mini-Primrose pool in YNP (lab pH 2.71) was adjusted with HCl or NaOH to make a set of solutions with pH ranging from 1.99 to 7. Each solution was purged using N_2 to remove all of the oxygen in solution. After purging each solution the pH was measured again and sulfide was added to a concentration of 28 μM. The solution was quickly stirred and a set of CV scans was run at 1000 mV/sec. The

electrode was held at –0.1 V for two seconds before running a scan from –0.1 V to –1.8 V.

Polysulfide Determination by Au-amalgam Microelectrodes

A solution of 0.1 M KCl was purged with N_2 to remove all the oxygen from solution. Polysulfide (S_2^{2-}, S_4^{2-}, S_5^{2-}) stock solutions were used to make standard 23 μM additions of polysulfide to the purged KCl. The conditioning step used for most experiments was –0.1 V for 2 seconds; however, some experiments were conducted in which the conditioning times were changed or no conditioning was applied. Oxidation experiments of polysulfides were conducted to determine the product of polysulfide oxidation with O_2. Oxygen was added to 0.1 M KCl solutions containing 60 μM S_5^{2-} and a small amount of thiosulfate by bubbling air through the solution with an aquarium pump. The solution was then purged with N_2 to remove the oxygen from the solution.

Polysulfide Electrochemical Signal Dependence on pH and Temperature

To determine how the S_5^{2-} signal changes with pH and temperature, a matrix of experiments were conduced changing the pH, temperature, and polysulfide salt. To purged 0.1 M KCl S_2^{2-}, S_4^{2-}, and S_5^{2-}, 20 μM additions were made at pH ranging from 2-7 and temperature ranging from 20-80 °C. Temperatures were kept constant by doing this matrix of experiments in an insulated cell, where water from a water bath was circulated between the walls of the cell.

S_5^{2-} Formation by Reaction between Sulfide and Elemental Sulfur

Thiosulfate (50 μM) was added to 0.1 M KCl solution, acidified with HCl to pH 1. The formation of the elemental sulfur can be seen as a white precipitate that forms when the acid is added to the solution containing thiosulfate (Johnston and McAmish, 1973).

$$S_2O_3^{2-}{}_{(aq)} + 2\ H^+{}_{(aq)} \rightarrow S_{(s)} + SO_{3\ (g)} + H_2O. \qquad (4.20)$$

The solution was then buffered back to pH 5 with NaOH. Sulfide was then added (10 μM) to the solution to create polysulfide ions (reaction 4.7). Electrochemical scans were collected through the entire process using CV scans at 1000 mV/sec, conditioning at –0.1 V for two seconds and running the scans from –0.1 to –1.8 V. Scans were collected continuously until polysulfide ions were no longer being formed.

Elemental Sulfur Electrochemical Signal

To determine the electrochemical signal for elemental sulfur, reagent grade elemental sulfur was dissolved in 0.1 M KCl by using sodium dodecysulfate (SDS) and hexadecyl(trimethyl)ammonium bromide (CTAB) to make an elemental sulfur stock solution (after Steudel and Holdt, 1988). The stock solution includes both dissolved elemental sulfur and colloidal elemental sulfur. Additions of the elemental sulfur solution were made to purged 0.1 M KCl, and both electrochemical data and UV absorption spectra were collected. The KCl/elemental sulfur solution was then filtered through a 0.45 μM filter to determine if the size of the elemental sulfur effects the electrochemical and UV-VIS signals. Electrochemical data and UV absorption spectra were collected for the filtered sample.

Identification of Electrochemical Signals in Yellowstone's Hot Springs

Water sampled from the three Yellowstone hot springs was used as the matrix water for additional laboratory experiments. Additions of polysulfide, sulfide, and thiosulfate were made to purged matrix waters for each hot spring at the pH and temperature reflecting the *in situ* conditions. Electrodes used in the field were eventually destroyed by repeated use in extreme temperatures; therefore, the same electrodes used in the field could not be used for calibration in the lab. Even though this is not the ideal situation, calibration curves for each chemical species in each hot springs sampled water were made at the *in situ* conditions with new solid-state Au-amalgam microelectrodes. Between different electrodes, there is less than 5% error for peak potential and 10% error for peak height of identical calibrations.

Intermediate Sulfur Species and Bioenergetics in Hot Spring Environments

The amount of chemical energy potentially available to microbial communities from a particular redox reaction can be quantified by calculating the Gibbs free energy:

$$\Delta G_r = \Delta G_r^o + RT\ln Q, \tag{21}$$

where, ΔG_r is the free energy change for a particular reaction, ΔG_r^o is the standard Gibbs free energy, R is the gas constant (8.3141 kJ/mol*K), T is the *in situ* temperature in degrees Kelvin, and Q is the activity product of compounds involved in the reaction.

The activity product, Q, was solved for all reactions of interest by:

$$Q = \Pi\, a_i{}^{r}{}_{(products)} / \Pi\, a_i{}^{r}{}_{(reactants)}, \tag{4.22}$$

where, $a_{i\ (products/reactants)}$ is the activity of the *i*th (product/reactant) chemical species involved in the reaction and r is the stoichiometric reaction coefficient for the *i*th chemical species. The activity (a_i) of a particular chemical species was calculated by

$$a_i = \gamma_i \bullet m_i, \tag{4.23}$$

where, m_i is the molar concentration of the particular chemical species and the Debye-Hückel theory is used to solve the activity coefficient (γ) from the molar concentration and the charge of the ion. The activities of all the potential chemical species in solution are solved using PHREEQC Interactive 2.10 for the *in situ* conditions of the environment. The standard Gibbs free energy, ΔG_r^o, is calculated at *in situ* temperature and 1 bar pressure for reaction of interest through:

$$\Delta G_r^o = \Sigma\ r \bullet \Delta G_i^o, \tag{4.24}$$

where, ΔG_i^o is the Gibbs free energy of formation for the *i*th chemical species and r is the stoichiometric reaction coefficient for the *i*th chemical species and is negative for reactants and positive for products. The values of ΔG_r^o were calculated using SUPCRT92 and a custom thermodynamic database including all chemical species of interest at 80 °C (Amend and Shock, 2001).

Microbial Culturing

Methods

Microbial samples collected through the sampling tube were cultured through the following process. Enrichment cultures were made in 125 mL septum bottles by filling the bottle half full of filtered site water (collected through the sampling tube) and half full

of beowolf media. Selected chemical species including: sulfide, thiosulfate, wackenroeder solution (a mix of sulfide and elemental sulfur), and $FeCO_3$ were added to the culture bottles. Cultures were allowed to grow for several months, being transferred to new septum bottles once a month to encourage growth.

DNA Extractions

Community DNA was extracted from a 1 mL sample of the cultures by bead beating, using the UltraClean Microbial DNA isolation kit (MoBio #12224-50). For a complete description of the extraction procedure, refer to Appendix 1.

Polymerase Chain Reaction (PCR)

The extracted environmental DNA is used as a template for the PCR amplification of SSU rRNA genes, 16S for bacteria (Spear et al., 2005). PCR primers used for full-length bacterial rRNA gene sequences in this study include fluorescently tagged 8F (5'AGAGTTTGATCCTGGCTCAG3') and 1492R (5'GGTTACCTTGTTACGACTT3') (Lane, 1991). All PCR reactions were incubated in a thermocycler at 94 ºC for 2 min, followed by 25 cycles at 94 ºC for 30 sec, 47 ºC for 1.5 min, and 72 ºC for 3 min, followed by a single 72 ºC step for 10 min. Each 24 µL PCR reaction contained 2.5 µL 10X Buffer, 0.5 µL DNTP, 0.5 µL of each primer, 0.15 µL Taq, 18.85 µL water, and 1 µL of the extracted DNA template**.** For a more detailed description of the PCR procedure used, refer to Appendix 1.

Terminal Restriction Fragment Length Polymorphism (T-RFLP)

PCR products were cleaned with a PCR Cleanup Kit (Qiagen) before running a restriction digest. PCR products were cut with Alu1, HinP1, and Msp1restriction endonucleases for three hours at 37 ºC, then 20 min at 65 ºC. Each restriction digest reaction contained 2 µL 10X NEB2, 2 µL 0.1% Triton X100, 0.1 µL HinP1, 0.2 µL MSP1, 0.2 µL Alu1, 5.5 µL water, and 10 µL of the PCR product**.**

Terminal-restriction fragment length polymorphism (T-RFLP) was run on all samples to fingerprint the overall microbial community cultured. The T-RFLP results are given as a peak, with an associated height or area, at every size fragment that exists in the sample. Peaks smaller than 100 were neglected and considered to be absent at that size fraction. To compare similarity between two samples, the presence or absence of peaks at particular size fragments are compared between samples. Size fractions were binned visually and samples having a peak within the bin were defined as having a peak present, while samples without a peak present were defined as being absent of a peak. The binned data was used for the analysis of the T-RFLP results. For more detailed information on T-RFLP methods, refer to Appendix 1.

T-RFLP Analysis

The Jaccard Index of compositional similarity is a statistical approach that allows two samples to be compared to one another. The Jaccard Index, JI = J/r, where J is the number of shared species at size fractions where both samples have a shared peak and r is the sum of number of peaks present in sample one and the number of peaks present in sample two minus the number of shared peaks (J).

To compare the T-RFLP results of this study to a database of cultured and uncultured microbial sequences, the tRFLP fragment sorter program was used (Fragsort can be downloaded for free from http://www.oardc.ohio-state.edu/trflpfragsort/). Into Fragsort, a database of microbial T-RFLP sequences that have been cultured with the same specific primer sets and restriction enzymes, must be entered. Microbial Community Analysis III (MICA III) is a database that allows you to extract T-RFLP sequences with specific primer sets and restriction enzymes, that have been cultured by other people. At http://mica.ibest.uidaho.edu/digest.php a MICA database can be created to use with the Fragsort program. Fragsort readsT-RFLP results as a list of the base pair size fragments and the percentage of the total fragments that make up that base pair size. Once this data and the MICA database are input into Fragsort, the program provides the possible microbial sequences that best match the fragments sizes cut by the specified restriction enzymes.

4.3 Results & Discussion

4.3.1 Thiosulfate in Natural Solutions

Thiosulfate has an electrochemical signal that can be detected by the Au-amalgam microelectrode (Figure 4.3.1). The addition of thiosulfate to 0.1 M KCl yields a current peak at a $E_{1/2}$ potential of –0.12 V. This peak potential can change slightly (-0.1 to –0.2 V) from one electrode to another; therefore, it is important to determine the thiosulfate peak potential for individual electrodes. The thiosulfate peak potential is also slightly affected by temperature and change from –0.1 to –0.3 V, as temperature is increased from 20 ºC to 80 ºC.

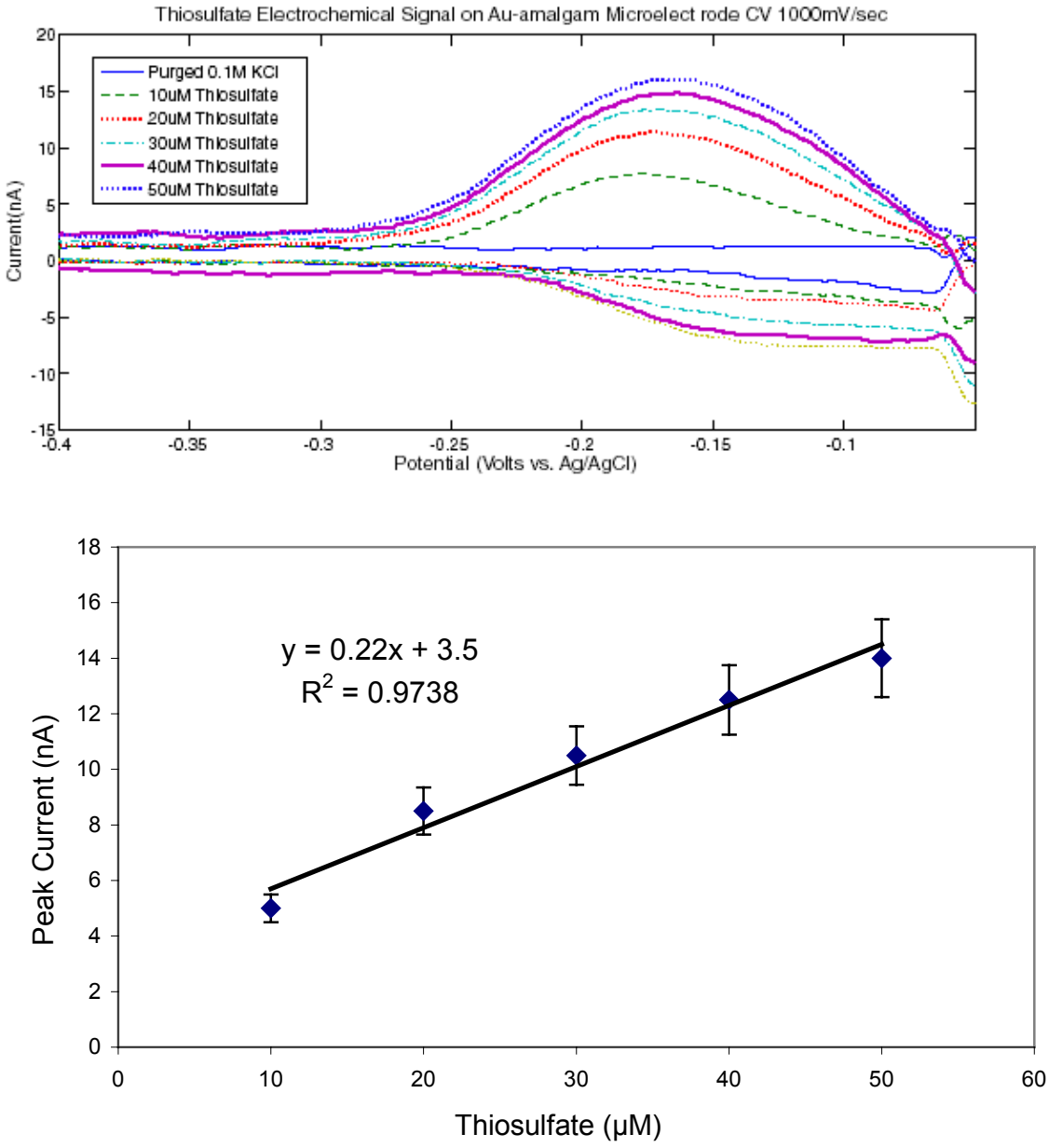

Figure 4.3.1. Top) Thiosulfate voltammetric signal on Au-amalgam microelectrodes in 0.1M KCl at 1000 mV/sec. Bottom) Concentration curve for above additions with 10% error bars.

4.3.2 Sulfide Electrochemical Signal Dependence on pH and Temperature

Sulfide can be detected at nanomolar concentrations in natural solutions using Au-amalgam microelectrodes (Ciglenecki et al., 1996; Rozan et al., 1999; Luther et al., 1990). Research using Au-amalgam microelectrodes for detecting sulfide *in situ* has primarily been conducted in buffered systems like the ocean where pH is constant and does not effect the voltammetric peak (Rozan et al., 2000). Environments such as Yellowstone's hot springs vary significantly in pH (1 to 10) and temperature (29.8 ºC to 93 ºC) from spring to spring (Ball et al., 2002), so understanding the effect pH and temperature have on the sulfide voltammetric peak is important. Aqueous sulfide in solution is preconcentrated on the electrode mercury surface during a conditioning step, using stripping voltammetry techniques, forming HgS at the electrode surface (4.25).

$$Hg(0) + HS^- \rightarrow HgS + 2e^- + H^+. \quad (4.25)$$

This HgS is reduced (4.26) as the forward voltammetric scan is run and a current peak is generated (Figure 4.3.2).

$$HgS + 2e^- + H^+ \rightarrow Hg(0) + HS^-. \quad (4.26)$$

Since this reaction is electrochemically reversible (Rozan et al., 2000), a current peak is also generated when the reverse cyclic voltammetry (CV) scan is run (Figure 4.3.2).

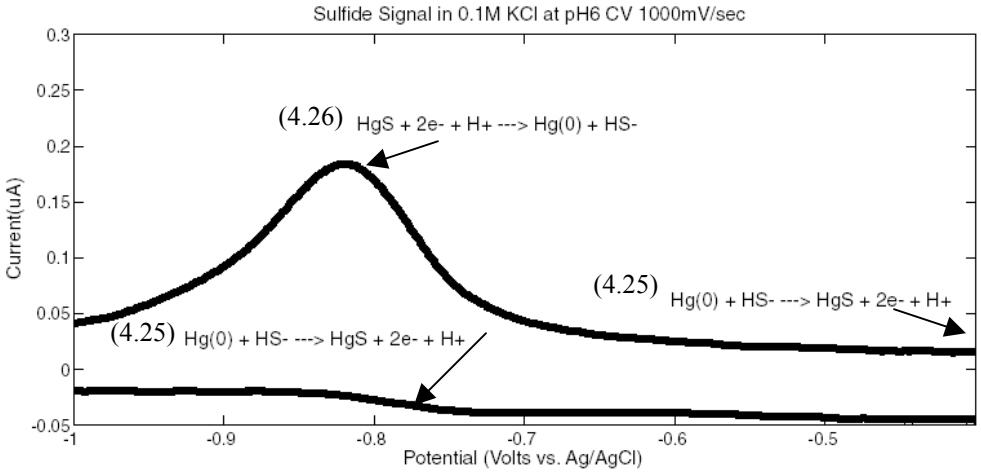

Figure 4.3.2. Sulfide Electrochemical Signal on Au-amalgam microelectrode.

The current peak occurs at a particular potential and is dependent on the pH of the solution (Figure 4.3.3). As pH increases the peak potential for sulfide becomes more negative. The reason the sulfide peak potential shifts with pH could be due to the activity of H^+ ions in solution. At lower pH values the activity of H^+ would be greater, therefore needing a lower potential to drive the stripping reaction (4.26) forward. In water collected from Mini-Primrose hot spring in Yellowstone (Figure 4.3.3), the sulfide peak potential has the trend with respect to pH change:

$$\text{Potential (V)} = -0.07(\text{pH}) - 0.226. \qquad (4.28)$$

This trend can be used as a general reference for most natural solutions. To properly identify the peak potential for sulfide, electrochemical scans collected from the environment must be compared to lab scans of sulfide additions made to water collected from that environment. The pH of the water sample collected may change due to CO_2

degassing and must be buffered back to the field pH in order to properly identify the peak potential of chemical species.

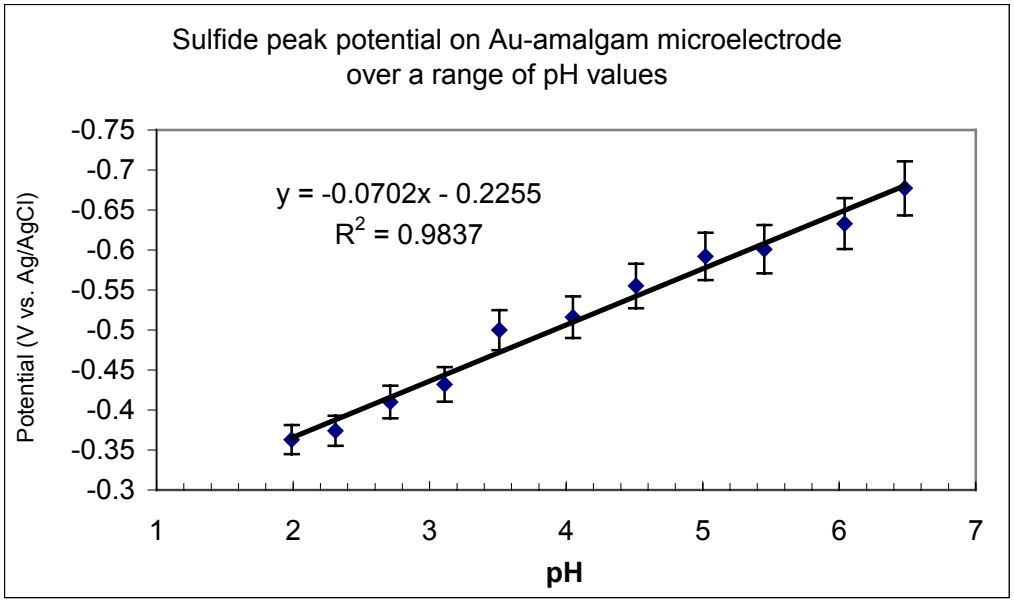

Figure 4.3.3. Sulfide electrochemical signal dependence on pH at 60 ºC from Mini-Primrose hot spring in Yellowstone National Park with 5% error bars.

The sulfide peak potential is also dependent on the temperature of the environment being sampled (Figure 4.3.4). The peak potential, E_p, shifts to more negative potentials with increasing concentration; however, the $E_{1/2}$ potential does not change with concentration (Figure 4.3.4), so assessing how the $E_{1/2}$ changes with temperature for sulfide is appropriate. The reduction of sulfide at the mercury surface will occur at more positive potentials as the temperature increases, changing from $E_{1/2} = -0.78$ at 20 ºC to $E_{1/2} = -0.68$ at 80 ºC. Changes in temperature shift the potential of the sulfide signal due to temperature affects on the diffusion characteristics around the surface of the electrode and have a small effect on the potential at which the chemical species reacts. The temperature shift is much less then the peak shift due to changes in

pH, but is still significant in correctly identifying and quantifying aqueous sulfide. Again, to properly identify the peak potential for sulfide, electrochemical scans collected from the environment must be compared to lab scans of sulfide additions made to water collected from that environment at the *in situ* pH and temperature.

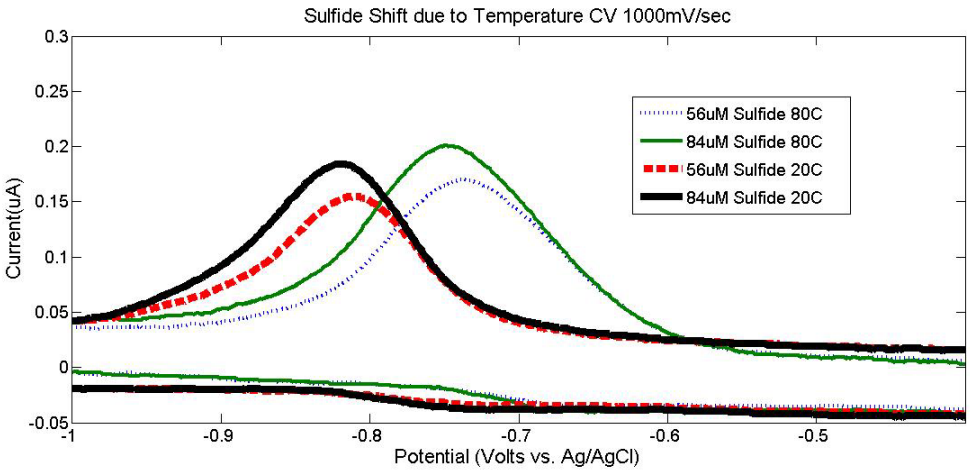

Figure 4.3.4. Sulfide dependence on temperature. Done in 0.1 M KCl at CV 1000 mV/sec.

4.3.3 Elemental Sulfur Electrochemical Signal

Elemental sulfur in natural solutions can be detected with Au-amalgam microelectrodes, but the size of the sulfur particles is critical to detection. To dissolve elemental sulfur in water and determine its electrochemical signal, several organic surfactents were used to dissolve elemental sulfur in a micellar structure (Steudel and Holdt, 1988). Kleinjan et al. (2005b) showed that two sizes of elemental sulfur colloids from biologically produced sulfur exist, a smaller 0.3 µm size and a 1 µm size, while other work has suggested that elemental sulfur is dissolved as an S_8 ring (Steudel and Holdt, 1988). More work needs to be done to determine the size distribution of elemental sulfur that is dissolved in solution; for the purpose of this explanation elemental sulfur

less than 0.45 µm (dissolved or undissolved) is considered small elemental sulfur colloids and dissolved elemental sulfur greater than 0.45 µm is large elemental sulfur colloids. With the aid of sodium dodecysulfate (SDS), dissolved elemental sulfur was able to be detected using Au-amalgam microelectrodes. Elemental sulfur dissolved by SDS yields the two electrochemical peaks (Figure 4.3.5).

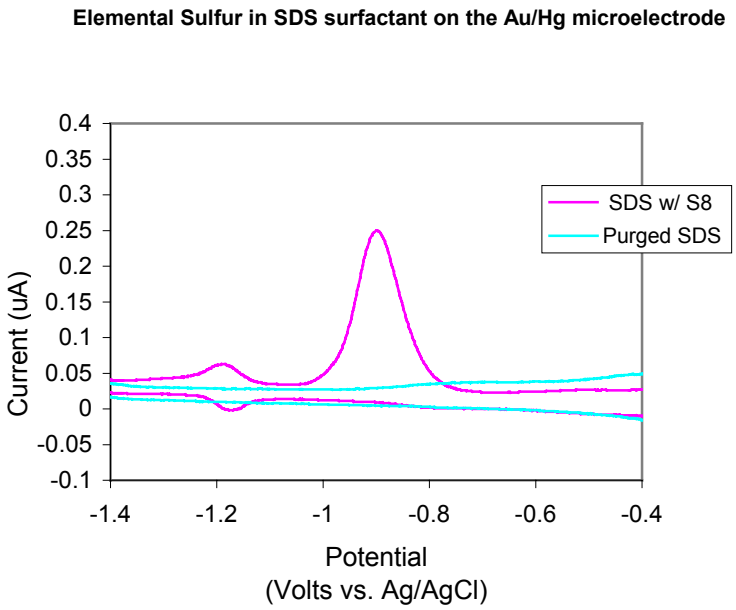

Figure 4.3.5. Elemental Sulfur electrochemical signal.

The more positive peak for elemental sulfur represents larger sized particles of elemental sulfur that can be filtered out with a 0.45µm filter (Figure 4.3.6). The more negative of the two sulfur peaks does decrease slightly when the solution is filtered; however, it is still present after filtration and represents small elemental sulfur colloids that are smaller than 0.45µm. UV-VIS data representing the same filtered and unfiltered samples show a slight change in the spectroscopic signal for elemental sulfur in solution due to filtration (Figure 4.3.7).

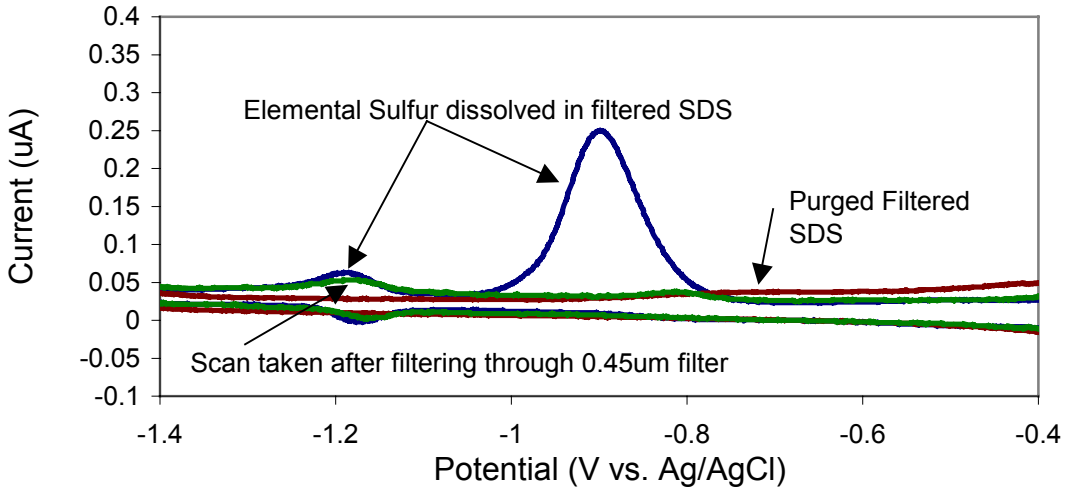

Figure 4.3.6. Electrochemical signals for a filtered and unfiltered sample of elemental sulfur dissolved in SDS.

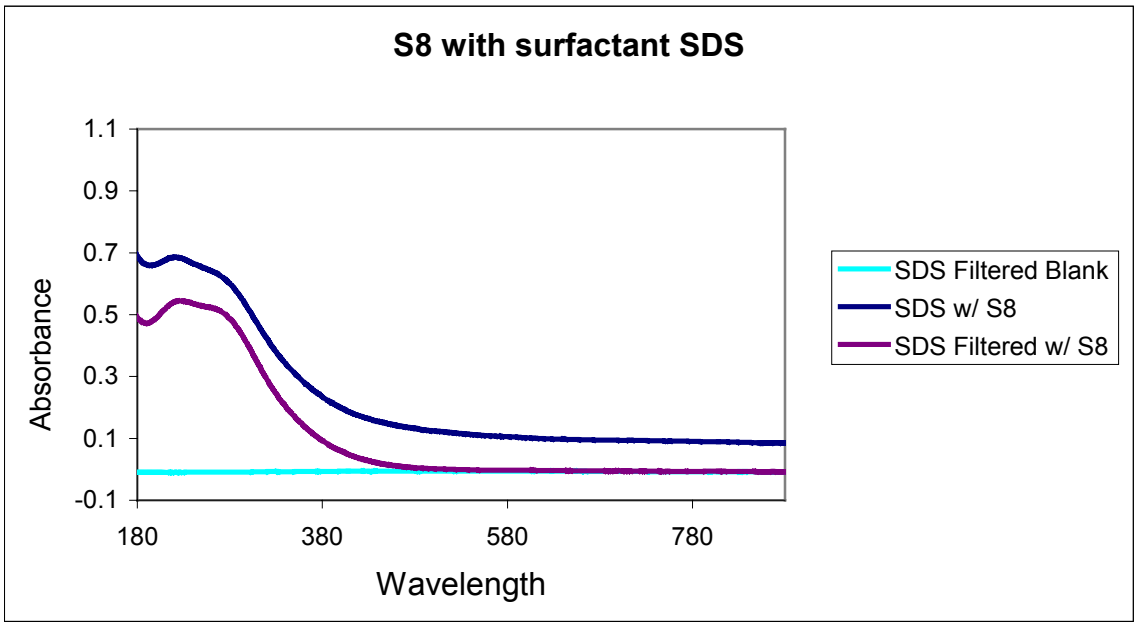

Figure 4.3.7. Spectroscopic peak of filtered and unfiltered elemental sulfur dissolved with SDS.

The decrease in the more negative voltammetric peak (Figure 4.3.6) and the decrease in the spectroscopic peak (Figure 4.3.7) after filtration show that some of the large elemental sulfur colloids were filtered out, as would be expected. This set of experiments

suggests that elemental sulfur, both particles larger than 0.45 μm and those less than 0.45 μm, are electroactive and has a peak potentials of –0.9 V and –1.2 V respectively. A necessary step to quantifying these signals must begin with a size-defined elemental sulfur standard in order to quantify the amount of elemental sulfur detected in an environment by Au-amalgam microelectrodes; however, Au-amalgam microelectrodes give us the ability to determine the presence of elemental sulfur *in situ*. The presence of elemental sulfur and its peak potential on the Au-amalgam microelectrode can also tell us more about the environment being studied. A large, dissolved elemental sulfur peak, those at –1.2 V, has been observed in several natural environments and are probably representative of biologically produced elemental sulfur or solubilized S_8. Biologically produced elemental sulfur is known to be much smaller in size and hydrophilic (Kleinjan et al., 2005b), making is possible for large concentrations to be present in dissolved phase (Janssen et al., 1996, 1999). The hydrophilic properties of the small sized elemental sulfur may explain why it reacts at a more negative potential than the larger hydrophobic elemental sulfur particles. The mercury surface, being extremely hydrophobic, would more easily react with another hydrophobic species, requiring less of a potential to drive the reaction forward.

4.3.4 Polysulfide Determination by Au-amalgam Microelectrodes

Polysulfides can be determined by the use of the Au-amalgam solid-state microelectrode, and the following electrochemical reactions potentially occur at the electrode surface in the presence of polysulfide and sulfide:

$$Hg(0) + S_x^{2-} \rightarrow HgS_x^{0} + 2e^{-}; \quad (4.28)$$

$$Hg(0) + HS^- \rightarrow HgS^0 + 2e^- + H^+; \quad (4.29)$$
$$HgS^0 + 2e^- + H^+ \rightarrow Hg(0) + HS^-; \quad (4.30)$$
$$HgS_x{}^0 + 2e^- \rightarrow Hg(0) + S_x{}^{2-}. \quad (4.31)$$

A plating reaction occurs (reactions 4.28 & 4.29) when the microelectrode is conditioned at a potential of –0.1 V for a certain amount of time. Both polysulfide and sulfide will form an amalgam with the mercury surface of the electrode. Polysulfides ($S_{(4,5)}{}^{2-}$) are better nucleophiles then aqueous sulfide (HS^-) at near-neutral pH (Luther, 1990), making polysulfides more reactive and allowing them to form a stronger bond at the mercury surface of the electrode (Rozan et al., 2000). Because the polysulfide and mercury surface form a stronger bond then sulfide does with the mercury surface, it will require more energy to break this bond and reduce the mercury (4.31), leading to a peak potential for polysulfide that is more negative then the sulfide peak potential. A longer conditioning step allows more polysulfide to bond to the mercury surface, increasing the size of the reduction peak (Figure 4.3.8).

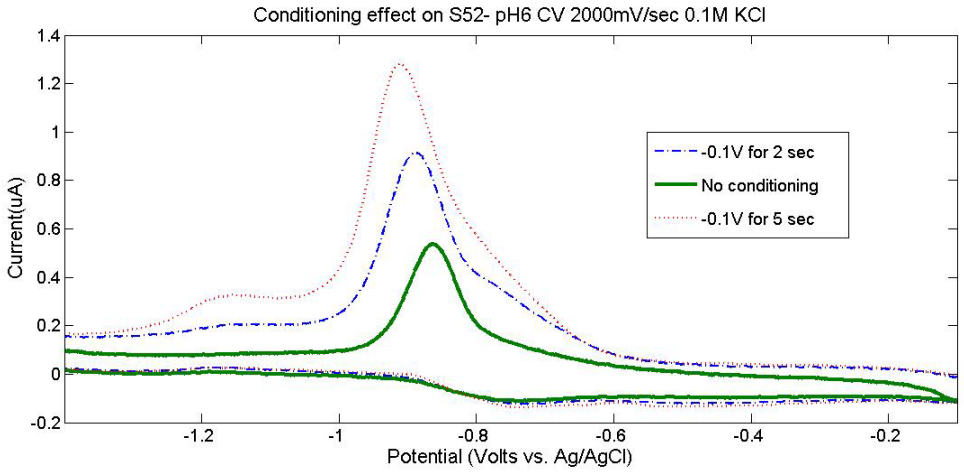

Figure 4.3.8. The effect that conditioning has on the polysulfide ($S_5{}^{2-}$) signal.

When the cyclic voltammetric scan is run the sulfide in the polysulfide standard that plated to the mercury surface (4.29) during the conditioning step is released into solution (4.30) forming the first peak, an inflection on the larger second peak. The second peak is the reduction of mercury-polysulfide complex (4.31) on the surface of the electrode. This peak is the one that can be used to quantify polysulfides. A third peak, sometimes present when polysulfide standards are added to a solution, represent the elemental sulfur in the polysulfide standard, and will be discussed further in the elemental sulfur section.

Increasing concentration of polysulfide ions in solution increases the size of the polysulfide peak and shifts the peak to more negative potentials (Figure 4.3.9). 'Pure' polysulfide standards added to 0.1 M KCl, have a small sulfide inflection on the polysulfide peak but until concentrations become high (>100 μM) have no observed elemental sulfur peak (Figure 4.3.9). The purest polysulfide standards we were able to synthesize, still have small amounts of sulfide and elemental sulfur in them, which increase proportionally with polysulfide when additions are made. Impure polysulfide standards or standards that are not carefully made can have large amounts of elemental sulfur and sulfide, resulting in three peaks and smaller polysulfide peaks that should not be used for calibration of electrodes.

There is a slight difference between S_2^{2-}, S_4^{2-}, and S_5^{2-} peak potentials for polysulfide salts; however, S_2^{2-}, S_4^{2-} and S_5^{2-} peaks are hard to differentiate because their peak potentials and peak heights are very close to one another (Figure 4.3.10).

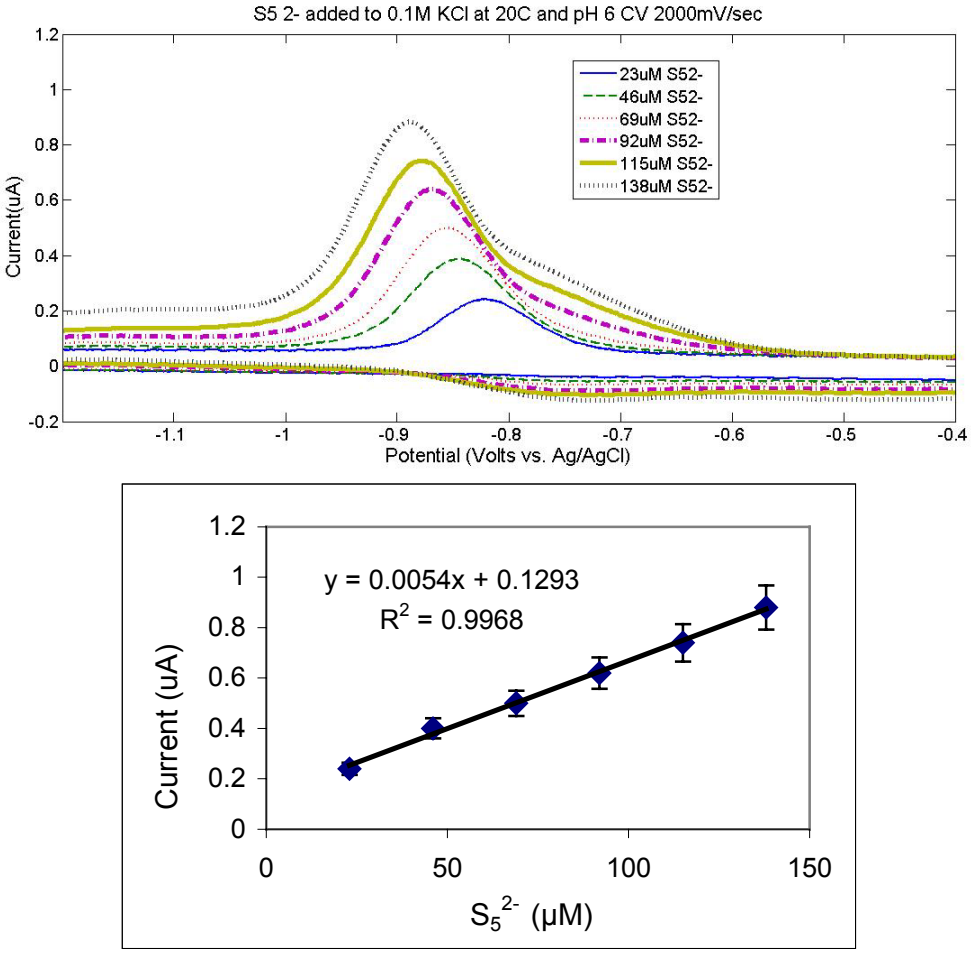

Figure 4.3.9. Top) Polysulfide additions to 0.1 M KCl. Bottom) Concentration curve for above additions with 10% error bars.

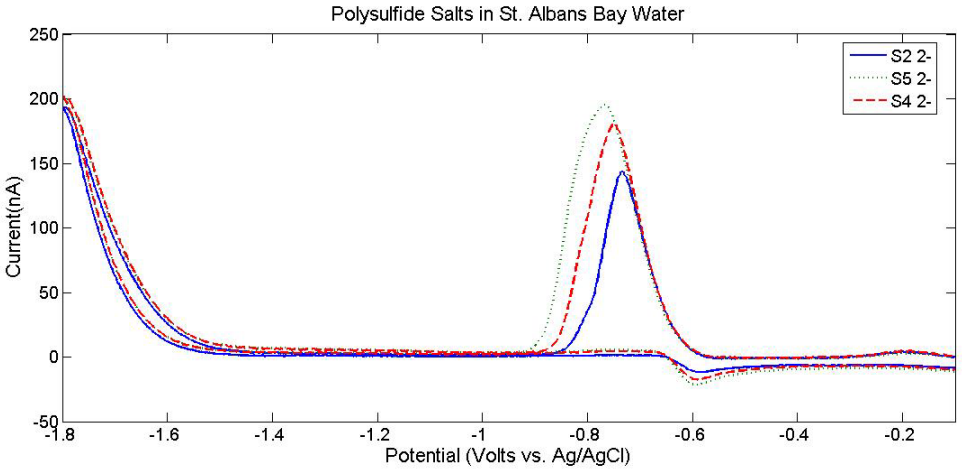

Figure 4.3.10. S_2^{2-}, S_4^{2-}, and S_5^{2-} 40µM additions made to St. Albans Bay Water CV 1000 mV/sec.

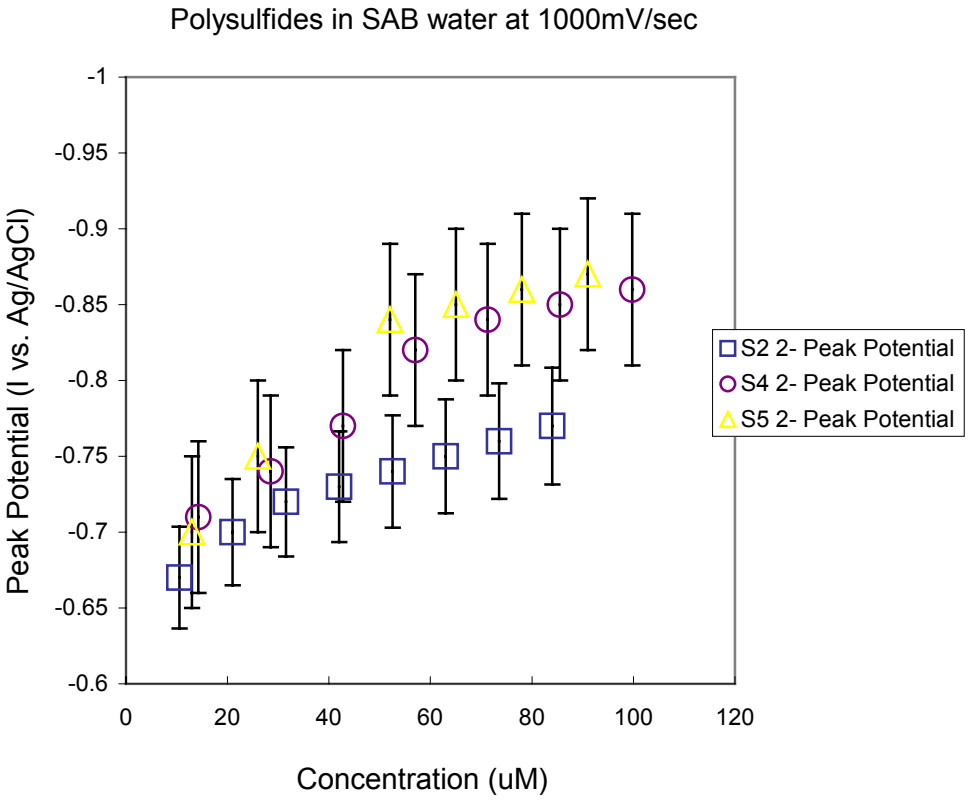

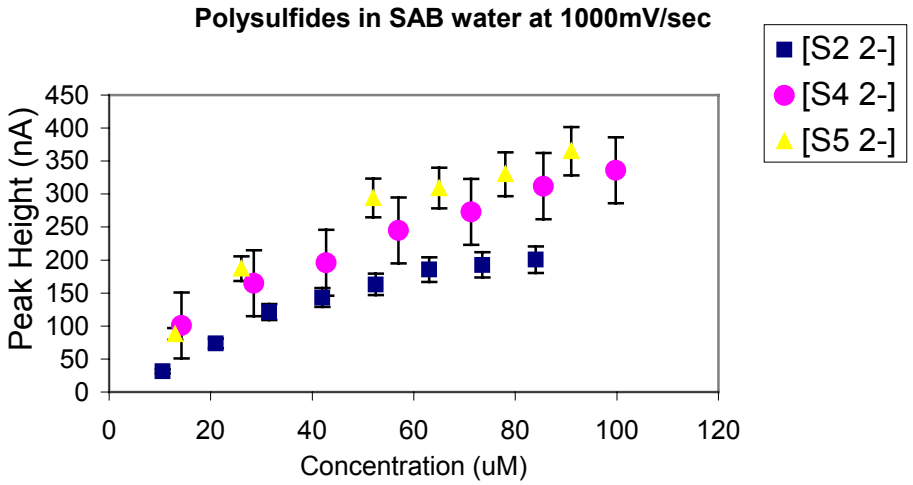

Figure 4.3.11. Three polysulfide ions S_2^{2-}, S_4^{2-} , S_5^{2-} change in Top) Peak potential with 5% error bars Bottom) Peak height with 10% error bars.

Standard additions of S_2^{2-} have a different potential and form much smaller peaks than S_4^{2-} and S_5^{2-} at similar concentrations (Figure 4.3.11). S_4^{2-} and S_5^{2-} peak potentials and peak heights across a range of concentrations are very similar and cannot be differentiated from one another. S_2^{2-} is known to decompose in natural solutions below pH 11 into aqueous sulfide and S_4^{2-} through the following pathway (Steudel, 2003):

$$3\ S_2^{2-} + H_2O \leftrightarrow 2HS^- + OH^- + S_4^{2-}. \quad (4.32)$$

It is possible that the S_2^{2-} decomposes when the laboratory standard is made and the electrochemical signal collected for S_2^{2-} is representative of the S_4^{2-} concentration in the solution (Figure 4.3.11). When 85 μM of S_2^{2-} was added to solution, the peak height was 180 nA (Figure 4.3.11), which would represent 35 μM S_4^{2-} if S_2^{2-} in fact reacted to S_4^{2-}. This result doesn't support this pathway (4.32) of polysulfide decomposition because no sulfide could be detected by the electrode and it is still unclear why the S_2^{2-} signal is different from signals for S_4^{2-} and S_5^{2-}. From this study of polysulfides in solution, S_4^{2-} and S_5^{2-} are the only polysulfide ions that can truly be quantified in natural solutions with pHs below 11, the pH range for most natural environments.

The products of polysulfide oxidation by molecular oxygen, reaction 4.19, has been a topic of much discussion in past literature (Chen and Morris, 1972; Steudel, 1986; Pasiuk-Bronikowska et al., 1992; Steudel, 1996). The Au-amalgam microelectrode gives us the ability to directly observe if thiosulfate is the product of polysulfide oxidation. From experiments run in our lab, small amounts of thiosulfate are formed due to bubbling oxygen through a solution containing polysulfide (Figure 4.3.12). The thiosulfate formed is equal to the difference in the signal between the thiosulfate present when the

polysulfide addition is made, the dark green scan, and the purged scan after the oxygen has been bubbled through, the purple scan (Figure 4.3.12). The difference, 0.05 uA is equal to 6.7 μM thiosulfate, which does not equal, through equation 4.19, to the 30 μM change in the polysulfide that was oxidized. The polysulfide could have also oxidized to SO_3^{2-}, which is electroactive at pH 6 but would probably not last long and may be the reason it was not detected.

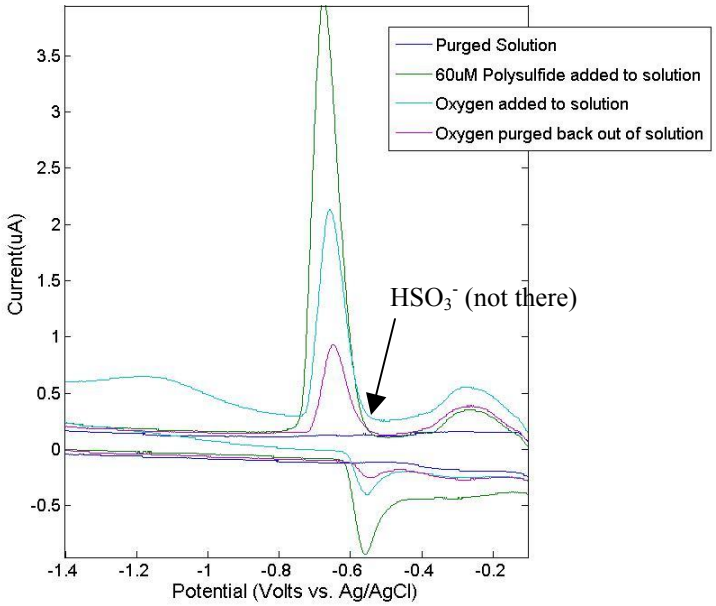

Figure 4.3.12. The oxidation of polysulfide with atmospheric oxygen at pH 6 and 20ºC.

4.3.5 Polysulfide Electrochemical Signal Dependence on pH and Temperature

Polysulfide, mainly $S_{(4,5)}^{2-}$, is stable in natural solution above pH 5.5; however, below pH 5.5 it will disproportionate into sulfide and elemental sulfur with some polysulfide remaining in solution above pH 2.5 (Figure 4.3.13).

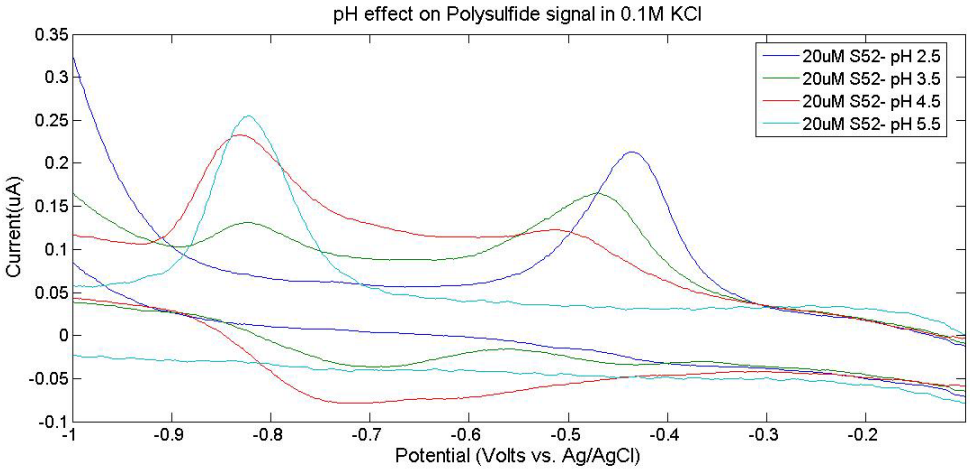

Figure 4.3.13. Polysulfide dependence on pH. At 20 ºC and 2000 mV/sec pH changed from 2.5 to 5.5.

This disproportionation reaction occurs quickly (< 10 sec) through the reverse reaction pathway of reactions (4.11 & 4.12) (Kamyshny et al., 2003). The formation of elemental sulfur from a polysulfide standard being added to low pH solution can be observed because the solution turns a cloudy white color almost instantaneously. Only one peak (E_p= -0.43) is detected with Au-amalgam microelectrodes when a polysulfide standard is added to a solution of pH 2.5 (Figure 4.3.13), representing the sulfide generated from the disproportionation reaction. The formation of elemental sulfur at pH 2.5 can be observed; however, there is no electrochemical signal for it, indicating the elemental sulfur that forms from the disproportionation of polysulfides is bigger than the electrode can detect. The size dependence of elemental sulfur on its electrochemical signal is discussed in the elemental sulfur section (4.3.3). Polysulfide standards added to solutions between pH 3 and 5 form two peaks (Figure 4.3.13), the more positive one representing the sulfide formed from the disproportionation reaction and the more negative representing the polysulfide, $S_{(4,5)}^{2-}$. There is more polysulfide and less sulfide present as the pH of the solution increases. The reason for this is still unknown and could be

determined through more careful experimentation; however, it is outside of the scope of this study. Polysulfides will only be present at low pH if some type of equilibrium or steady state between sulfide and elemental sulfur is reached within the system. The polysulfide peak potential does not shift with pH like the sulfide signal does, making the separation between the polysulfide and sulfide peaks greater as the pH of a solution decreases.

The polysulfide peak potential is dependent on the temperature of the environment being sampled (Figure 4.3.14). The peak potential, E_p, shifts to more negative potentials with increasing concentration; however, the $E_{1/2}$ potential does not change with concentration (Figure 4.3.14), so assessing how the $E_{1/2}$ changes with temperature for sulfide is appropriate.

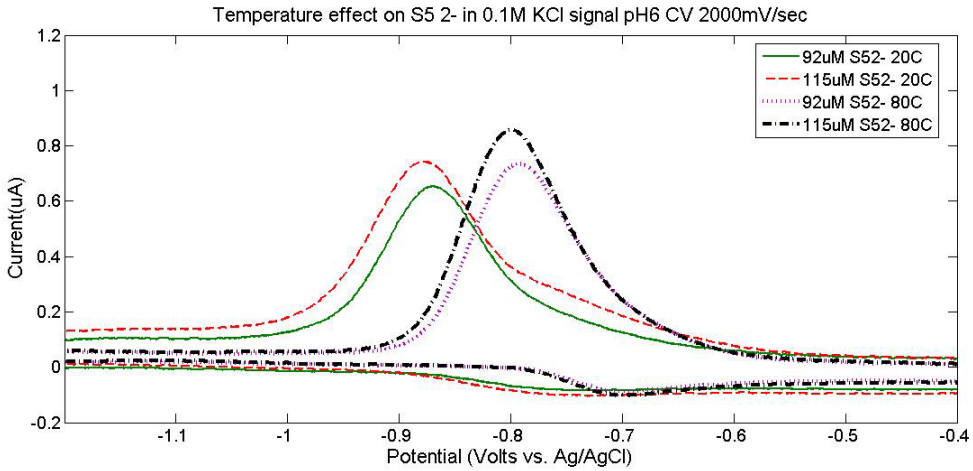

Figure 4.3.14. Polysulfide dependence on Temperature.

The reduction of polysulfide at the mercury surface will occur at more positive potentials as the temperature increases, changing from $E_{1/2} = -0.82$ at 20 ºC to $E_{1/2} = -0.72$ at 80 ºC, and is linear with the sulfide temperature shift from $E_{1/2} = -0.78$ at 20 ºC to $E_{1/2} = -0.68$ at 80 ºC. Changes in temperature shift the potential of the sulfide signal due to a

temperature effect on the diffusion characteristics around the surface of the electrode, having a small effect on the potential at which the chemical species reacts.

4.3.6 S_5^{2-} Formation by Reaction between Sulfide and Elemental Sulfur

Polysulfide, particularly S_5^{2-}, is known to be the product of a reaction between elemental sulfur and aqueous sulfide (a Wackenroeder solution; See equation 4.6). The acidification of thiosulfate can form elemental sulfur in solution reaction 4.20. Aqueous sulfide added to a solution containing elemental sulfur, formed through the acidification of thiosulfate, forms pentasulfide and the reaction can be detected using Au-amalgam microelectrodes (Figure 4.3.15).

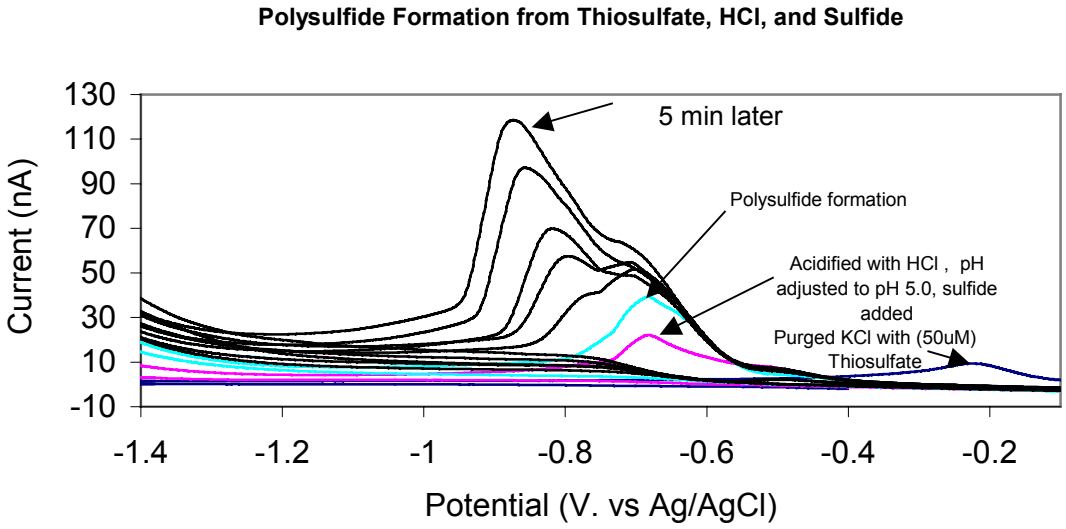

Figure 4.3.15. Polysulfide formation from elemental sulfur and aqueous sulfide. Thiosulfate was acidified with HCl to pH <2, readjusted with NaOH to pH 5, and sulfide was added to form polysulfides.

Thiosulfate added to an aqueous solution can be detected by the Au-amalgam microelectrode; however, when the solution is acidified a sulfur precipitate forms and the thiosulfate peak disappears immediately. The sulfur precipitate that forms cannot be detected with the Au-amalgam microelectrode because it is too big, as discussed in the

elemental sulfur section (4.3.3). The pH is readjusted back to a more neutral pH so that the polysulfides being formed can be detected. Once aqueous sulfide is added to the solution polysulfide ions begin to form immediately. Polysulfide ions continue to form until either all the sulfide or all the elemental sulfur is consumed by the reaction.

The creation of polysulfide ions through this reaction pathway is relatively slow and the polysulfide peak has been observed to continuously increase for over 20 minutes. The cyclic voltammetric polysulfide signal created by the reaction between elemental sulfur and sulfide (Figure 4.3.15) is a $S_{(4,5)}^{2-}$ signal and has the same potential as $S_{(4,5)}^{2-}$ standards (Figure 4.3.9).

4.3.7 Overlay of Multiple Sulfur Species

Polysulfide, sulfide, colloidal elemental sulfur, and dissolved elemental sulfur all have different peak potentials and can be detected in the same solution using the same Au-amalgam microelectrode (Figure 4.3.16).

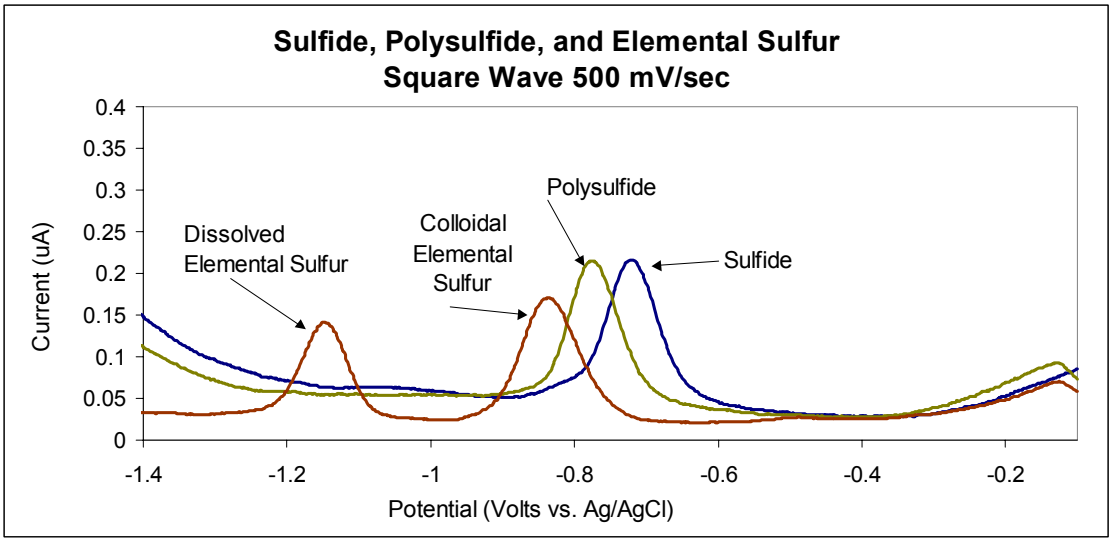

Figure 4.3.16. Overlay of Sulfide, Polysulfide, colloidal elemental sulfur, and dissolved elemental sulfur in 0.1 M KCl.

Because of the colloidal elemental sulfur, polysulfide, and sulfide peaks close proximity to one another, fast scan rates, square wave voltammetry, or differential pulse polarography should be used to separate the peaks.

4.3.8 Identification of Electrochemical Signals in Yellowstone's Hot Springs

Evening Primrose

In August 2004, Evening Primrose Spring (Latitude: 44º41'30"N; Longitude: 110º46'36"W), located in the Sylvan Springs Group of Gibbon Geyser Basin, was visited and *in situ* electrochemical data was collected to better define the redox chemistry of the hot spring (Figure 4.3.17).

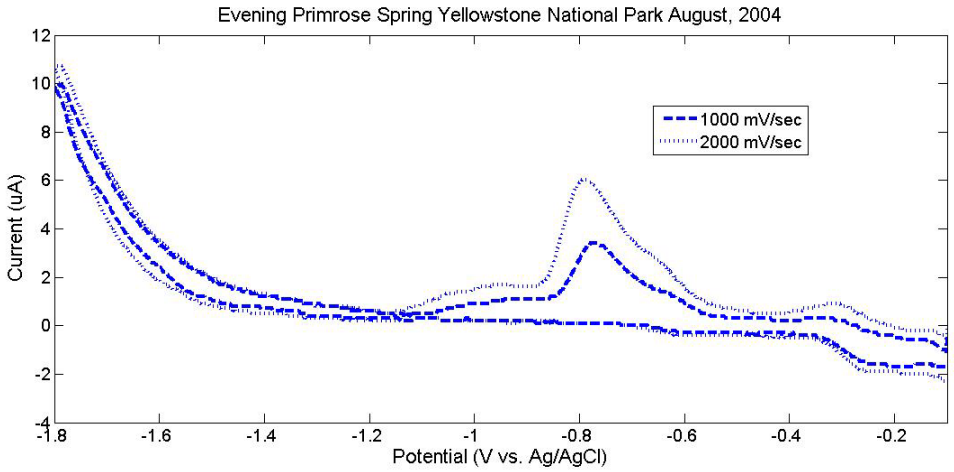

Figure 4.3.17. Field Scans Collected from Evening Primrose Spring.

Gases bubbling through the water in the hot spring created large amounts of turbulence increasing the background noise of the electrochemical signals being collected by affecting the diffusion at the electrode surface. In order to enhance the signal to noise ratio and collect the *in situ* redox chemistry with Au-amalgam microelectrodes, fast scan rates (>1000 mV/sec) and small working electrodes (100 μm diameter surface) were

used. Cyclic voltammetric scans at scan rates of 1000 mV/sec and 2000 mV/sec had better signal to noise ratios and are the scans that were used to quantify the redox chemistry of Evening Primrose Spring (Figure 4.3.17).

Identification and quantification of the peaks, representing different redox species, was done in the laboratory. Water collected from the hot spring was used to make additions of chemical species at *in situ* temperature and pH. It is critical that the pH, temperature, scan rate, and water matrix are the same as the *in situ* conditions when trying to match peaks and quantify chemical redox species. Polysulfide, S_5^{2-}, additions were made to an Evening Primrose water sample for calibration (Figure 4.3.18), allowing polysulfide to be quantified in the hot spring (Figure 4.3.19).

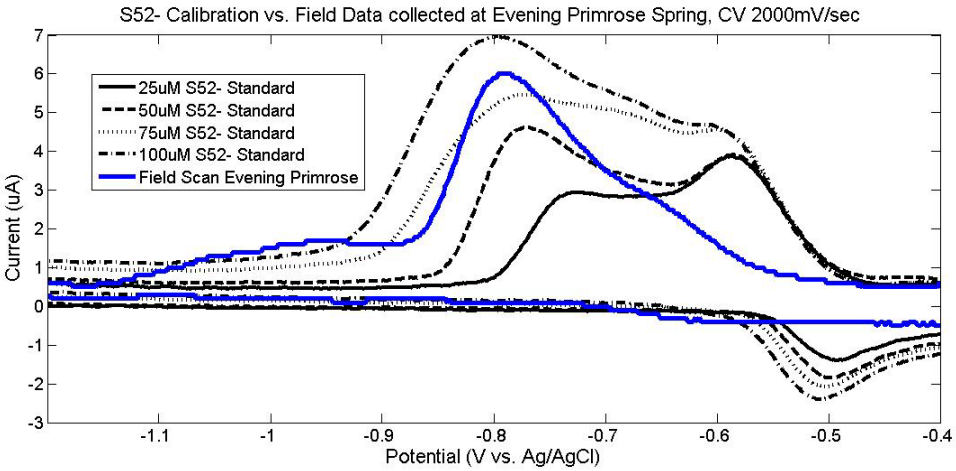

Figure 4.3.18. Polysulfide additions made to Evening Primrose water compared to the field scan collected from the spring.

From standard addition experiments conducted in the laboratory at *in situ* conditions the equation presented in Figure 4.3.19 gives us the ability to quantify the S_5^{2-} in Evening Primrose hot spring, which was consistently changing and ranged from 84 µM to 322 µM.

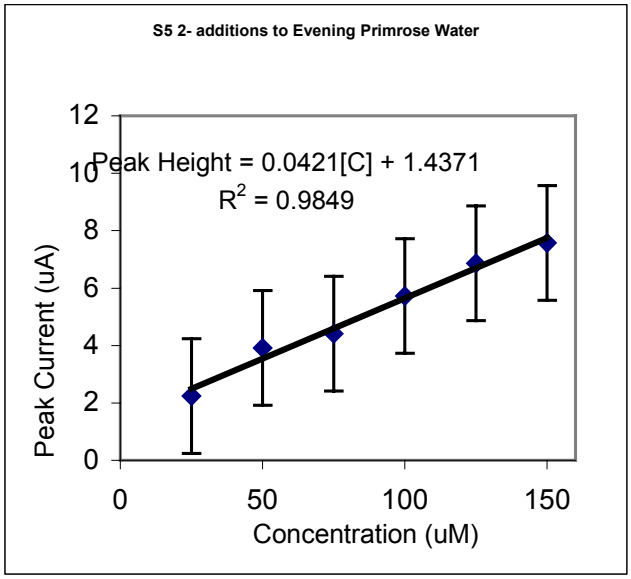

Figure 4.3.19. Concentration curves for polysulfide in Evening Primrose water with 5% error bars.

Matching peaks on the electrochemical data is extremely important in determining the chemical species present in the environment being sampled. Laboratory additions, done at the *in situ* pH and temperature of the spring, confirmed the peak positions for sulfide and polysulfide in water collected from Evening Primrose (Figure 4.3.20).

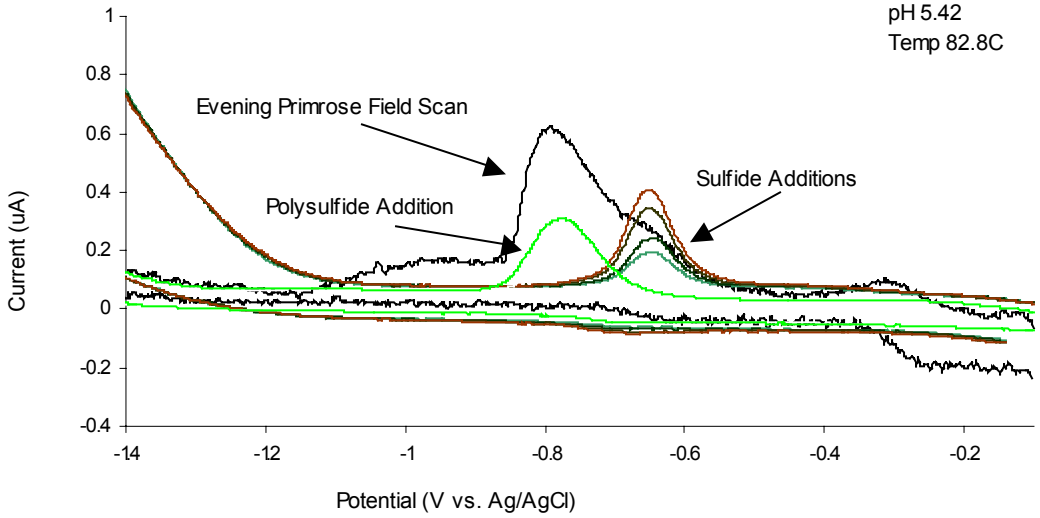

Figure 4.3.20. Sulfide and Polysulfide overlay of Evening Primrose Field Scans

Once addition experiments are conducted in the laboratory, the peaks on electrochemical scans collected from Evening Primrose can be labeled (Figure 4.3.21). Elemental sulfur is the only peak that cannot be quantified, but the peak potential tells us the elemental sulfur is a colloidal form.

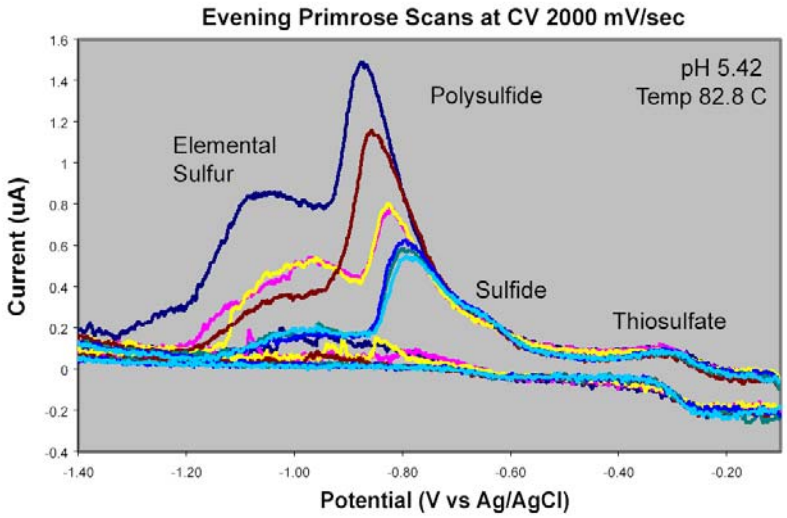

Figure 4.3.21. Evening Primrose Field Scans with labeled peaks.

Over the hour that microbial samples were collected from Evening Primrose Spring, the chemistry of the pool was constantly changing (Figure 4.3.21). The thiosulfate (4.48 mg/L) and sulfide (2.11 mg/L) concentrations in the pool didn't change; however, the polysulfide (13.4 to 51.5 mg/L) and elemental sulfur signal changed significantly. The change in the elemental sulfur signal may be due to either a change in elemental sulfur concentration or a change in the size of the elemental sulfur in Evening Primrose Pool.

Scans collected at different times throughout the sampling event at Evening Primrose (Figure 4.3.21) indicate the intermediate sulfur chemistry of the pool was

constantly changing. The aqueous sulfide concentration of the pool did not change over the course of sampling; however, violent off gassing was continuous, suggesting equilibrium between H_2S gas and aqueous H_2S. Polysulfide and colloidal elemental sulfur dynamics seem to be correlated, suggesting that the following reaction pathway is taking place in Evening Primrose Spring:

$$H_2S_{(g)} \leftrightarrow H_2S_{(aq)} + S_{8(dissolved)} \rightarrow S_5^{2-} \rightarrow S_{8(colloidal)} + S_2O_3^{2-}{}_{(aq)};$$

where the intermediate sulfur chemistry of the Evening Primrose system is controlled by the amount of H_2S gas coming into the system. The thiosulfate concentration also remained constant throughout the entire sampling event, suggesting that the oxygen needed to oxidize polysulfide to thiosulfate is controled by diffusion into the surface of hot spring.

Cinder Pool

In August 2004, Cinder Pool (Latitude: 44º43'57.5"; Longitude: 110º42'32.7"), located in the 100 Spring Plain of Norris Geyser Basin, was visited and *in situ* electrochemical data was collected to better define the redox chemistry of the hot spring (Figure 4.3.22). Previous studies of Cinder Pool provided insight into the potential intermediate sulfur redox chemistry present in the pool (Xu et al., 2000; Druschel et al., 2003; McCleskey et al., 2005). Thiosulfate was found to exist in Cinder Pool in much higher concentration than expected for a hot spring with a pH < 5 (Xu et al., 2000). Thiosulfate is not stable under low pH conditions and rapidly disproportionates to elemental sulfur and sulfite (reaction 32). The Xu et al. (2000) study of Cinder Pool did

not look at the polysulfide concentrations in the hot spring, which could play a critical part in their proposed sulfur cycle.

Fast scan rates were preformed in Cinder Pool because turbulence, due to off gassing in Cinder Pool, contributes to electrochemical singal noise as in Evening Primrose Spring. Voltammetric scans collected from Cinder Pool consisted of two large peaks (Figure 4.3.22). No thiosulfate was detected with the Au-amalgam microelectrode, and should have showed up as a small peak (10-20 nA; see Figure 4.3.1) if the concentrations reported by Xu et al. (2000), 35.6 -71.0 μM, were present in Cinder Pool. The more positive peak did not change significantly over the sampling event (approximately 1 hour), in several locations of the pool. The more negative peak constantly changed in size shown in Figure 4.3.22.

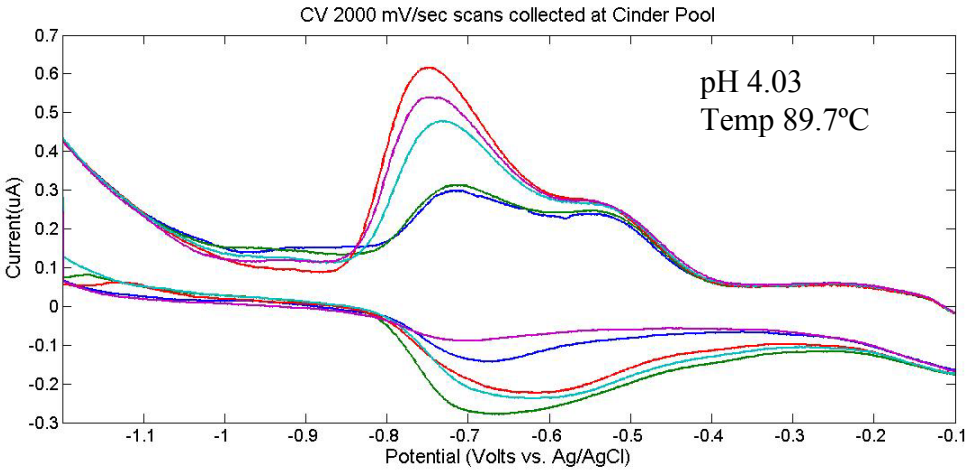

Figure 4.3.22. CV scans collected from Cinder Pool

Identification and quantification of the peaks, representing redox species, was preformed in the laboratory. Water collected from Cinder Pool was used to make additions of chemical species at *in situ* temperature and pH. It is critical that the pH, temperature, scan rate, and water matrix are the same as the *in situ* conditions when

trying to match peaks and quantify chemical redox species. Laboratory polysulfide, S_5^{2-}, standard additions to water collected from Cinder Pool overlay the more negative peak on the Cinder Pool field voltammograms (Figure 4.3.23). Laboratory additions of a sulfide standard overlay the more positive peak on Cinder Pool voltammograms (Figure 4.3.23).

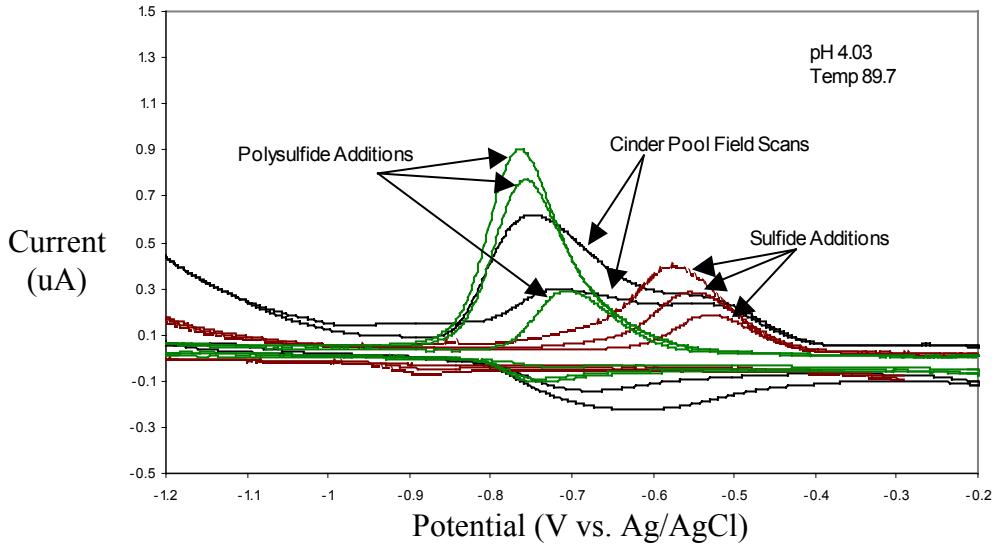

Figure 4.3.23. Overlays of Sulfide and Polysulfide to Cinder Pool.

The *in situ* concentrations of these chemical species changed over time as we sampled the pool and ranged from 15 to 25 µM sulfide and 46 to 100 µM S_5^{2-}. Thiosulfate had previously been reported (Xu et al., 2000; Ball et al., 2001) to exist in Cinder Pool but was not found during this investigation and could still exist at concentrations less than 10 µM, which is the detection limit for thiosulfate on the Au-amalgam microelectrode. Elemental sulfur was also not detected with the Au-amalgam microelectrode. This may be because the particle size may be too large to be detected with the electrodes.

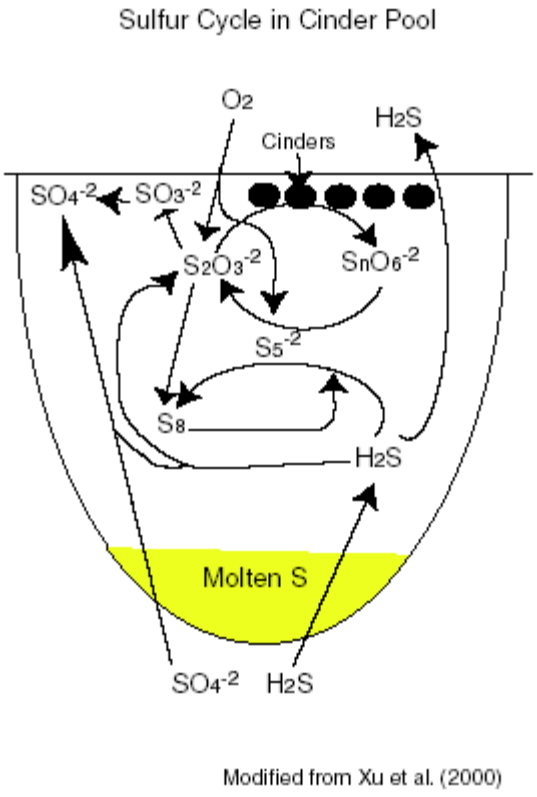

Figure 4.3.24. Schematic diagram of Cinder Pool proposed sulfur cycle modified from Xu et al., 2000.

Based on the sulfur cycle of Cinder Pool presented by Xu et al. (2000), we have added polysulfide to the schematic (Figure 4.3.24). Just like the Evening Primrose system, aqueous sulfide is probably in equilibrium with hydrogen sulfide gas. The H_2S gas input into Cinder Pool is controlling the formation of polysulfides within Cinder Pool; however, as we have determined from our experiments, polysulfide is not completely stable below pH 5.5, and would therefore disproportionate into elemental sulfur and sulfite upon formation. The disproportionation of polysulfides may explain the variability in the sulfide concentration detected. Some type of steady state could be reached within the system creating a cycle of disproportionation and polysulfide

formation, allowing polysulfide to be present in the system. This cycle would then be controlled by the amount of H_2S entering the system. In the presence of oxygen, polysulfides will easily oxidize to thiosulfate; however, in Cinder Pool thiosulfate would not be stable and would easily disproportionate into elemental sulfur and sulfite, and could explain why thiosulfate concentrations are lower than 10 μM. Previous studies found similar concentrations of H_2S: (16-48 μM, Xu et al., 2000), (10 μM, Ball et al., 2001), and (16 μM, Ball et al., 2002), to the 15-25 μM found in this study. The thiosulfate found in previous studies may be from the direct oxidation of polysulfides in the sample collected from Cinder Pool, or the concentration may have been below detection limits on the Au-amalgam microelectrode the day we sampled Cinder Pool.

Mini-Primrose

In August 2004, Mini-Primrose Spring (Latitude: 44º42'1.3"N; Longitude: 110º 45'58"W), located in the Sylvan Springs Group of Gibbon Geyser Basin, was visited; and *in situ* electrochemical data was collected to better define the redox chemistry of the hot spring (Figure 4.3.25). This hot spring was selected for sampling due to the similar visual characteristics of Evening Primrose. However, the *in situ* chemistry was surprisingly different then that encountered at Evening Primrose. The pH of Mini-Primrose was 3.3 and the temperature was 59.6 ºC. Over an extended period of time, approximately 2 hours, electrochemical data was collected from the Mini-Primrose spring and two peaks were consistently seen in the hot spring environment (Figure 4.3.25, Red Scan) until the hot spring would "belch", suddenly releasing a large amount of gas.

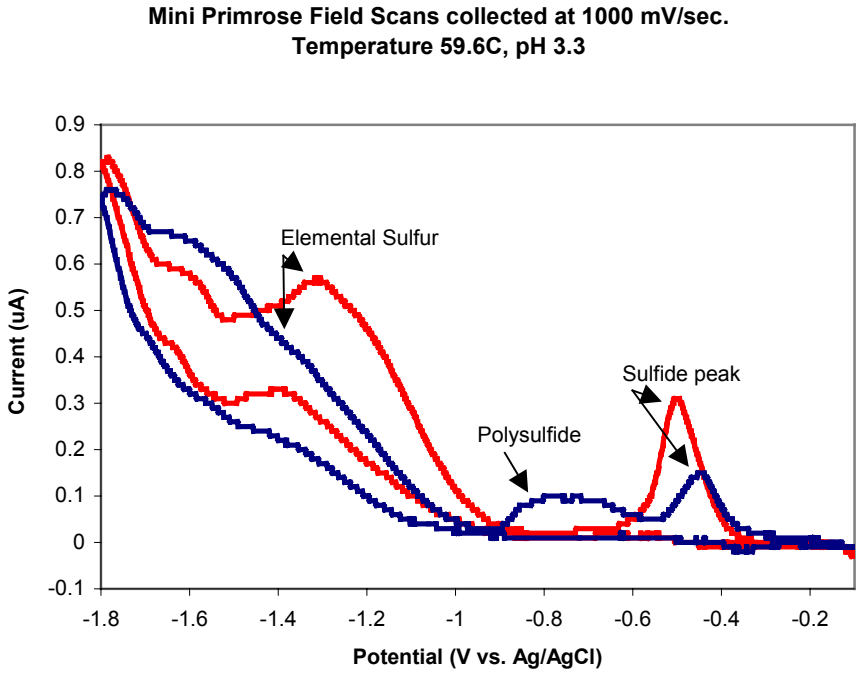

Figure 4.3.25. Field Scans collected from Mini-Primrose.

A scan collected only seconds after gases had been released from the hot spring, showed a decrease in both of the predominate peaks and the formation of a new peak (Figure 4.3.25, Blue scan). The peak labeled as sulfide was determined by making standard sulfide additions to water collected from Mini-Primrose. The addition of sulfide to Mini- Primrose water recreated the broad peak seen after gas release from the hot spring (Figure 4.3.26). Increased rates of hydrogen sulfide gas input into the hot spring caused an increase in the polysulfide concentration within the spring. This is a supporting example of the steady-state existence of the polysulfide species, where the production of polysulfide ions is dependent on the rate of H_2S entering the hot spring.

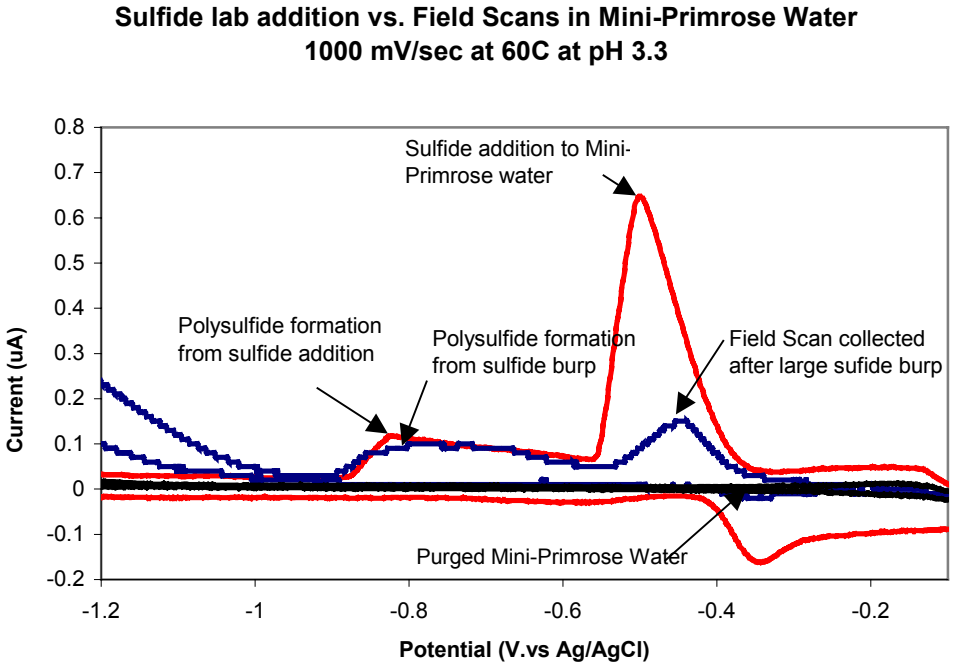

Figure 4.3.26. Lab Scan overlay on Mini-Primrose Field Scan.

The polysulfides formed in Mini-Primrose due to the temporary increase in H_2S input do not last long due to the pH of the spring, easily disproportionating to sulfide and elemental sulfur within a matter of seconds. The large elemental sulfur peaks observed in the field, representing small sized elemental sulfur, were not detected when water collected from Mini-Primrose was voltammetrically analyzed in the lab.

4.3.9 Intermediate Sulfur Species and Bioenergetics in Hot Spring Environments

Sulfur, iron, manganese, arsenic and many other chemical redox species are sensitive to oxidation when they are removed from their natural environment and exposed to atmospheric oxygen during sampling. The ability to quantify sulfur, iron, manganese, and arsenic redox species *in situ*, through the use of Au-amalgam microelectrodes, yields a more complete geochemical data set than was previously possible. It also eliminates

the possibility for speciation changes in a collected water sample due to oxidation or precipitation. For example, polysulfide would oxidize to thiosulfate when exposed to small amounts of oxygen, or would disproportionate into sulfide and elemental sulfur if a collected water sample was acidified to preserve metals. Adding intermediate redox species, which could not previously be defined by traditional analytical techniques, to an environment's geochemical data set allows the energetics of reactions involving these intermediate redox species to be defined.

Electrochemical data collected from the hot springs visited in YNP was interpreted by calibrating the electrodes used in the field to determine the concentration of sulfide, polysulfide, and thiosulfate. If oxygen, iron, arsenic, or manganese were present in concentrations high enough to be determined with the Au-amalgam microelectrodes, the associated redox species concentrations could also be determined. Water samples collected from the hot springs were run on an ICP-OES to determine the concentrations of chemical species that cannot be defined with the microelectrodes. The ICP-OES was not sensitive enough to detect all chemical species known to exist (Ball et al., 2001) in Cinder Pool and Evening Primrose therefore, data presented in their report was used for the chemical species we were unable to detect. Also data on the amount of NH_4 and hydrogen gas present in Cinder Pool had previously been determined by Spear et al. (2005) and was used for this study. The geochemical data set used to perform bioenergetic calculations for two of the hot springs visited in Yellowstone is shown in Table 4.3.1.

Table 4.3.1. Analytical data for hot springs.[1] Defined by Au-amalgam microelectode. [2] From Ball et al., 2001. [3] From Spear et al., 2005.

	Evening Primrose	Cinder Pool
Temp	82.8	89.7
pH	5.42	4.03
	mg/L	mg/L
Ca	10	6.3
Mg	0.43	0.017
Sr	0.029	0.021
Ba	0.076	0.019
Na	330	430
K	36	65
Li	1.1	5.6
F	3.1	5.5
Cl	390	670
Br	1.1	2.2
Si	240	370
B	7.8	12
Al	10	0.71
Mn	0.2	0.0005
Cu	0.0005	0.004
Zn	0.012	0.0005
Cr	0.001	0.0005
C(2)	0.0005	0.002
Ni	0.01	0.01
Cd	0.0005	0.0005
Pb	0.016	5.00E-05
Be	0.001	5.00E-05
V	0.001	0.0005
Se	0.00015	0.00015
As	1.7	2.6
Fe(3)	2.01	0
Fe(2)	2.55	0.043
S_5^{2-}	13.4-51.5[1]	7.4-16[1]
SO_4	1700[2]	43[2]
S_2O_3	4.48[1]	0[1]
H_2S	2.11[1]	0.5-0.58[1]
NH_4	No Data	1.8[3]
H_2	No Data	0.034[3]

Activities of aqueous species (Table 4.3.2) were calculated using PHREEQC Interactive 2.10 with the chemical data presented in Table 4.3.1, for the *in situ* conditions of Cinder Pool and Evening Primrose.

Table 4.3.2. Activities of aqueous chemical species in Cinder Pool and Evening Primrose and Gibbs free energy of formation at 80ºC from Amend and Shock (2001).

	Evening Primrose	Cinder Pool	
Species	Activity	Activity	ΔG_i^o
H^+	1.45E-02	4.786E-05	0
H_2	2.33E-14	5.023E-07	13.39
H_2O	9.99E-01	1	-241.81
H_2S	1.28E-05	5.888E-10	-36.39
HS^-	2.70E-10	3.707E-12	8.33
HSO_3^-	2.88E-06	1.66E-08	-536.12
O_2	3.41193E-49	1.82E-39	8.81
OH^-	2.16E-11	6.252E-09	-156.02
S_8	1	1	-2.04
$S_2O_3^{-2}$	1.93E-05	3.35E-05	-525.44
S_4^{-2}	4.18E-12	1.265E-09	63.86
S_5^{-2}	8.67E-10	1.109E-06	58.13
SO_2	1	1	-311.88
SO_4^{-2}	1.36E-03	0.0002118	-744.32

Table 4.3.2 also includes the Gibbs free energy of formation, ΔG_i^o (from Amend and Shock, 2001), for each chemical species at 80ºC. The energetic potential of 28 reactions involving intermediate sulfur species, including polysulfide, elemental sulfur, sulfide, and thiosulfate, that could potentially yield metabolic energy to microorganisms are given in Table 4.3.3. Some of the reactions presented in Table 4.3.3 have previously been looked at in hot spring environments (Amend et al., 2003; Spear et al., 2005) for their energetic

potential; however, reactions involving polysulfides have not been investigated for their potential energy gain at YNP.

Table 4.3.3. Selected reactions involving intermediate sulfur species and the electrons transferred (e^-).

Reaction #	Reaction	e^-
1	$SO_4^{-2} + 4\ H_2 + 2\ H^+ = H_2S + 4\ H_2O$	8
2	$S_2O_3^{-2} + 2\ O_2 + H_2O = 2\ SO_4^{-2} + 2\ H^+$	8
3	$5\ S_2O_3^{-2} + H_2O + 4\ O_2 = 6\ SO_4^{-2} + 2\ H^+ + 4\ S_8$	16
4	$S_2O_3^{-2} + H_2O = SO_4^{-2} + H_2S$	8
5	$S_2O_3^{-2} + 2\ H^+ + 4\ H_2 = 2\ H_2S + 3\ H_2O$	8
6	$S_8 + 1.5\ O_2 + H_2O = SO_4^{-2} + 2\ H^+$	6
7	$4\ S_8 + 4\ H_2O = SO_4^{-2} + 3\ H_2S + H^+$	6
8	$S_8 + H_2 = H_2S$	2
9	$H_2S + 2\ O_2 = SO_4^{-2} + 2\ H^+$	8
10	$2\ H_2S + 2\ O_2 = S_2O_3^{-2} + H_2O + 2\ H^+$	8
11	$H_2S + 0.5\ O_2 = S_8 + H_2O$	2
12	$H_2 + 0.5\ O_2 = H_2O$	2
13	$2\ S_5^{-2} + 2\ H^+ = 2\ HS^- + S_8$	4
14	$2\ HS^- + S_8 = 2\ S_5^{-2} + 2\ H^+$	4
15	$0.5\ S_8 + 4\ H_2O = 3\ HS^- + SO_4^{-2} + 5\ H^+$	6
16	$S_4^{-2} + 1.5\ O_2 = S_2O_3^{-2} + 0.25\ S_8$	6
17	$4\ S_4^{-2} + H_2O = HS^- + OH^- + 3\ S_5^{-2}$	2
18	$S_5^{-2} + 3\ OH^- = S_2O_3^{-2} + 3\ HS^-$	6
19	$S_2O_3^{-2} + OH^- = SO_4^{-2} + HS^-$	4
20	$S_4^{-2} + 3\ H_2 = 4\ HS^- + 2\ H^+$	6
21	$S_5^{-2} + 4\ H_2 = 5\ HS^- + 3\ H^+$	8
22	$2\ S_4^{-2} + 4H^+ + O_2 = S_8 + 2\ H_2O$	4
23	$S_2O_3^{-2} + 0.25\ S_8 = S_4^{-2} + 1.5\ O_2$	6
24	$S_2O_3^{-2} + 3\ HS^- = S_5^{-2} + 3\ OH^-$	6
25	$S_2O_3^{-2} + H^+ = S_8 + HSO_3^-$	2
26	$SO_4^{-2} + 3\ H_2S + 2H^+ = 4\ S_8 + 4\ H_2O$	6
27	$3\ HS^- + SO_4^{-2} + 5\ H^+ = 0.5\ S_8 + 4\ H_2O$	6
28	$HS^- + OH^- + 3\ S_5^{-2} = 4\ S_4^{-2} + H_2O$	2

The electrons transferred during each reaction (e^-) are presented in Table 4.3.3 and are used to normalize the Gibbs free energy values. Investigating reactions for which microbial metabolisms are unknown, such as those involving polysulfides and other

intermediate sulfur species, allows us to determine their energetic potential as possible modes of metabolism for microorganisms in these environments. Sulfate reduction (reactions 1, 26, and 27) is known to be used by species of Thermodesulfobacterium (Jeanthon et al., 2002) and Archaeoglobus (Burggraf et al., 1990) among others; while the oxidation of elemental sulfur (reactions 6) is used by Acidianus, Aquifex, Sulphurococcus, and Thermothrix; and the reduction of elemental sulfur (reactions 8) is used by many thermophilic bacteria for metabolic energy (Amend et al., 2003). The Gibbs free energy of the above reactions (ΔG_r^o) and the calculated overall Gibbs free energy (ΔG_r) for two of the hot springs visited in Yellowstone National Park is reported in Table 4.3.4.

Table 4.3.4. Values of ΔG_r^o for each reaction, the energy provided in each environment by the reactions ΔG_r, and the normalized values of the Gibbs free energy $\Delta G_r/e^-$ (kJ/mol).

		Evening Primrose	Evening Primrose	Cinder Pool	Cinder Pool
Reaction	ΔG_r^o	ΔG_r	$\Delta G_r/e^-$	ΔG_r	$\Delta G_r/e^-$
1	-312.87	72.32715	9	-118.971	-15
2	-739.01	-106.6053	-13	-286.714	-36
3	-1640.31	-292.6054	-18	-634.813	-40
4	-13.46	-34.33081	-4	-71.2526	-9
5	-326.33	37.99634	5	-190.224	-24
6	-513.685	-60.10525	-10	-199.689	-33
7	121.91	-10.9809	-2	-122.754	-20
8	-47.74	12.18239	6	-67.8361	-34
9	-725.55	-72.27448	-9	-215.462	-27
10	-712.09	-37.94367	-5	-144.209	-18
11	-211.865	-12.16923	-6	-15.7721	-8
12	-259.605	0.013167	0	-83.6082	-42
13	-101.64	-83.35348	-21	-117.492	-29
14	101.64	83.35348	21	117.492	29
15	248.93	-30.60962	-5	-159.485	-27
16	-603.025	-58.86795	-10	-174.274	-29
17	13.07	0.01617	0	-0.012	0

18	-90.52	-38.14639	-6	-146.749	-24
19	-54.53	-34.33755	-9	-71.1636	-18
20	-70.71	0.054269	0	-252.878	-42
21	-70.04	0.083434	0	-337.193	-42
22	-622.19	-83.38547	-21	-116.078	-29
23	603.025	58.86795	10	174.274	29
24	90.52	38.14639	6	146.7493	24
25	-12.72	-5.766805	-3	-5.769	-3
26	-121.91	10.9809	2	122.7536	20
27	-248.93	30.60962	5	159.4849	27
28	-13.07	-0.01617	0	0.012003	0

The calculated overall Gibbs free energies that are negative provide a source of energy to microorganisms that are able to couple the chemical species involved in the reaction (termed exergonic); therefore, Gibbs free energies that are positive do not provide energy to microorganisms (termed endergonic) and will not be used formetabolic processes. The overall Gibbs free energy is normalized per electron transferred ($\Delta G_r/e^-$) for each reaction in order to provide a more straightforward comparison of the energetics of redox reactions (Amend et al., 2003).

For Evening Primrose the oxidation and disproportionation of polysulfides (Reactions 13 and 22) yield the most energy. A total of 15 of the 28 calculated reactions (Table 4.3.5) have negative values for ΔG_r, yielding energy and possible sources of metabolic energy for microorganisms.

Table 4.3.5. Reactions yielding energy in Evening Primrose $\Delta G_r/e^-$.(kJ/mol).

Reaction #	$\Delta G_r/e^-$	Reaction
22	-21	$2\ S_4^{-2} + 4H^+ + O_2 = S_8 + 2\ H_2O$
13	-21	$2\ S_5^{-2} + 2\ H^+ = 2\ HS^- + S_8$
3	-18	$5\ S_2O_3^{-2} + H_2O + 4\ O_2 = 6\ SO_4^{-2} + 2\ H^+ + 4\ S_8$

2	-13	$S_2O_3^{-2} + 2\ O_2 + H_2O = 2\ SO_4^{-2} + 2\ H^+$
6	-10	$S_8 + 1.5\ O_2 + H_2O = SO_4^{-2} + 2\ H^+$
16	-10	$S_4^{-2} + 1.5\ O_2 = S_2O_3^{-2} + 0.25\ S_8$
9	-9	$H_2S + 2\ O_2 = SO_4^{-2} + 2\ H^+$
19	-9	$S_2O_3^{-2} + OH^- = SO_4^{-2} + HS^-$
18	-6	$S_5^{-2} + 3\ OH^- = S_2O_3^{-2} + 3\ HS^-$
11	-6	$H_2S + 0.5\ O_2 = S_8 + H_2O$
15	-5	$0.5\ S_8 + 4\ H_2O = 3\ HS^- + SO_4^{-2} + 5\ H^+$
10	-5	$2\ H_2S + 2\ O_2 = S_2O_3^{-2} + H_2O + 2\ H^+$
4	-4	$S_2O_3^{-2} + H_2O = SO_4^{-2} + H_2S$
25	-3	$S_2O_3^{-2} + H^+ = S_8 + HSO_3^-$
7	-2	$4\ S_8 + 4\ H_2O = SO_4^{-2} + 3\ H_2S + H^+$

For Cinder Pool, energy from 21 of the 28 calculated reactions is energonic, having some large negative ΔG_r values for a number of the reactions (Table 4.3.6). It is interesting to note that the reaction between S_5^{2-} and aqueous hydrogen gas yield the largest amount of energy in the system.

Table 4.3.6. Reaction providing energy to Cinder Pool $\Delta G_r/e^-$.(kJ/mol).

Reaction #	$\Delta G_r/e^-$	Reaction
21	-42	$S_5^{-2} + 4\ H_2 = 5\ HS^- + 3\ H^+$
20	-42	$S_4^{-2} + 3\ H_2 = 4\ HS^- + 2\ H^+$
12	-41	$H_2 + 0.5\ O_2 = H_2O$
3	-40	$5\ S_2O_3^{-2} + H_2O + 4\ O_2 = 6\ SO_4^{-2} + 2\ H^+ + 4\ S_8$
2	-36	$S_2O_3^{-2} + 2\ O_2 + H_2O = 2\ SO_4^{-2} + 2\ H^+$
8	-34	$S_8 + H_2 = H_2S$
6	-33	$S_8 + 1.5\ O_2 + H_2O = SO_4^{-2} + 2\ H^+$
13	-29	$2\ S_5^{-2} + 2\ H^+ = 2\ HS^- + S_8$
16	-29	$S_4^{-2} + 1.5\ O_2 = S_2O_3^{-2} + 0.25\ S_8$
22	-29	$2\ S_4^{-2} + 4H^+ + O_2 = S_8 + 2\ H_2O$
9	-27	$H_2S + 2\ O_2 = SO_4^{-2} + 2\ H^+$
15	-27	$0.5\ S_8 + 4\ H_2O = 3\ HS^- + SO_4^{-2} + 5\ H^+$
18	-24	$S_5^{-2} + 3\ OH^- = S_2O_3^{-2} + 3\ HS^-$
5	-24	$S_2O_3^{-2} + 2\ H^+ + 4\ H_2 = 2\ H_2S + 3\ H_2O$
7	-21	$4\ S_8 + 4\ H_2O = SO_4^{-2} + 3\ H_2S + H^+$
10	-18	$2\ H_2S + 2\ O_2 = S_2O_3^{-2} + H_2O + 2\ H^+$
19	-18	$S_2O_3^{-2} + OH^- = SO_4^{-2} + HS^-$

1	-15	$SO_4^{-2} + 4\ H_2 + 2\ H^+ = H_2S + 4\ H_2O$
4	-9	$S_2O_3^{-2} + H_2O = SO_4^{-2} + H_2S$
11	-8	$H_2S + 0.5\ O_2 = S_8 + H_2O$
25	-3	$S_2O_3^{-2} + H^+ = S_8 + HSO_3^-$

In a study done by Spear et al. (2003), Aquificales Hydrogenobaculum spp. was found to dominate the system, making up the entire microbial population and using reaction 12 for metabolic energy. From our calculations, it seems possible that microbial populations in Cinder Pool could gain significant metabolic energy through the use of polysulfides and aqueous hydrogen gas (reactions 20 and 21).

4.3.10 Importance of In Situ Redox Chemistry to Microbial Culturing

Microbial samples collected from the hot springs of Yellowstone National Park were cultured using oxygen as the terminal electron acceptor and the redox species sulfide, thiosulfate, wackenroeder solution, and $FeCO_3$ as the substrate. The DNA from these cultures was extracted and amplified using PCR. Of the 26 microbial cultures collected from the hot springs visited, 14 grew (Table 4.3.7) on the media they were provided and were able to be amplified with the selected universal bacteria primers.

Table 4.3.7. Microbial samples cultured from Yellowstone's Hot Springs.

Sample Name	YNP Hot Spring	Site within hot spring	Media and Substrate
RS-172	Realgar Spring	Site 3, green biofilm before convergence with red stream	½ Beowolf ½ site H_2O
RS-178 (Sulfide)	Realgar Spring	Site 5, downstream filaments	½ Beowolf ½ site H_2O (Sulfide)
MM-125 (FeCO3)	Mini Primrose	Pool 1	½ Beowolf ½ site H_2O ($FeCO_3$)
MM-125	Mini Primrose	Pool 1	½ Beowolf ½ site H_2O

Sample Name	YNP Hot Spring	Site within hot spring	Media and Substrate
MM-126 (Sx)	Mini Primrose	Pool 1	½ Beowolf ½ site H_2O Wackenroeder
MM-128	Mini Primrose	Pink edge of pool 1	½ Beowolf ½ site H_2O
MM-130 (S_2O_3)	Mini Primrose	Pool 4	½ Beowolf ½ site H_2O (S_2O_3)
MM-131 ($FeCO_3$)	Mini Primrose	Pool 4	½ Beowolf ½ site H_2O ($FeCO_3$)
MM-132 (Sx)	Mini Primrose	Pool 4	½ Beowolf ½ site H_2O Wackenroeder
MM-133 (Sx)	Mini Primrose	Pool 2	½ Beowolf ½site H_2O Wackenroeder
MM-134 ($FeCO_3$)	Mini Primrose	Pool 2	½ Beowolf ½ site H_2O ($FeCO_3$)
MM-134 (Dup)	Mini Primrose	Pool 2	½ Beowolf ½ site H_2O ($FeCO_3$)
MM-135 (Sulfide)	Mini Primrose	Pool 2	½ Beowolf ½ site H_2O (Sulfide)
CP-163 (Sx)	Cinder Pool	Pool water under cinders	½ Beowolf ½ site H_2O Wackenroeder

Restriction digests using three restriction enzymes were run to cut the PCR product into small fragments for T-RFLP analysis. Comparing the similarity of the T-RFLP results can help determine whether using different substrates for microbial culturing shifted the microbial community fingerprint, represented by the presence or absence fragments of a certain base pair fragment size. The Jaccard Index is mainly used as a statistical approach for assessing the similarity of species in biodiversity studies (Chao et al., 2005); however, it can be useful in determining the similarity between microbial communities cultured using different substrates (Mummey and Stahl, 2003). The microbial cultures from Yellowstone National Park were compared using the Jaccard Index and the results

are presented in Table 4.3.8. The Jaccard Index is a measure of similarity varying from 0 to 1, where a Jaccard Index of 1 would indicate an identical match and 0 would indicate that there is nothing shared between the two samples. Field duplicates of sample MM-134 were collected from the same location, cultured under the same conditions, and run through the same PCR and T-RFLP process simultaneously, and these samples were calculated to be 62% similar to one another (Table 4.3.8) after binning the data by two base pairs per bin. It is expected that a cultured field duplicate would not be identical, because of the existence of multiple microbial communities in a sample. The DNA extracted from sample MM-131 was diluted 10 times and 100 times before PCR was run and were found to be 61-65% similar (Table 4.3.8), after binning data by two base pairs. Previous studies have shown that decreasing the DNA concentration in PCR by dilution will decrease the number of 5'-termainal restriction fragments in a T-RFLP sample (Osborn et al., 2000). These missing peaks in diluted samples would explain why identical samples that were diluted before PCR do not have a Jaccard Index close to 1. Since there was no control used in this set of experiments, the error associated with the Jaccard index is unknown and other information must be used to assess the similarity between microbial samples.

Table 4.3.8 Jaccard Index of Yellowstone's Microbial Samples T-RFLP results.

	RS-178 (Sulfide)	RS-172	CP-163 (Sx)	MM-132 (Sx)	MM-130 (S2O3)	MM-131 (FeCO3)	MM-131 (FeCO3)	MM-131 (FeCO3)	MM-135 (Sulfide)	MM-134 (FeCO3)	MM-134 (FeCO3)	MM-133 (Sx)	MM-128	MM-126 (Sx)	MM-125 (FeCO3)
MM-125 (FeCO3)															
MM-126 (Sx)															0.33
MM-128														0.30	0.38
MM-133 (Sx)													0.35	0.49	0.45
MM-134 (FeCO3)												0.49	0.43	0.42	0.31
MM-134 (FeCO3)											0.62	0.51	0.46	0.50	0.35
MM-135 (Sulfide)										0.41	0.33	0.33	0.31	0.67	0.31
MM-131 (FeCO3)									0.30	0.47	0.49	0.45	0.48	0.40	0.35
MM-131 (FeCO3)								0.63	0.32	0.46	0.61	0.44	0.52	0.39	0.26
MM-131 (FeCO3)							0.65	0.61	0.31	0.53	0.59	0.47	0.45	0.41	0.29
MM-130 (S2O3)						0.31	0.38	0.33	0.64	0.38	0.33	0.49	0.28	0.70	0.31
MM-132 (Sx)					0.67	0.38	0.41	0.36	0.64	0.47	0.42	0.49	0.35	0.66	0.38
CP-163 (Sx)				0.47	0.37	0.53	0.55	0.52	0.40	0.53	0.64	0.47	0.45	0.44	0.38
RS-172			0.63	0.40	0.40	0.53	0.50	0.47	0.50	0.57	0.54	0.61	0.41	0.50	0.38
RS-178 (Sulfide)		0.53	0.59	0.40	0.30	0.53	0.55	0.57	0.30	0.49	0.45	0.47	0.50	0.34	0.46

A microbial program that compares and assesses T-RFLP data based on the restriction enzymes used can be used for another comparison between microbial community fingerprints. A database from MICA is input into the program and is used to assess T-RFLP results. The information this database uses to assess T-RFLP data is the base pair size of the fragments and the percentage of the sample that falls into that base pair size. Sequenced microbial communities from the MICA database were compared to our T-RFLP results. Uncultured iron oxidizers dominate in the samples that were given an $FeCO_3$ substrate; however, no sulfur oxidizers were found in samples given sulfur species substrates. Microbial cultures may have been left too long in culture and run out of substrate, allowing another microbial community such as heterotrophs to take over. These microorganisms could utilize the original culture microorganisms as a food source for growth and destroy the validity of the samples.

Results from this study are not appropriate to discuss culturing technique successes, as it is still unknown whether the substrate used for culturing will effect the microbial community being cultured. Methods and lessons learned from this study can be used as a base point for a future study. I would recommend that procedures for culturing be carefully analyzed before a future study is done. Sampling procedures and DNA extraction procedures from this study can still be followed; however, the procedure for restriction digests should be examined. Each sample should be run with only one restriction enzyme each before adding multiple enzymes together. This may help resolve some of the errors associated with so many fragments in T-RFLP results.

4.4 Conclusion

Using Au-amalgam microelectrodes to determine the existence of sulfide, polysulfide, elemental sulfur, and thiosulfate *in situ* is useful in better defining sulfur cycling in natural environments. The quantification of polysulfide is possible through careful calibrations of microelectrodes with pure standards. The ability to determine and quantify polysulfide is an important step to understanding complex sulfur systems, such as Cinder Pool, where polysulfide may have been overlooked in the past due to the inability to determine its presence. Defining polysulfide in microbial habitats could lead to culturing novel organisms that use polysulfide as a substrate. Energetic calculations involving intermediate sulfur species provide adequate energy for microbial metabolism and proper culturing techniques using polysulfide as a substrate and hydrogen as an electron acceptor may yield novel microorganisms.

Concentrations of substrates that are added to microbial cultures can be defined by the concentration found in the natural environment from the location where the microbial sample was taken from, through the use of Au-amalgam microelectrodes. This can guide the selection of one microbial community over another in environmental samples and help to study microbial community shifts due to substrate selection.

Comprehensive Bibliography

Aiuppa, A., D'Alessandro, W., Federico, C., Palumbo, B., and Valenza, M., 2003, The aquatic geochemistry of arsenic in volcanic groundwaters from southern Italy: Applied Geochemistry, v. 18, p. 1283-1296.

Allen, E.T. and Day, A.L., 1935, Hot springs of the Yellowstone National Park: Carnegie Institution of Washington Publication Number 466, 525 p.

Allen, E.T., 1936, The hot springs of the Yellowstone National Park: Carnegie Institution of Washington News Service Bull. School ed., v. 4, p. 1-20.

Amend, J.P. and Shock, E.L., 2001, Energetics of overall metabolic reactions of thermophilic and hyperthermophilic Archaea and Bacteria: FEMS Microbiology Reviews, v. 25, p. 175-243.

Amend, J.P., Rogers, K.L., Shock, E.L., Gurrieri, S., and Inguaggiato, S., 2003, Energetics of chemolithoautotrophy in the hydrothermal system of Vulcano Island, southern Italy: Geobiology, v. 1, p. 37-58.

Amirbahman, A., Kent, D.B., Curtis, G.P., and Davis J.A., 2006, Kinetics of sorption and abiotic oxidation of arsenic(III) by aquifer materials: Geochimica et Cosmochimica Acta, v. 70, p. 533-547.

Anderson, G.L., Williams, J., and Hille, R., 1992, The purification and characterization of arsenite oxidase from *Alcaligenes faecalis*, a molybdenum-containing hydroxylase: Journal of Biological Chemistry, v. 267, p. 23674-23682.

Arai, Y., Elzinga, E.J., and Sparks, D.L., 2001, X-ray absorption spectroscopic investigation of arsenite and arsenate at the aluminum oxide-water interface: Journal of Colloid Interface Science, v. 235, p. 80-88.

Archer, D., Emerson, S., and Reimers, C., 1989, Dissolution of calcite in deep-sea sediments - pH and O_2 microelectrode results: Geochimica et Cosmochimica Acta, v. 53, p. 2831-2845.

Ball, J. W., Nordstrom, D.K., Jenne, E.A., and Vivit, D.V., 1998, Chemical Analyses of Hot Springs, Pools, Geysers, and Surface Waters from Yellowstone National Park, Wyoming, and Vicinity, 1974-1975: U.S. Geological Survey Open-File Report 98-182, 45 p.

Ball, J.W., Nordstrom, D.K., McCleskey, R.B., Schoonen, M.A.A., and Xu, Y., 2001, Water-Chemistry and On-Site Sulfur-Speciation Data for Selected Springs in Yellowstone National Park, Wyoming, 1996-1998: U.S. Geological Survey Open-File Report 01-49, 42 p.

Ball, J.W., McKleskey, R.B., Nordstrom, D.K., Holloway, J.M., and Verplanck, P.L., 2002, Water-chemistry data for selected springs, geysers, and streams in Yellowstone National Park, Wyoming, 1999–2000: with a section on activity of thermal features of Norris Geyser Basin, 1998 by S.A. Sturtevant: U.S. Geological Survey, Open-file Report 02-382.

Ballantyne, J. and Moore, J., 1988, Arsenic geochemistry in geothermal systems: Geochimica et Cosmochimica Acta, v. 52, p. 475-483.

Banciu, H., Sorokin, D.Y., Kleerebezem, R., Muyzer, G., Galinski, E.A., and Kuenen, J.G., 2004, Growth kinetics of haloalkaliphilic, sulfur-oxidizing bacterium Thioalkalivibrio versutus strain ALJ 15 in continuous culture: Extremophiles, v. 8, p. 185–192.

Barns, S., Fundyga, R., Jeffries, M., and Pace, N., 1994, Remarkable archaeal diversity detected in a Yellowstone-National-Park hot-spring environment: Proceedings of the National Academy of Sciences of the United States of America, v. 91, p. 1609-1613.

Batley, G.E. and Gardner, D., 1978, Copper, lead and cadmium speciation in some estuarine and coastal marine waters: Estuarine Coastal Marine Science, v. 7, p. 59-70.

Bernhard, J.M., Visscher, P.T., and Bowser, S.S., 2003, Submillimeter life positions of bacteria, protists, and metazoans in laminated sediments of the Santa Barbara Basin: Limnology and Oceanography, v. 42, p. 813-828.

Blank, C.E., Cady, S.L., Pace, N.R., 2002, Microbial composition of near-boiling silica depositing thermal springs throughout Yellowstone National Park: Applied and Environmental Microbiology, v. 68, p. 5123–5135.

Brannon, J.M., and Patrick, W.H., 1987, Fixation, transformation, and mobilization of arsenic in sediment: Environmental Science and Technology, v. 21, p. 450-459.

Brendel, P.J. and Luther, G.W., 1995, Development of a gold amalgam voltammetric microelectrode for the determination of dissolved Fe, Mn, O_2, and S^{-2} in porewaters of marine and fresh-water sediments: Environmental Science and Technology, v. 29, p. 751-761.

Brock, T.D., 1978, Thermophilic Microorganisms and Life at High Temperatures: Springer-Verlag, New York.

Buisman, C., IJspeert, P., Janssen, A., and Lettinga, G., 1990, Kinetics of chemical and biological sulfide oxidation in aqueous solutions: Water Research, v. 24, p. 667–671.

Burgess, J.E., Parsons, S.A., and Stuetz, R.M., 2001, Developments in odor control and waste gas treatment biotechnology: a review: Biotechnology Advances, v. 19, p. 35–63.

Burggraf, S., Jannasch, H. W., Nicolaus, B. and Stetter, K. O., 1990, *Archaeoglobus profundus* sp. nov., represents a new species within the sulfur-reducing *Archaebacteria*: Systematic and Applied Microbiology, v. 13, p. 24-28.

Cai, W.J. and Reimers, C.E., 1993, The development of pH and pCO2 microelectrodes for studying the carbonate chemistry of pore waters near the sediment-water interface: Limnology and Oceanography, v. 38, p. 1762-1773.

Cai , W.J. and Reimers, C.E., 1995, Benthic oxygen flux, bottom water oxygen concentration and core top organic carbon content in the deep northeast Pacific Ocean: Deep-Sea Research Part I-Oceanographic Research Papers, v. 42, p. 1681-1699.

Capodaglio, G., Coale, K., and Bruland, K., 1990, Lead speciation in surface waters of the eastern north pacific: Marine Chemistry, v. 29, p. 221-233.

Chao, A., Chazdon, R. L., Colwell, R. K., and Shen, T.J, 2005, A new statistical approach for assessing compositional similarity based on incidence and abundance data: Ecology Letters, v. 8, p. 148-159.

Chen, K.Y. and Morris, J.C., 1972, Kinetics of oxidation of aqueous sulfide by O_2: Environmental Science and Technology, v. 6, p. 529–537.

Cherry, J.A., Shaik, A.U., Tallman, D.E. and R.V. Nicholson, 1979, Arsenic species as an indicator of redox conditions in groundwater: Journal of Hydrology, v. 43, p. 373-392.

Christiansen, R., 2001, The geology of Yellowstone National Park: The Quaternary and Pliocene Yellowstone plateau volcanic field of Wyoming, Idaho, and Montana, U.S. Geological Survey Professional Paper 729-G, 145p.

Chui, V.Q., and Hering, J.G., 2000, Arsenic adsorption and oxidation at manganite surface. 1. Method for simultaneous determination of adsorbed and dissolved arsenic species: Environmental Science and Technology, v. 34, p. 2029-2034.

Ciglenecki, I., Kodba, Z., and Cosovic, B., 1996, Sulfur species in Rogoznica Lake: Marine Chemistry, v. 53, p. 101-110.

Craig, H.B. and White, D.E., 1956, Isotope geochemistry of thermal waters: National Academy Science National Research Council Publication 400, p. 29-39.

Cummings, D.E., Caccavo Jr., F., Fendorf, S., and Rosenzweig, R.F., 1999, Arsenic mobilization by the dissimilatory Fe(III)-reducing bacterium *Shewanella alga* BrY: Environmental Science and Technology, v. 33, p. 723-729.

deBeer, D., Schramm, A., Santegoeds, C.M., and Kuhl, M., 1997, A nitrite microsensor for profiling environmental biofilms: Applied and Environmental Microbiology, v. 63, p. 973-977.

de Beer, D. and Vandenheuval, J.C., 1988, Response of ammonium-selective microelectrodes based on the neutral carrier nonactin: Talanta, v. 35, p. 728-730.

Dixit, S., and Hering, J.G., 2003, Comparison of arsenic(V) and arsenic(III) sorption onto iron oxide minerals: implications for arsenic mobility: Environmental Science and Technology, v. 37, p. 4182-4189.

Donahoe-Christiansen, J., D'Imperio, S., Jackson, C., Inskeep, W., and McDermott, T., 2004, Arsenite oxidizing Hydrogenobaculum strain isolated from an acid-sulfate-chloride geothermal spring in Yellowstone National Park: Applied and Environmental Microbiology, v. 70, p. 1865-1868.

Druschel, G.K., Schoonen, M.A.A., Nordstrom, D.K., Ball, J.W., Xu, Y., and Cohn, C.A., 2003, Sulfur geochemistry of hydrothermal waters in Yellowstone National Park, Wyoming, USA. III. An anion-exchange resin technique for sampling and preservation of sulfoxyanions in natural waters: Geochemical Transactions, v. 4, p. 12-19.

Druschel, G.K., Sutka, R., Emerson, D., Luther, G.W., Kraiya, C., and Glazer., B., 2004, Voltammetric investigation of Fe-Mn-S species in a microbially active wetland, *in* Wanty, R.B., and Seal, R.R., eds., Eleventh International Symposium on Water-Rock Interaction WRI-11, Volume 2: Saratoga Springs, NY USA, Balkema, p. 1191-1194.

Eckert, W. and Truper, H.G., 1993, Microbially-related redox changes in a subtropical lake .1. In-situ monitoring of the annual redox cycle: Giogeochemistry, v. 21, p. 1-19.

Electrochemistry Dictionary, 2006, http://electrochem.cwru.edu/ed/dict.htm.

Ellis, A.J. and Mahon, W.A.J., 1964, Natural hydrothermal systems and experimental hot water/rock interactions (Pt I.): Geochimica et Cosmochimica Acta, v. 28, p. 1323–1357.

Ellis, A.J. and Mahon, W.A.J., 1967, Natural hydrothermal systems and experimental hot water/rock interactions (Pt II.): Geochimica et Cosmochimica Acta, v. 31, p. 519–538.

Ellis, A.J. and Mahon, W.A.J., 1977, Chemistry and geothermal systems: Academic Press, New York, 392 p.

Emett, M., and Khoe, G., 2001, Photochemical oxidation of arsenic by oxygen and iron in acidic solutions: Water Research, v. 35, p. 649-656.

Ewers, G.R. and Keays, R.R., 1977, Volatile and precious metal zoning in the Broadlands Geothermal Field, New Zealand: Economic Geology, v. 72, p. 1337-1354.

Feeney, R., and Kounaves, S., 2000, Microfabricated ultramicroelectrode arrays: Developments, advances, and applications in environmental analysis: Electroanalysis, v. 12, p. 677-684.

Feeney, R., Kounaves, S.P, 2000, On-site analysis of arsenic in groundwater using a microfabricated gold ultramicroelectrode array: Analytical Chemistry, v. 72, p. 2222-2228.

Feeney, R., Kounaves, S.P., 2002, Voltammetric measurement of arsenic in natural waters: Talanta, v. 58, p. 23-31.

Federal Register, 2001, National Primary Drinking Water Regulations; Arsenic and Clarifications to Compliance and New Source Contaminants Monitoring: 40CFR Parts 141 and 142, v. 66, p. 42974-42975

Ferreira, M., and Barros, A., 2002, Determination of As(III) and arsenic(V) in natural waters by cathodic stripping voltammetry at a hanging mercury drop electrode: Analytica Chimica Acta, v. 459, p. 151-159.

Fishbain, S., Dillon, J., Gough, H., and Stahl, D., 2003, Linkage of high rates of sulfate reduction in Yellowstone hot springs to unique sequence types in the dissimilatory sulfate respiration pathway: Applied and Environmental Microbiology, v. 69, p. 3663-3667.

Florence, T., 1986, Electrochemical aproaches to trace-element speciation in waters- a review: Analyst, v. 111, p. 489-505.

Forsberg, G., O'Laughlin, J.W., and Megargle, R.G., 1975, Determination of Arsenic by Anodic Stripping Voltammetry and Differential Pulse Anodic Stripping Voltammetry: Analytical Chemistry, v. 47, p. 1586-1592.

Fournier, R.O., 1989, Geochemistry and dynamics of the Yellowstone National Park hydrothermal system: Annual Review of Earth and Planetary Sciences, v. 17, p. 13-53.

Fournier, R.O., Thompson, J.M., and Hutchinson, R.A., 1992, The geochemistry of hot spring waters at Norris Geyser Basin, Yellowstone National Park, USA, in Kharaka, Y.K. and Maest, A.S., eds., Proceedings, 7th International Symposium on Water-Rock Interaction, Park City, Utah, p. 1289-1292.

Francesconi, K., and Kuehnelt, D., 2004, Determination of arsenic species: A critical review of methods and applications, 2000-2003: Analyst, v. 129, p. 373-395.

Gerischer, H., 1949, Uber die Auflo¨sungsgeschwindigkeit von Schwefel in Sulfide und Polysulfidlosungen: Journal of Inorganic and General Chemistry, v. 259, p. 220.

Giggenbach W., 1971, Optical spectra of highly alkaline sulfide solutions and the second dissociation constant of hydrogen sulfide: Inorganic Chemistry, v. 10, p. 1333–1338.

Gigganbach, W., 1974, Equilibria involving polysulfide ions in aqueous sulfide solutions up to 240ºC: Inorganic Chemistry, v. 13, p. 1724-1730.

Gihring, T.M., Druschel, G.K., McCleskey, R.B., Hamers, R.J., and Banfield, J.F., 2001, Rapid arsenic oxidation by *Thermus aquaticus*and *Thermus thermophilus*: Field and laboratory investigations: Environmental Science and Technology, v. 35, p. 3857-3862.

Ginzburg, B., Dor, I., Chalifa, I., Hadas, O., and Lev, O., 1999, Formation of dimethyloligosulfides in Lake Kinneret: Biogenic formation of inorganic oligosulfide intermediates under oxic conditions: Environmental Science and Technology, v. 33, p. 571-579.

Glud, R., Gundersen, J., Revsbech, N., and Jorgensen, B., 1994, Effects on the benthic diffusive boundary-layer imposed by microelectrodes: Limnology and Oceanography, v. 39, p. 462-467.

Gooch, F.A. and Whitfield, J.E., 1888, Analysis of the waters of the Yellowstone National Park, with an account of methods of analysis employed: U.S. Geological Survey Bulletin 47. 84p.

Gnaiger E., Forstner H., 1983, Polarographic oxygen sensors. Aquatic and physiological applications. Berlin, Heidelberg, New York. Springer Verlag.

Graber, J.R., Kirshtein, J., Speck, M., Reysenbach, A.L., 2001, Community structure along a thermal gradient in a stream near Obsidian Pool, Yellowstone National Park. In Thermophiles: Biodiversity, Ecology and Evolution (eds Reysenbach AL Voytek M, Mancinelli R). Klewer Academic/Plenum Publishers, New York, pp. 81–89. Microbiology, v. 180, p. 60–68.

Greulach, U., and Henze, G., 1995, Analysis of arsenic(V) by cathodic stripping voltammetry: Analytica Chimica Acta, v. 306, p. 217-223.

Gundersen, J. and Jorgensen, B., 1990, Microstructure of diffusive boundary-layers and the oxygen-uptake of the sea-floor: Nature, v. 345, p. 604-607.

Gundersen, J., Jorgensen, B., Larsen, E., and Jannasch, H., 1992, Mats of giant sulfur bacteria on deep-sea sediments due to fluctuating hydrothermal flow: Nature, v. 360, p. 454-456.

Gunter, B.D., Musgrave, B.C., 1966, Gas chromatographic measurements of hydrothermal emanations at Yellowstone National Park: Geochimica Cosmochimica Acta, v. 30, p. 1175-1189.

Hague, A., 1911, Origin of the thermal waters of the Yellowstone Park: Bulletin for Geological Society of America, v. 22, p. 103-119.

Hartler, N., Libert, J., and Teder, A., 1967, Rate of sulfur dissolution in aqueous sodium sulfide: Industrial and Engineering Process Design and Development, v. 6, p. 398.

Heinrich, C. and Eadington, P., 1986, Thermodynamic predictions of the hydrothermal chemistry of arsenic and their significance for the paragenetic sequence of some cassiterite-arsenopyrite-base metal sulfide deposits: Economic Geology, v. 81, p. 511-529.

Helz, G., Tossell, J., Charnock, J., Pattrick, R., Vaughan, D., and Garner, C., 1995, Oligomerization in As(III) sulfide solutions - Theoretical constraints and spectroscopic evidence: Geochimica et Cosmochimica Acta, v. 59, p. 4591-4604.

Henneke, E., Luther, G., and Delange, G., 1991, Determination of inorganic sulfur speciation with polarographic techniques- some preliminary-results for recent hypersaline anoxic sediments: Marine Geology, v. 100, p. 115-123.

Herdan, J., Feeney, R., Kounaves, S., Flannery, A., Storment, C., Kovacs, G., and Darling, R., 1998, Field evaluation of an electrochemical probe for in situ screening of heavy metals in groundwater: Environmental Science and Technology, v. 32, p. 131-136.

Hitchman, M., 1978, Measurement of Dissolved Oxygen: Chemical Analysis, v. 49, New York: John Wiley & Sons.

Holak, W., 1980, Determination of Arsenic by Cathodic Stripping Voltammetry with a Hanging Mercury Drop Electrode: Analytical Chemistry, v. 52, p. 2189-2192.

Huber, R., Eder, W., Heldwein, S., Wanner, G., Huber, H., Rachel, R., and Stetter, K., 1998, Thermocrinis ruber gen. nov., sp. nov., a pink-filament-forming hyperthermophilic bacterium isolated from Yellowstone National Park: Applied and Environmental Microbiology, v. 64, p. 3576-3583.

Hugenholtz, P., Pitulle, C., Hershberger, K.L., and Pace, N.R., 1998, Novel division level bacterial diversity in a Yellowstone hot spring: Journal of Bacteriology, v. 180, p. 366–376.

Hung, D., Nekrassova, O., and Compton, R., 2004, Analytical methods for inorganic arsenic in water: a review: Talanta, v. 64, p. 269-277.

Inskeep, W.P., Macur, R.E., Harrison, G., Bostick, B.C., and Fendorf, S., 2004, Biomineralization of As(V)-hydrous ferric oxyhydroxide in microbial mats of an acid-sulfate-chloride geothermal spring, Yellowstone National Park: Geochimica et Cosmochimica Acta, v. 68, p. 3141-3155.

Janssen, A., de Keizer, A., van Aelst, A., Fokkink, R., Yangling, H., and Lettinga, G., 1996, Surface characteristics and aggregation of microbiologically produced sulphur particles in relation to the process conditions. Colloids Surface B: Biointerfaces, v. 6, p. 115.

Janssen, A.J.H., Lettinga, G., and de Keizer, A., 1999, Removal of hydrogen sulphide from wastewater and waste gases by biological conversion to elemental sulphur. Colloidal and interfacial aspects of biologically produced sulphur particles. Colloids Surface A—Physicochemical Engineering Aspects, v. 151, p. 389–397.

Jeanthon, C., L'Haridon, S., Cueff, V., Banta, A., Reysenbach, A.L., Prieur, D., 2002, Thermodesulfobacterium hydrogeniphilum sp nov., a thermophilic, chemolithoautotrophic, sulfate-reducing bacterium isolated from a deep-sea hydrothermal vent at Guaymas Basin, and emendation of the genus Thermodesulfobacterium: International Journal of Systematic and Evolutionary Microbiology, v. 52, p. 765-772.

Jensen, K., Revsbech, N.P., and Nielsen, L.P., 1993, Microscale distribution of nitrification activity in sediment determined with a shielded microsensor for nitrate: Applied and Environmental Microbiology, v. 59, p. 3287-3296.

Jeroschewski, P. and Braun, S., 1996, A flow analysis system with an amperometric detector for the determination of hydrogen sulphide in waters: Fresenius Journal of Analytical Chemistry, v. 354, p. 169-172.

Jeroschewski, P., Sollig, M., and Berge, H., 1988, Amperometric dtermination of hydrogen-sulfide: Zeitschrift fur Chemie, v. 28, p. 75-75.

Ji, G., Silver, S., Garber, A.E., Ohtake, C., Cervantes, C., and Corbisier, P., 1983, Bacterial molecular genetics and enzymatic transformations of arsenate, arsenite, and chromate, p. 529-539. *In* Torma, A.E., Apel, M.L., and Brierly, C.L.(ed.), Biohydrometallurgical techniques. The Minerals, Metals, and Materials Society, Warrendale, Pa.

Johnston, F. and McAmish, L., 1973, A study of the rates of sulfur production in acid thiosulfate solutions using S-35. Journal of Colloid. Interf. Science, v. 42, p. 112–119.

Kamyshny, A., Goifman, A., Rizkov, D., and Lev, O., 2003, Kinetics of disproportionation of inorganic polysulfides in undersaturated aqueous solutions at environmentally relevant conditions: Aquatic Geochemistry, v. 9, p. 291-304.

Kariuki, S., Morra, M.J., Umiker, K.J., and Cheng, I.F., 2001, Determination of total polysulfides by differential pulse polarography: Analytica Chimica Acta, v. 442, p. 277-285.

Kester, D.R., 1975, Dissolved gasses other than CO: In J. P. Riley and G. Skirrow (eds.), Chemical Oceanography, Academic Press, London, v. 1, Chap. 8. p. 497-556.

Kim, J., Korshin, G.V., Frenkel, A.I., and Velichenko, A.B., 2006, Electrochemical and XAFS studies of effects of carbonate on the oxidation of Arsenite: Environmental Science and Technology, v. 40, p. 228-234.

Kleinjan, W.E., de Keizer, A., Janssen, A.J.H., 2005a, Kinetics of the chemical oxidation of polysulfide anions in aqueous solution: Water Research, v. 39, p. 4093-4100.

Kleinjan, W.E., de Keizer, A., Janssen, A.J.H., 2005b, Kinetics of the reaction between dissolved sodium sulfide and biologically produced sulfur: Industrial and Engineering Chemistry Research, v. 44, p. 309–317.

Kotoucek, M., Vasicova, J., and Ruzicka, J., 1993, Determination of arsenic by cathodic stripping voltammetry at a hanging mercury drop electrode: Mikrochimica Acta, v. 111, p. 55-62.

Kounaves, S.P., 1997, "Voltammetric Techniques", in Handbook of Instrumental Techniques for Analytical Chemistry, F.A.Settle (Ed.) Prentice Hall PTR, Upper Saddle River, NJ.

Kuhl, M., Steuckart, C., Eickert, G., and Jeroschewski, P., 1998, A H_2S microsensor for profiling biofilms and sediments: application in an acidic lake sediment: Aquatic Microbial Ecology, v. 15, p. 201-209.

Kumaresan, M., and Riyazuddin, P., 2001, Overview of speciation chemistry of arsenic: Current Science, v. 80, p. 837-846.

Lane, D.J., 1991, 16S/23S rRNA sequencing. In nucleic acid techniques in bacterial systematics, ed. E. Stackebrandt and M. Goodfellow, NewYork: John Wiley and Sons, p. 115-175.

Larsen, L.H., Kjaer, T., and Revsbech, N.P., 1997, A microscale NO3- biosensor for environmental applications: Analytical Chemistry, v. 69, p. 3527-3531.

Li, H., and Smart, R., 1996, Determination of sub-nanomolar concentration of arsenic(III) in natural waters by square wave cathodic stripping voltammetry: Analytica Chimica Acta, v. 325, p. 25-32.

Luther G. W. III, 1990, The frontier-molecular-orbital theory approach in geochemical Processes: In Aquatic Chemical Kinetics (ed. W. Stumm), pp. 173–198. Wiley.

Luther, G.W. III, Brendel, P.J., Lewis, B.L., Sundby, B., Lefrancois, L., Silverberg, N., and Nuzzio, D.B., 1998, Simultaneous measurements of O_2, Mn, Fe, I^-, and S(-II) in marine pore waters with a solid-state voltammetric microelectrode. Limnology Oceanography, v. 43, p. 325– 333.

Luther, G.W. III, Giblin, A.E., and Versolona, R., 1985, Limnology Oceanography, v. 30, p. 727.

Luther, G.W., Glazer, B.T., Hohmann, L., Popp, J.I., Taillefert, M., Rozan, T.F., Brendel, P.J., Theberge, S.M., and Nuzzio, D.B., 2001, Sulfur speciation monitored in situ with solid state gold amalgam voltammetric microelectrodes: polysulfides as a special case in sediments, microbial mats and hydrothermal vent waters: Journal of Environmental Monitoring, v. 3, p. 61-66.

Luther, G.W., Glazer, B., Ma, S., Trouwborst, R.E., Moore, T.S., Kraiya, C., Waite, T.J., Druschel, G., Sundby, B., Taillefert, M., Nuzzio, D.B., and Shank, T.M., 2005, Use of voltammetric solid-state (micro)electrodes for studying biogeochemical processes: laboratory measurements to real time measurements with an in situ electrochemical analyzer (ISEA). Marine Chemistry.

Luther, G., Reimers, C., Nuzzio, D., and Lovalvo, D., 1999, In situ deployment of voltammetric, potentiometric. and amperometric microelectrodes from a ROV to determine dissolved O-2, Mn, Fe, S(-2), and pH in porewaters: Environmental Science and Technology, v. 33, p. 4352-4356.

Luther, G.W. III, Shellenbarger, P.A., and Brendel, P.J., 1996, Dissolved organic Fe(III) and Fe(II) complexes in salt marsh porewaters: Geochimica et Cosmochimica Acta, v. 60, p. 951–960.

Mambote, R., Krijgsman, P., and Reuter, M., 2003, Hydrothermal precipitation of arsenic compounds in the ferric-arsenic (III)-sulfate system: thermodynamic modeling: Minerals Engineering, v. 16, p. 429-440.

Manning, B.A., Fendorf, S.E., and Goldberg, S., 1998, Surface structures and stability of arsenic(III) on goethite: spectroscopic evidence for inner-sphere complexes: Environmental Science and Technology, v. 32, p. 2383-2388.

Manning, B.A., and Goldberg, S., 1997, Adsorption and stability of arsenic(III) at clay mineral-water interface: Environmental Science and Technology, v. 31, p. 2005-2011.

Mazor, E. and Fournier, R.O., 1973, More on noble gases in Yellowstone National Park hot waters: Geochimica Cosmochimica Acta, v. 37, p. 515-525.

Mazor, E. and Wasserburg, G.J., 1965, Helium, neon, argon, krypton, and xenon in gas emanations from Yellowstone and Lassen Volcanic National Parks: Geochimica Cosmochimica Acta, v. 29, p. 443-454.

McCleskey, R.B., Ball, J.W., Nordstrom, D.K., Holloway, J.M., and Taylor, H.E., 2005, Water-chemistry data for selected springs, geysers, and streams in Yellowstone National Park Wyoming, 2001-2002: U.S. Geological Survey Open-File Report 2004-1316, 94 p.

McCleskey, R., Nordstrom, D., and Maest, A., 2004, Preservation of water samples for arsenic(III/V) determinations: an evaluation of the literature and new analytical results: Applied Geochemistry, v. 19, p. 995-1009.

Meyer-Dombard, D., Price, R., Pichler, T., and Amend, J., 2004, Geochemical-microbial processes in hydrothermal sediments, Ambitle Island, Papua New Guinea: Geochimica et Cosmochimica Acta, v. 68, p. A410-A410.

Microbial Community Analysist III, 2005, http://mica.ibest.uidaho.edu/digest.php, University of Idaho.

Millero, F. J. and Sohn, M. L., 1992, Chemical Oceanography. CRC Press. Boca Raton, Ann Arbor, London: 531 p.

Mukhopadhyay, R., Rosen, B. P., Phung, L. T., and Silver, S., 2002, Microbial arsenic: from geocycles to genes and enzymes: FEMS Microbiol. Rev., v. **26,** p. 311-325.

Mummey, D.L. and Stahl, P.D., 2003, Spatial and temporal variability of bacterial 16S rDNA-based T-RFLP patterns derived from soil of two Wyoming grassland ecosystems: FEMS Microbiology Ecology, v. 46, p. 113.

Munoz, E., and Palmero, S., 2005, Analysis and speciation of arsenic by stripping potentiometry: a review: Talanta, v. 65, p. 613-620.

Myers, D.J., and Osteryoung, J., 1973, Determination of Arsenic(III) at the Parts-per Billion Level by Differential Pulse Polarography: Analytical Chemistry, v. 45, p. 267-271.

National Research Council, 1999. Arsenic in Drinking Water. National Academy Press, Washington, DC.

Newman, D.K., Ahmann, D., and Morel, F.M.M., 1998, A brief review of microbial arsenate respiration: Geomicrobiology, v. 15, p. 255-268.

Nolan, M.A. and Gaillard, J.F., 2002. Probing zinc speciation in contaminated sediments by square wave voltammetry at a Hg/Ir microelectrode. In: Taillefert, M., Rozan, T.F. (Eds.), Environmental Electrochemistry: Analyses of Trace Element Biogeochemistry, American Chemical Society, Symposium Series 811, Washington, DC, p. 210–226.

Nolan, M., and Kounaves, S., 2000, The source of the anomalous cathodic peak during ASV with in situ mercury film formation in chloride solutions: Electroanalysis, v. 12, p. 96-99.

Nunan, N., Wu, K., Young, I.M., Crawford, J.W. and Ritz, K., 2002, In situ spatial patterns of soil bacterial populations, mapped at multiple scales, in an arable soil: Microbiolgy and Ecology, v. 44, p. 296-305.

Nunan, N., Ritz, K., Crabb, D., Harris, K., Wu, K.J., Crawford, J.W. and Young, I.M., 2001, Quantification of the in situ distribution of soil bacteria by large-scale imaging of thin sections of undisturbed soil: FEMS Microbiolgy and Ecology, v. 37, p. 67-77.

Oremland, R., Kulp, T., Blum, J., Hoeft, S., Baesman, S., Miller, L., and Stolz, J., 2005, A microbial arsenic cycle in a salt-saturated, extreme environment: Science, v. 308, p. 1305-1308.

Oremland, R. and Stolz, J., 2005, Arsenic, microbes and contaminated aquifers: Trends in Microbiology, v. 13, p. 45-49.

Osborn, M., Moore, E.R.B., and Timmis, K.N., 2000, An evaluation of terminal restriction fragment length polymorphism (T-RFLP) analysis for the study of microbial community structure and dynamics: Environmental Microbioogy, v. 2, p. 39-50.

Oscarson, D.W., Huang, P.M., and Liaw, W.K., 1981, Role of manganese in the oxidation of arsenite by freshwater lake sediments: Clay Clay Minerals, v. 29, p. 219-225.

Pasiuk-Bronikowska, W., Ziajka, J., Bronikowski, T., 1992, In: Brimblecombe, P. (Transl. Ed.), Autoxidation of Sulphur Compounds. Ellis Horwood Limited, Chichester.

Piotrowicz, S., Springeryoung, M., Puig, J., and Spencer, M., 1982, Anodic-stripping voltammetry for evaluation of organic-metal interactions in sea-water: Analytical Chemistry, v. 54, p. 1367-1371.

Raven, P.R., Jain, A., and Loeppert, R.H., 1998, Arsenite and arsenate adsorption on ferrihydrite: Kinetics, equialbrium, and absorption envelopes: Environmental Science and Technology, v. 32, p. 344-349.

Reimers, C., Fischer, K., Merewether, R., Smith, K., and Jahnke, R., 1986, Oxygen microprofiles measured in situ in deep ocean sediments: Nature, v. 320, p. 741-744.

Reimers, C.E., 1987, An *in situ* microprofiling instrument for measuring interfacial pore water gradients: methods and oxygen profiles from the North Pacific Ocean: Deep-Sea Research, v. *34*, p. 2019-2035.

Revsbech, N., Nielsen, L., Christensen, P., and Sorensen, J., 1988, Combined oxygen and nitrous-oxide microsensor for denitrification studies: Applied and Environmental Microbiology, v. 54, p. 2245-2249.

Reysenbach, A. and Shock, E., 2002, Merging genomes with geochemistry in hydrothermal ecosystems: Science, v. 296, p. 1077-1082.

Reysenbach, A., Wickham, G., and Pace, N., 1994, Phylogenetic analysis of the hyperthermophilic pink filament community in octopus spring, Yellowstone-National-Park: Applied and Environmental Microbiology, v. 60, p. 2113-2119.

Rochette, E., Bostick, B., Li, G., and Fendorf, S., 2000, Kinetics of arsenate reduction by dissolved sulfide: Environmental Science and Technology, v. 34, p. 4714-4720.

Rosen, E. and Tegman, R., 1971, A Preparative and X-ray Powder Diffraction Study of the Polysulfides Na_2S_2, Na_2S_4, and Na_2S_5: Acta Chemica Scandinavica, v. 25: p. 3329-3336.

Roychoudhury, A.N., 2004, Sulfate respiration in extreme environments: A kinetic study: Geomicrobiology, v. 21, p. 33-43.

Rozan, T.F., Benoit, G., and Luther, G.W. III, 1999, Measuring metal sulfide complexes in oxic river waters with square wave voltammetry: Environmental Science and Technology, v. 33, p. 3021.

Rozan, T.F., Theberge, S.M., and Luther, G.W. III, 2000, Quantifying elemental sulfur (S^0), bisulfide (HS^-), and polysulfides (S_x^{2-}) using a voltammetric method: Analytica Chimica Acta, v. 415, p. 175-184.

Rubinson, K.A., Rubinson, J.F., 2000, Contemporary Instrumental Analysis. Prentice Hall: Upper Saddle River, NJ.

Sadana, R.S., 1983, Determination of arsenic in the presence of copper by differential pulse cathodic stripping voltammetry at a hanging mercury drop electrode: Analytical Chemistry, v. 55, p. 304–307.

Santini, J.M., Sly, L. I., Schnagl, R. D., and Macy, J. M. 2000, A new chemoautotrophic arsenite-oxidizng bacterium isolated from a gold mine: phylogenetic, physiological, and preliminary biochemical studies: Applied Environmental Microbiology, v. 66, p. 92 – 97.

Setchell, W.A., 1903, The upper temperature limits of life: Science, v. 17, p. 934–937.

Sharma, P., 1995, Sequential Trace Determination of Arsenic(III) and Arsenic(V) by Differential-Pulse Polarography: Analytical Sciences, v. 11, p. 261-262.

Sheppard, D., Truesdell, A., and Janik, C., 1992, Geothermal gas compositions in Yellowstone-National-Park, USA: Journal of Volcanology and Geothermal Research, v. 51, p. 79-93.

Shock, E.L., Holland, M., Meyer-Dombard, D.R., Amend, J.P., 2005, Geochemical sources of energy for microbial metabolism in hydrothermal ecosystems: Obsidian Pool, Yellowstone National Park, USA. In Geothermal Biology and Geochemistry in Yellowstone National Park (eds Inskeep WP, McDermott TR). Thermal Biology Institute, Montana State University, Bozeman, MT, p. 95–112.

Skirnisdottir, S., Hreggvidsson, G.O., Hjorleifsdottir, S., Marteinsson, V.T., Petursdottir, S.K., Holst, O., and Kristjansson, J.K., 2000, Influence of sulfide and temperature on species composition and community structure of hot spring microbial mats: Applied Environmental Microbiology, v. 66, p. 2835-2841.

Skoog, D.A. and Leary, J.J., 1998, Principles of Instrumental Analysis: 5th edition, Saunders College Publishing, TX.

Smedley, P.L., Kinniburgh, D.G., 2002. A review of the source, behavior, and distribution of arsenic in natural waters. Applied Geochemistry, v. 17, p. 517-568.

Sonne, K. and Dasgupta, P.K., 1991, Simultaneous photometric flow-injection determination of sulfide, polysulfide, sulfite, thiosulfate, and sulfate: Analytical Chemistry, v. 63, p. 427.

Spear, J.R., Walker, J.J., McCollom, T.M., and Pace, N.R., 2005, Hydrogen and bioenergetics in the Yellowstone geothermal ecosystem: PNAS Early Edition.

Squibb, K.S. and Fowler, B.A., 1983. “The toxicity of arsenic and its compounds.” In B.A. Fowler (Ed.), Biological and Environmental Effects of Arsenic. Elsevier, Amsterdam, 233-263.

Stauffer, R.E. and J.M. Thompson. 1984. Arsenic and antimony in geothermal waters of Yellowstone National Park, Wyoming, USA. Geochimica et Cosmochimica Acta, v. 48, p. 2547-2561.

Steudel, R., 1996, Mechanism for the formation of elemental sulfur from aqueous sulfide in chemical and microbiological desulfurization processes: Industrial and Engineering Chemistry Research, v. 35, p. 1417–1423.

Steudel, R., 2003, Inorganic polysulfides S_n^{2-} and radical anions $S_n^{\cdot -}$: Top. Curr. Chem., v. 231, p. 127–152.

Steudel, R., Holdt, G., Nagorka, R., 1986, On the autoxidation of aqueous sodium polysulfide: Z. Naturforsch. B, v. 41, p. 1519–1522.

Steudel, R. and Holdt, G., 1988, Solubilization of Elemental Sulfur in Water by Cationic and Anionic Surfactants.: Angew. Chem. Int. Ed. Engl., v. 27, p.

Stuben, D., Braun, S., Jeroschewski, P., and Haushahn, P., 1998, Application of in-situ and on-line measurements to environmental studies in Lake Muritz, northern Germany: Applied Geochemistry, v. 13, p. 379-389.

Sun, X., and Doner, H.E., 1998, Adsorption and oxidation of arsenite on goethite: Soil Science, v. 163, p. 278-287.

Sundby, B., Caetano, M., Vale, C., Gobeil, C., Luther, G., and Nuzzio, D., 2005, Root induced cycling of lead in salt marsh sediments: Environmental Science and Technology, v. 39, p. 2080-2086.

Sweerts, J.P.R.A. and deBeer, D., 1989, Microelectrode measurements of nitrate gradients in the littoral and profundal sediments of a meso-eutrophic lake (Lake Vechten, the Netherlands): Applied and Environmental Microbiology, v. 55, p. 754-757.

Taillefert, M., Luther, G.W. III, and Nuzzio, D.B., 2000, The application of electrochemical tools for in situ measurements in aquatic systems: Electroanalysis, v. 12, p. 401-412.

Tani, Y., Miyata, N., Ohashi, M., Ohnuki, T., Seyama, H., Iwahori, K., and Soma, M., 2004, Interaction of inorganic arsenic with biogenic manganese oxide produced by Mn-oxidizing fungus, strain KR21-2: Environmental Science and Technology, v. 38, p. 6618-6624.

Tankere, S.P.C., Bourne, D.G., Muller, F.L.L., and Torsvik, V., 2002, Microenvironments and microbial community structure in sediments: Environmental Microbiology, v. 4, p. 97- 105.

Teder, A., 1971, The equilibrium between elementary sulfur and aqueous polysulfide Ions: Acta Chemica Scandinavica, v. 25, p. 1722–1728.

Tengberg, A., De Bovee, F., Hall, P., Berelson, W., Chadwick, D., Ciceri, G., Crassous, P., Devol, A., Emerson, S., Gage, J., Glud, R., Graziottin, F., Gundersen, J., Hammond, D., Helder, W., Hinga, K., Holby, O., Jahnke, R., Khripounoff, A., Lieberman, S., Nuppenau, V., Pfannkuche, O., Reimers, O., Rowe, G., Sahami, A., Saylers, F., Schurter, M., Smallman, D., Wehrli, B., and De Wilde, P., 1995, Benthic chamber and profiling landers in oceanography – a review of design, technical solutions and functioning: Progress in Oceanography, v. 35, p. 253-292.

Tercier, M., Buffle, J., and Graziottin, F., 1998, Novel voltammetric in-situ profiling system for continuous real-time monitoring of trace elements in natural waters: Electroanalysis, v. 10, p. 355-363.

Tercier-Waeber, M., Belmont-Hebert, C., and Buffle, J., 1998, Real-time continuous Mn(II) monitoring in lakes using a novel voltammetric in situ profiling system: Environmental Science and Technology, v. 32, p. 1515-1521.

Thamdrup, B., Fossing, H., and Jørgensen, B.B., 1994, Manganese, iron, and sulfur cycling in a coastal marine sediment, Aarhus Bay, Denmark: Geochimica et Cosmochimica Acta, v. 58, p. 5115-5129.

Theberge, S. M. and G. W. Luther, III. 1997. Determination of the electrochemical properties of a soluble aqueous FeS cluster present in sulfidic systems. Aquatic Geochemistry 3, 191-211.

Thompson, J. M. and Hutchinson, R. A., 1980, Boundary Creek thermal area of Yellowstone National Park: II. Thermal water analyses: Trans. Geothermal Resource Council, v. 4, p. 189-92.

Thompson, J. M. and Hutchinson, R. A., 1981, Chemical analyses of waters from the Boundary Creek Thermal Area, Yellowstone National Park, Wyoming: U.S. Geological Survey Open-File Report 81-1310, 15 p.

Tighe, M., Lockwood, P., Wilson, S., and Lisle, L., 2004, Comparison of digestion methods for ICP-OES analysis of a wide range of analytes in heavy metal contaminated soil samples with specific reference to arsenic and antimony: Communications in Soil Science and Plant Analysis, v. 35, p. 1369-1385.

Tossell, J., 1997, Theoretical studies on arsenic oxide and hydroxide species in minerals and in aqueous solution: Geochimica et Cosmochimica Acta, v. 61, p. 1613-1623.

tRFLP Fragment Sorter, 2006, http://www.oardc.ohio-state.edu/trflpfragsort/index.php: The Ohio State University, Stephen M. Sciarini.

Truesdell, A.H. and Fournier, R.O., 1976, Conditions in the deeper parts of hot spring systems of Yellowstone National Park, Wyoming: U.S. Geological Survey Open-File Report 76, 29 p.

Truesdell, A.H., Nathenson, M., and Rye, R.O., 1977, The effects of subsurface boiling and dilution on the isotopic compositions of Yellowstone thermal waters: Journal of Geophysical Research, v. 82, p. 3694-3704.

Truesdell, A. H. and Thompson, J. M., 1982, The geochemistry of Shoshone Geyser Basin, Yellowstone National Park: Guidebook for Wyoming Geological Association Annual Field Conference, 33rd, p. 153-59.

Van den Berg, C.M.G., 1984, Determination of the complexing capacity and conditional stability constants of complexes of copper (II) with natural organic ligands in seawater by cathodic stripping voltammetry of copper-catechol complex ions: Marine Chemistry, v. 15, p. 1-18.

Vasil'ev, A., Temerdashev, Z., and Tsyupko, T., 1999, Voltammetric determination of arsenic(III) using a gold-glassy-carbon electrode: Journal of Analytical Chemistry, v. 54, p. 642-645.

Visscher, P.T., Beukema, J., and Vangemerden, H., 1991, In-situ characterization of sediments – measurements of oxygen and sulfide profiles with a novel combined needle electrode: Limnology and Oceanography, v. 36, p. 1476-1480.

Wang, J. and Ariel, M., 1978, The Rotating Disc Electrode in Flowing Systems. Part II: Flow system for Automated ASV Analysis of Discrete Samples: Analytica Chimica Acta, v. 101.

Wang B. and Greene, J. 1983, Determination of Arsenic(III) in Flowing Streams by Anodic Stripping Voltammetry: Journal of Electroanalytical Chemistry, v. 154, p. 261.

Wang, J., Larson, D., Foster, N., Armalis, S., Lu, J.M., Rongrong, X., Olsen, K., and Zirino, A., 1995, Remote electrochemical sensor for trace-metal contaminants: Analytical Chemistry, v. 67, p. 1481-1485.

Webster, J.G. and Nordstrom, D.K., 2003, Geothermal Arsenic, in Welch, A.H., and Stollenwerk, K.G., eds., Arsenic in Ground Water: Geochemistry and Occurrence: Boston, Kluwer Academic Publishers, p. 101-126.

Welhan, J.A., 1981, Carbon and hydrogen gases in hydrothermal systems; the search for a mantle source: PhD. thesis Univ. Calif., San Diego, La Jolla. 216 p.

Weres, O., 1988, Environmental Protection and Chemistry of Geothermal Fluids: Geothermal Science and Technology, v. 1, p. 253-302.

White, D.E., Muffler, L.J.P., and Truesdell, A.H., 1971, Vapor-dominated hydrothermal systems compared with hot-water systems: Economic Geology, v. 66, p. 75-97.

WHO, 1993. Guidelines for Drinking-Water Quality, vol. 1: Recommendations, second ed. WHO, Geneva.

Williamson, M.A. and Rimstidt, J.D., 1992, Correlation between structure and thermodynamic properties of aqueous sulfur species: Geochimica et Cosmochimica Acta, v. 56, p. 3867-3880.

Xu, Y., 1997, Kinetics of the redox transformations of aqueous sulfur species: The role of intermediate sulfur oxyanions and mineral surfaces. Ph.D. dissertation, State University of New York at StonyBrook.

Xu, Y. and Schoonen, M.A.A., 1995, The stability of thiosulfate in the presence of pyrite in low-temperature aqueous solutions: Geochimica Cosmochimica Acta, v. 59, p. 4605-4622.

Xu, Y., Schoonen, M.A.A., Nordstrom, D.K., Cunningham, K.M., and Ball, J.W., 1998, Sulfur geochemistry of hydrothermal waters in Yellowstone National Park: I. The origin of thiosulfate in hot spring waters: Geochimica et Cosmochimica Acta, v. 62, p. 3729-3743.

Xu, Y., Schoonen, M.A.A., Nordstrom, D.K., Cunningham, K.M., and Ball, J.W., 2000, Sulfur geochemistry of hydrothermal waters in Yellowstone National Park, Wyoming, USA. II. Formation and decomposition of thiosulfate and polythionate in Cinder Pool: Journal of Volcanology and Geothermal Research, v. 97, p. 407-423.

Zima, J., and Vandenberg, C., 1994, Determination of Arsenic in Sea Water by Cathodic Stripping Voltammetry in the Presence of Pyrrolidine Dithiocarbamate: Analytica Chimica Acta, v. 289, p. 291-298.

Zobrist, J., Dowdle, P.R., Davis, J.A., and Oremland, R.S., 2000, Mobilization of arsenite by dissimilatory reduction of adsorbed arsenate: Environmental Science and Technology, v. 34, p. 474-475.

Appendix A: DNA Extraction, PCR, and T-RFLP Techniques

DNA Extraction

1) Use UltraClean Microbial DNA Isolation Kit (MoBio #12224-50) for environmental samples and cultures and the UltraClean Soil DNA Kit (MoBio #12800-100) for environmental soil samples, to extract DNA. These kits are used for the isolation of DNA from microorganisms and the instruction manual that comes with the kit should be followed. Gloves should be worn at all times during the DNA isolation and extraction. The following steps are a reworded version of the instruction manual provided with the Microbial DNA isolation kit.

    a. Add 1.8 mL of bacterial culture to the provided microcentrifuge tube and centrifuge for 30 seconds at 10,000 x g. Decant the supernatent and centrifuge the tubes again for 30 seconds at 10,000 x g. Remove all remaining media supernatent with a pipet tip being careful not to touch the pellet on the bottom of the tube. Use a new pipet tip for each sample.
    b. Resuspend the cell pellet by adding 300 uL of the provided MicroBead Solution and gently vortex to mix. Transfer resuspended cells to the provided MicroBead tube.
    c. Add 50uL of Solution MD1 to the MicroBead tube. Optional: To increase yields, heat at 65 ºC for 10 minutes.
    d. Secure bead tubes to the vortex via a flat plate and tape so that the tubes lay horizontal. Vortex at maximum speed for 10 minutes.
    e. Centrifuge the MicroBead tubes for 30 seconds at 10,000 x g. Be sure not to exceed 10,000 x g or the tubes will break. Transfer the supernatent to a clean microcentrifuge tube provided with the kit. This is best done using a pipet and drawing the supernatent in very slowly. Remember use a clean tip for each sample. (Expect 300-350 uL)
    f. Add 100uL of Solution MD2 to the supernatent. Vortex 5 seconds. Incubate at 4 ºC for 5 minutes (Refrigerator works for this).
    g. Centrifuge for 1 minute at 10,000 x g. Avoiding the pellet, transfer the entire volume of supernatent to a clean 1.9 mL microcentrifuge tube that is provided. You can expect approximately 450 uL in volume.
    h. Add 900 uL of Solution MD3 to the supernatent and vortex for 5 seconds.
    i. Load about 700 uL into the spin filter and centrifuge for 30 seconds at 10,000 x g. Discard the flow through, add the remaining supernatent to the spin filter and centrifuge again for 30 seconds at 10,000 x g. Discard all flow through liquid.
    j. Add 300 uL of Solution MD4 and centrifuge for 30 seconds at 10,000 x g. Discard the flow through. Centrifuge again for 1 minute at 10,000 x g.
    k. Being careful not to splash liquid on the filter basket, place the spin filter in a new 1.9 mL tube that is provided.

l. Add 50 uL of Solution MD5 to the center of the white filter membrane. Centrifuge for 30 seconds at 10,000 x g. Discard spin filter.
m. DNA in the tube should be frozen at –20 ºC until it is to be used.

PCR

2) Run PCR reaction using the following method per reaction:
(for **n** reactions…multiply volume by **n**)

10X Buffer	2.5 uL
$MgCl_2$	1 uL (Only add if buffer doesn't have it)
DNTP	0.5 uL
8F Primer	0.5 uL (This Primer must have Fluorescent tag)
1492R Primer	0.5 uL
Taq	0.15 uL (goes in last)
H_2O	17.85 uL (Add 1uL water if no Mg is added)
	23 uL per reaction
+ Template	1 uL (extracted DNA)
Total Reaction	24 uL

PCR Thermocycler Sequence:
2 min at 94 ºC

Cycle next three steps 25x:
30 sec at 94 ºC
1.5 min at 47 ºC
3 min at 72 ºC

10 min at 72 ºC
Hold at 4 ºC

a. Defrost DNA isolated from the MoBio kit and add 1 uL DNA (template) to the small 0.1 mL PCR tube.
b. Calculate and combine DNTP, 10x buffer, Primers, water, and Taq; making sure to add the Taq last (amount/reaction X # of reactions + 2). If your 10X buffer doesn't have Mg then you need to add it to the reaction; otherwise, add 1 uL/ reaction water to make the total reaction volume 23 uL.
c. Add 23 uL mixture to each PCR tube.
d. Mix or vortex for 5 seconds and place in thermocycler.
e. Program thermocycler to the above PCR reaction program.

f. Once finished store at –20 ºC.

Gel Electrophoresis

3) Make electrophoresis gel.
    a) Make 0.8% agarose gel by adding 0.8 g to 100 mL of 1X TBE buffer in a 250 mL flask designated for this task.
    b) Heat mixture up in the microwave for 1 min or on a hot plate. and then let cool to 60 ºC (Should be able to hold the flask uncomfortably). Once it has cooled add 3 uL of Ethidium Bromide stock solution and swirl to mix. Dispose of tip in designated beaker.
    c) Pour gel into gel box use combs to remove any air bubbles, then place comb in proper location. Allow the gel to set up for at least 30 min.
    d) While waiting for gel to harden, dot 1 uL of dye on parafilm for each reaction you are running (this saves tips).
    e) Once gel is solid, remove comb(s) carefully.
    f) Add 4 uL of PCR product to 1 uL of dye and mix on parafilm. Add mixture to wells in the agarose gel left by the comb.
    g) Turn gel 90 degrees so the top set of wells is closer to the negative terminal. Remember DNA will migrate from negative to positive in gel. Pour TBE buffer into the gel box to cover the gel completely. Place the lid on the box and run for about 30 min at 150 V. Done when bands have migrated halfway between the upper and lower wells.
4) Take a picture of the PCR gel using the FotoAnalyst software and the camera with the ethidium bromide filter
    a) Make sure the Ethidium Bromide filter is loaded.
    b) Turn switch under glass to HIGH.
    c) Push the CAMERA and TRANS buttons on the box between the Camera and Computer (It should start beeping).
    d) In software go to acquire new image. Select Capture and expose for 200-300. You may need to change the exposure to get a clear image.
    e) Dispose of all Gloves and gel in the Solid Hazardous Waste under the sink.

5) If you find that your PCR product does have DNA (from running the gel) then clean up the PCR reaction product using a PCR cleanup kit (Qiagen). Follow the instructions contained in the kit.

Enzyme Digestions for RFLP

6) Run Double digest with the following per reaction:

10x NEB2	2 uL
0.1% triton X100	2 uL
2u/rxn HinPI	0.1 uL
2u/rxn MSPI	0.2 uL
PCR product temp.	10 uL
2u/rxn Alu1	0.2 uL
H_2O	5.5 uL

Run digest (all 20 uL) for 3hrs @ 37 ºC, then 20 min @ 65 ºC.

7) Check concentration on Nanodrop. Needs to be greater than 20 ug/L DNA.

Appendix B: MATLAB Code for Plotting Text Files

```
%%%%%%%%%%
%Greg Lorenson
%October 4, 2005
%Updated January 27, 2006
%%%%%%%%%%%%%%%%%%%%%%%%

%This program will take output text files from the Analysis program and
%plot the data for you.
%Inputs: Text Files
%Outputs: Voltammogram and data in excel spreadsheet

close all;
clear all;

dirname = uigetdir; %User can find directory where files are located.
d=dir(dirname);
addpath(dirname);
str = {d.name};
[s,v] = listdlg('PromptString','Select a file:',...
                'SelectionMode','multiple',...
                'ListString',str);
%Prompts the user to select the text files they want to use.User can choose
%more than one at a time.

data = str(s(1,:));
%Creates a matrix called (data) that includes the names of the files
%selected.
n = length(data)';
z = importdata(data{1,1});
c = class(z);
if c == 'struct';
   numdata = [z.data];
   datatext = {z.textdata};
   datatext = datatext{:,1};
   potential = numdata(:,1);
   FinalData = potential;
      for i=1:n;
      z=importdata(data{1,i});
      numdata = [z.data];
      current = numdata(:,:);
      current = current(:,3);
```

```
        Resultant(:,i)=current;
        FinalData(:,i+1)=Resultant(:,i);
        end;
else
    if c == 'double';
    potential = z(:,1);
    FinalData = potential;
        for i=1:n;
        z=importdata(data{1,i});
        current = z(:,:);
        current = current(:,3);
        Resultant(:,i) = current;
        FinalData(:,i+1)=Resultant(:,i);
        end;
    end;
end;

%All of the above sorted the data into a format that is easy to export to
%excel and plot.

%%%%%%%%%%%%
% These next set of functions allow the user to export the data to an excel
% file.
ex=input('Would you like to export this data to excel? (Y or N)','s');

if ex == 'Y';
    warning off MATLAB:xlswrite:AddSheet;
    name=input('What would you like to call this file?','s');
    xlswrite(name,FinalData,'Sheet1');
end;
if ex == 'y';
    warning off MATLAB:xlswrite:AddSheet;
    name=input('What would you like to call this file?','s');
    xlswrite(name,FinalData,'Sheet1');
end;

%Plots the data the user has choosen.

plot(potential(:,1),Resultant(:,:),'-');
title('Voltammogram');
xlabel('Potential (Volts vs. Ag/AgCl)');
ylabel('Current(uA)');
```